



SAPIENZA  
UNIVERSITÀ DI ROMA

Ph.D. Course in Mathematical Models for Engineering,  
Electromagnetics and Nanoscience

- Curriculum Materials Science-

XXXVI cycle

**A poly-hydroxyalkanoates (PHAs) multifaced  
study: extraction, characterization and  
applications**

**PhD student:** Sara Alfano

**Supervisor:** Prof. Andrea Martinelli

**PhD coordinator:** Prof. Lorenzo Giacomelli

Academic year 2023-2024



*[..] se ne usciva, ogni sera e più acutamente a fine corso, con la sensazione di avere "imparato a fare una cosa" il che, la vita lo insegna, è diverso dall'aver "imparato una cosa"*

Primo Levi, *Il segno del chimico* in *L'altrui mestiere*, 1985

## Abstract

In recent years, the problems associated with solid waste management and the dependence on petroleum-based plastics have created great interest, mainly focused on the development of bio-derived and biodegradable polymers. One of the most promising group of biopolymers that can be used as a fossil plastic substitute is the polyhydroxyalkanoates family (PHAs). PHAs are polyesters that can be naturally accumulated as intracellular granules by many prokaryotic microorganisms. The stored copolymer is a biodegradable thermoplastic material. Poly(3-hydroxybutyrate) [P(3HB)] and its copolymers, mainly with 3-hydroxyvalerate monomeric repeating unit [P(3HB-*co*-3HV)], are among the most investigated biopolymers of this class. The combination of thermoplasticity and biodegradability makes PHAs suitable for several applications, including packaging and biomedical devices.

However, problems related to the environmental and economic sustainability of the extraction and purification as well as PHA chemical modification limit the large-scale diffusion.

In this thesis, the transition toward eco-friendly methodologies has been addressed both for P(3HB-*co*-3HV) recovery from biomasses and for chemical functionalization. More in detail, the extraction of P(3HB-*co*-3HV) from biomass by dissolution in ethyl esters and through innovative coupled treatment based on cell lysis is proposed as an effective alternative to the commonly used chloroform solubilization.

As far as the application of PHA in the biomedical field, chemical modification is often necessary to increase the polymer hydrophilicity to hamper particles aggregation in body fluids as well as to favour the adhesion of cells and possible internalization processes. Then, a safer alternative to the main approaches described in literature has been proposed. It involves the use of the non-cytotoxic ionic liquid choline taurinate [Ch][Tau] for the surface modification of PHA films and for the preparation of self-surfactant systems, used in nanoparticles fabrication.

In addition to the mentioned economic and sustainability-related drawbacks, P(3HB-*co*-3HV) copolymers with low 3HV content are difficult to process, because of high melting



temperature, and the obtained items are brittle, because of the high crystallinity. The possibility of producing 3HV-rich copolymers leads to a reduction of crystallinity and, therefore, to better processability and mechanical properties. On the other hand, a gap of knowledge is still present about the effect of high 3HV concentration on copolymer properties. Then, part of this thesis is dedicated to a basic study of the structure-property relationships of P(3HB-*co*-3HV) copolymers with various 3HV content and to the evaluation of the effect of copolymer composition processing and compounding.

# Table of contents

<b>INTRODUCTION</b>	<b>11</b>
<i>FROM LINEAR TO CIRCULAR ECONOMY</i>	<b>12</b>
<i>PHA: A VIRTUOUS EXAMPLE OF INTEGRATED BIOREFINERY</i>	<b>17</b>
1. <i>PHAS BIOSYNTHESIS</i>	20
2. <i>PHA PRODUCTION: PURE CULTURE VS MIXED CULTURES</i>	21
3. <i>PHA LIFE CYCLE: FROM THE UPSTREAM TO FINAL APPLICATIONS</i>	23
4. <i>PHAS LIMITATION: HOW TO CIRCUMVENT THEM?</i>	26
<b>AIM AND RESEARCH PLAN</b>	<b>28</b>
<b>CHAPTER 1</b>	<b>30</b>
<b>CHALLENGES AND ADVANCEMENTS IN PHA RECOVERY</b>	<b>31</b>
<i>ETHYLIC ESTERS AS GREEN SOLVENTS FOR THE EXTRACTION OF INTRACELLULAR POLYHYDROXYALKANOATES PRODUCED BY MIXED MICROBIAL CULTURE</i>	<b>36</b>
1. <i>MATERIALS AND METHODS</i>	<b>37</b>
1.1 <i>PHA PRODUCTION</i>	37
1.2 <i>PRELIMINARY DISSOLUTION TESTS</i>	37
1.3 <i>EXTRACTION EXPERIMENTS</i>	38
1.4 <i>CHARACTERIZATION METHODS</i>	39
2. <i>RESULTS AND DISCUSSION</i>	<b>41</b>
2.1 <i>SCREENING OF DIFFERENT EES AS PHA-EXTRACTION SOLVENTS</i>	41
2.2 <i>EVALUATION OF PHA EXTRACTION PERFORMANCES WITH ETHYL ACETATE (EA)</i>	43
2.3 <i>FT-IR AND 1H-NMR ANALYSIS</i>	48
3. <i>CONCLUSIONS</i>	<b>50</b>
<i>CHLORINE-FREE EXTRACTIONS OF MIXED-CULTURE POLYHYDROXYALKANOATES PRODUCED FROM FERMENTED SEWAGE SLUDGE AT PILOT SCALE</i>	<b>52</b>
1 <i>MATERIALS AND METHODS</i>	<b>53</b>

1.1 <i>P(3HB-CO-3HV)</i> PRODUCTION	53
1.2 <i>P(3HB-CO-3HV)</i> EXTRACTION	53
1.2.1 ALKALINE AND OXIDATIVE CHLORINE-FREE TREATMENTS	53
1.2.2 ETHYL ACETATE EXTRACTION	54
1.3 <i>P(3HB-CO-3HV)</i> CHARACTERIZATION	54
<b>2 RESULTS AND DISCUSSIONS</b>	<b>55</b>
2.1 <i>P(3HB-CO-3HV)</i> EXTRACTION AND RECOVERY	55
2.2 VISCOSITY AVERAGE MOLECULAR WEIGHT ( $M_v$ )	57
2.3 THERMAL ANALYSIS	57
2.4 EXTRACTION AT A PILOT SCALE	60
2.5 ECONOMIC ANALYSIS	61
<b>3 CONCLUSIONS</b>	<b>63</b>
<b>CHAPTER 2</b>	<b>64</b>

---

**TOWARD A NEW STRATEGY FOR SUSTAINABLE CHEMICAL MODIFICATION OF PHAS**

---

**65**

<b>SUSTAINABLE SURFACE FUNCTIONALIZATION OF POLY(3HYDROXYBUTIRATE-CO-3HYDROXYHEXANOATE) (PHBHHx)</b>	<b>69</b>
<b>1. MATERIALS AND METHODS</b>	<b>70</b>
1.1 MATERIALS	70
1.2 FILMS PREPARATION AND FUNCTIONALIZATION	70
1.3 FTIR ANALYSIS	70
1.4 STATIC CONTACT ANGLE MEASUREMENTS	71
1.5 MORPHOLOGICAL CHARACTERIZATION	71
1.6 DYNAMIC LIGHT SCATTERING (DLS)	71
<b>2. RESULTS AND DISCUSSION</b>	<b>71</b>
2.1 STUDY OF THE EFFECT OF SOLVENTS ON CRYSTALLINITY	71
2.2 SCREENING OF DIFFERENT SOLVENTS FOR AMINOLYSIS	73
2.3 FRACTIONATION OF HETEROGENEOUS AMINOLYSIS PRODUCTS	76
<b>3. CONCLUSIONS</b>	<b>78</b>

<b>PREPARATION AND CHARACTERIZATION OF PHA-BASED SELF-SURFACTANT SYSTEMS</b>	<b>79</b>
<b>1. MATERIALS AND METHODS</b>	<b>80</b>
1.1 MATERIALS	80
1.2 NANOPARTICLES PREPARATION	80
1.3 FOURIER TRANSFORM INFRARED SPECTRA (FTIR)	81
1.4 GEL PERMEATION CHROMATOGRAPHY (GPC)	81
1.5 DYNAMIC LIGHT SCATTERING (DLS)	82
1.6 UV-VIS SPECTROSCOPY	82
<b>2 RESULTS AND DISCUSSION</b>	<b>83</b>
2.1 EVALUATION OF DIFFERENT REACTION TIME INFLUENCE	83
2.2 EVALUATION OF DIFFERENT [CH][TAU]: PHBHHX RATIOS EFFECT	85
2.2.1 CHARACTERIZATION OF NON-FRACTIONATED PRODUCTS (S <sub>PHBHHX<sub>TOT</sub></sub> )	85
2.2.2 CHARACTERIZATION OF FRACTIONATED PRODUCTS (S <sub>PHBHHX<sub>PREC</sub></sub> AND S <sub>PHBHHX<sub>SOL</sub></sub> )	88
2.2 SELF-SURFACTANT ACTIVITY OF S <sub>PHBHHX<sub>TOT</sub></sub>	90
2.3 APPARENT SOLUBILITY ( $\Delta A$ ) CALCULATION FOR ENCAPSULATION EFFICIENCY EVALUATION	92
2.4 S <sub>PHBHHX</sub> AS SURFACTANT FOR PHBHHX	94
<b>3 CONCLUSION</b>	<b>94</b>
<b>CHAPTER 3</b>	<b>95</b>
<hr/>	
<b><u>EXPLORING THE ROLE OF 3-HYDROXYVALERATE (3HV) CONTENT ON PROCESSABILITY, COMPOUNDING AND PROPERTIES OF P(3HB-CO-3HV)</u></b>	<b>96</b>
<b>1. MATERIALS AND METHODS</b>	<b>101</b>
1.1 MATERIALS	101
1.2 METHODS	102
1.2.1 PREPARATION OF P(3HB-CO-3HV)-BASED FILMS	102
1.2.2 THERMAL CHARACTERIZATION	103
1.2.3 TENSILE TESTS	104
1.2.4 POLARIZED OPTICAL MICROSCOPE MEASUREMENTS (POM)	104
1.2.5 SCANNING ELECTRON MICROSCOPY (SEM)	104
1.2.6 WATER VAPOR PERMEABILITY	104

<b>2. RESULTS AND DISCUSSION</b>	<b>105</b>
2.1 EFFECT OF 3HV CONTENT ON PROCESSABILITY AND MECHANICAL PROPERTIES	105
2.2 EFFECT OF BN ADDITION	108
2.3 EFFECT OF MCL-PHA ADDITION	113
2.4 SYNERGISTIC EFFECT OF BN AND MCL-PHA ADDITION	117
2.5 WVP MEASUREMENTS	119
<b>3. CONCLUSIONS</b>	<b>121</b>
<b>CHAPTER 4</b>	<b>122</b>
<hr/>	
<b>RAPID ESTIMATION OF POLY(3-HYDROXYBUTYRATE-CO-3-HYDROXYVALERATE) COMPOSITION BY ATR-FTIR</b>	<b>123</b>
<hr/>	
<b>1. MATERIALS AND METHODS</b>	<b>125</b>
1.1. MATERIALS	125
1.2. SAMPLE PREPARATION AND CHARACTERIZATION	126
1.3. DATA ANALYSIS	127
<b>2. RESULTS</b>	<b>128</b>
2.1. ATR-FTIR ANALYSIS	128
2.2 DATA ANALYSIS	132
<b>3 CONCLUSIONS</b>	<b>134</b>
<b>CONCLUDING REMARKS</b>	<b>136</b>
<hr/>	
<b>APPENDICES</b>	<b>137</b>
<hr/>	
<b>APPENDIX 1- SIDE RESEARCH ACTIVITIES</b>	<b>138</b>
PHAS PRODUCTION	138
PHAS APPLICATIONS	141
BIO-BASED REPROCESSABLE MATERIALS	143
<b>APPENDIX 2- ACTIVITIES REPORT</b>	<b>145</b>
1. LIST OF PUBLICATIONS	145
2. CONFERENCES	147

3. <i>ATTENDED COURSES</i>	149
4. <i>ATTENDED SEMINARS</i>	150
5. <i>TUTORING</i>	153
<b><u>ACKNOWLEDGEMENTS</u></b>	<b>154</b>
<b><u>REFERENCES</u></b>	<b>155</b>

## List of acronyms

[Ch][Tau]: choline taurinate

ATR: attenuated total reflection.

CAPEX: fixed costs

CHCl<sub>3</sub>: chloroform

COD: chemical oxygen demand

EA, EtOAc: ethyl acetate

EB: ethyl butyrate

EE: ethylic esters

EP: ethyl propionate

FTIR: Fourier-Transform infrared spectroscopy

H<sub>2</sub>O<sub>2</sub>: hydrogen peroxide

*lcl*-PHA: long chain length polyhydroxyalkanoates

*mcl*-PHA: medium chain length polyhydroxyalkanoates

MMC: mixed microbial cultures

M<sub>n</sub>: number average molecular weight

M<sub>v</sub>: viscosity average molecular weight

MW: molecular weight

M<sub>w</sub>: weight average molecular weight

NaOCl: sodium hypochlorite

NaOH: sodium hydroxide

NPs: nanoparticles

OFMSW: organic fraction of municipal solid waste

OPEX: operational costs

P4HB: poly(4-hydroxybutyrate)

PDI: polydispersity index

PHA: poly(hydroxyalkanoates)

PHB, P3HB: poly(3-hydroxybutyrate)

PHBV, P(3HB-co-3HV), PHB-HV : poly(hydroxybutyrate-co-3hydroxyvalerate)

SBR: sequencing batch reactor

*scl*-PHA: short chain length polyhydroxyalkanoates

VFA: volatile fatty acids

WAS: waste activated sludge

# **INTRODUCTION**



## **From linear to circular economy**

Since their introduction in the 1950s, plastics have revolutionized daily life habits. Rapid advances in material science technology have led to the production of new products with favourable mechanical integrity and excellent durability.

Plastic production increased from 2 million tons in 1950 to 380 Mt in 2015, becoming the bulk material with the strongest growth in global production [1]. Mostly derived from polymers based on petrochemicals, plastics offer a stable and lightweight material that can be easily moulded into a wide variety of shapes. These properties enable cost savings and enhanced functionality, from lightweight automotive and electronic components to widespread use in construction. Many medical, dental, and pharmaceutical advancements have been made with the use of new plastic materials to produce devices like heart valves and prostheses.

The low costs and the ease of processing of plastics have stimulated the production of single use objects including specialized packaging systems for the storage and delivery (i.e., blood transfusion bags, pouches for dental instruments) and single use manufactures (i.e., syringes, catheters, vials) able to ensure sterility and more hygienical conditions.

Single-use plastic packaging applications have played a key role in expanding the trade, distribution and consumption of industrial food and food preparations in recent decades. The advent of single-use plastic objects helps reach a more dynamic lifestyle, supporting fast technological development.

Despite the crucial role of plastic in the establishment of a high level of wellness in human life, there are many side aspects that can no longer be ignored. For many years, fast and easily usable packaging solutions as well as disposable objects, like spoons or forks, have been used and thrown after their use. As a result, a linear economy model has been established. The linear economic model is based on the take-make-dispose concept leading to the depletion of non-renewable resources, emission of greenhouse gases during manufacture and transportation as well as the generation of solid waste. In 2015, the plastics sector was responsible for 4.5% of global greenhouse gas (GHG) emissions. Following current growth rates, plastic production and their corresponding GHG emissions could

almost quadruple by 2050 [2]. Furthermore, plastics contribute to particulate matter emissions [3] and growing pollution [4].

Because petroleum plastic products are mostly not biodegradable, they are extremely persistent and, if improperly discarded as often occurs, they accumulate in the ecosystem, resulting in a significant burden on solid waste management. The most effective and alarming example is the so-called "great Pacific Garbage Patch" which literally is an island made of solid wastes, mainly plastic. Its existence was announced in 1988 by the National Oceanic and Atmospheric Administration (NOAA) of the United States (US) [5] and since then has been constantly expanding and constitutes a harmful presence for marine ecosystems.

Plastic pollution is not only a visible problem but also ubiquitous in daily life on a non-visible scale. Microplastics have been found in food, drinking water and air as well as in Arctic snow samples at concentrations up to  $14.4 \times 10^3$  items per litre [6]. The ice core of the Arctic Fram Strait contained a maximum concentration of  $1.2 \times 10^7$  microplastics per  $m^3$  [7]. Microplastics could potentially induce immune and stress responses, as well as interfere with reproductive functions and growth of animals [8]. Microplastics were found to adsorb other environmental pollutants, to release plastic additives and to provide surfaces for microbial growth, resulting in their altered or enhanced ecotoxicities [9].

It seems clear that the adoption of a linear economic model enhanced social wellness but caused ecological and health issues [10,11]. Many strategies have been proposed to counteract waste management-related problems, such as incineration, pyrolysis or landfilling but they are not effective in eliminating the always greater quantities of produced garbage.

In this scenario finding a solution is an urgent challenge for the mitigation of the cradle-to-grave environmental impacts associated with waste production.

To effectively deal with waste, the "make, use and dispose" approach should be substituted by the more sustainable "make, use, reuse and recycle" model [4,12,13] which is the basis of the circular economy.

The circular economy focuses on the retention of value in the material cycle through the reuse and recycling of materials such as plastic and preventing their uncontrolled release into the environment. Recycling ensures that post-use materials are returned to the factory as raw material thereby forming a circular loop. The scope of the circular economy is to prevent waste by conserving resources within the system according to the United Nations Sustainable Development Goal (SDG) number 12, which seeks to ensure sustainable consumption and production patterns [14].

However, recycling is not always the best solution since recycled plastic quality is often low due to the impossibility of separating different polymers and to the degradation that occurs during the recycling process. When the resulting recycled material is composed of a mix of different plastics, its heterogeneity affects mechanical, thermal and barrier properties. Additionally, recycled plastics often contain traces of contaminants deriving from their original usage as food packaging. Contaminants could be, as an example, degradation by-products of food residues (i.e. amines) which will be incorporated into the final manufacture. All these concerns limit the potentiality of recycling. Additionally, recycling is not a strategy which completely solve the plastic pollution issue since it simply “delay” the waste generation. In fact, objects made by recycled plastics are often not recyclable anymore.

An alternative approach which fits well with the principles of a circular economy model is the replacement of conventional plastics with materials characterized by similar properties and lower environmental impact. The latter means the possibility to re-introduce the material into bio-geochemical cycles in a timeframe compatible with human life.

Different classes of more sustainable materials have been individuated (Figure 1).

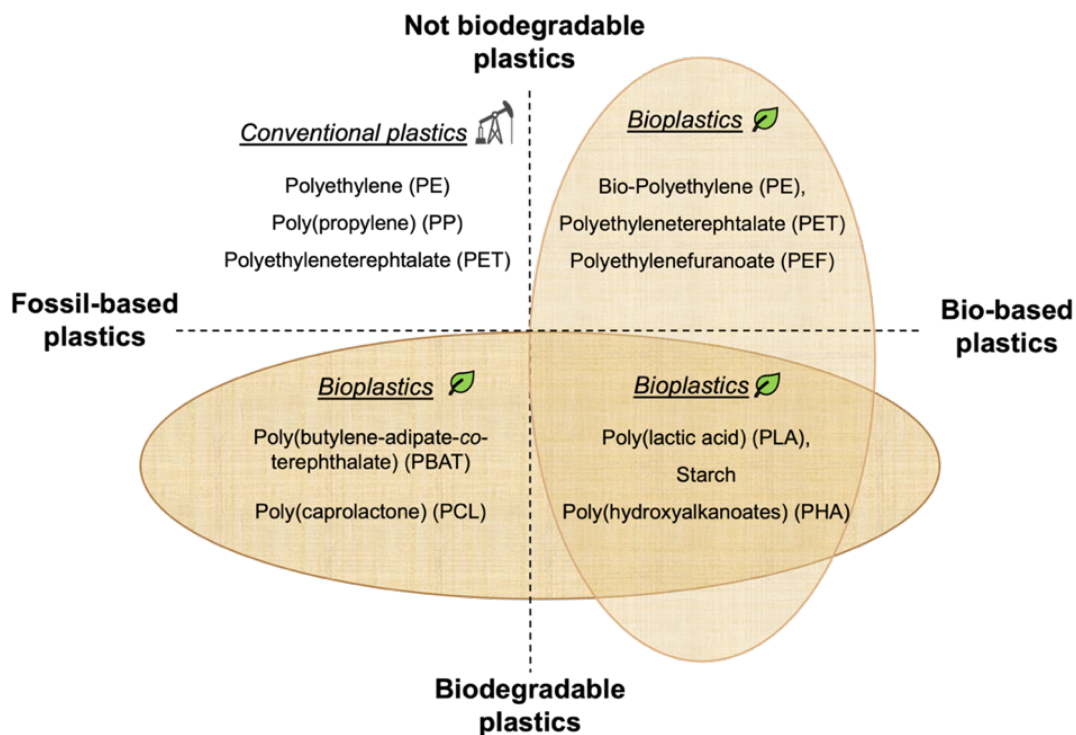


Figure 1 Classification of bioplastic.

As reported in Figure 1, the first distinction is between conventional (fossil-based) and bioplastic. Despite the term bioplastics is commonly used to indicate different materials, it should be noted that there are differences. Bioplastics is a general term that includes bio-based, biodegradable and both bio-based and biodegradable plastics. Plastics such as polyethylene (PE) or polyethylene terephthalate (PET) could be bio-based since their monomers can be produced starting from renewable resources (i.e. agri-food by-products or organic fractions of municipal wastes) instead of petroleum. As an example, bio-PE is produced starting from bio-ethylene obtained through catalytic dehydration of bioethanol in turn produced by enzymatic hydrolysis and subsequent fermentation of sugar cane, sugar beet, starch crops coming from maize, wheat or other grains and lignocellulosic materials [15,16]. In this case, sustainability is restricted only to the production process, in fact, biobased PE or PET end-of-life fate is landfilling, incineration or recycling. With respect to the oil-based polymers, their biodegradability remains unchanged.

On the other hand, bioplastic also indicates biodegradable plastics. Biodegradability is a key point in reducing plastic waste. A material is classified as biodegradable when, in the presence of microorganisms like fungi algae or bacteria, is completely converted into water,

carbon dioxide (CO<sub>2</sub>) and biomass over a period of 6 months meaning the re-introduction in the geo-chemical cycle of carbon (C cycle). If the abovementioned transformation occurs within 12 weeks at 58 °C, according to the European normative EN13432, the material can be classified as compostable at industrial scale. For home composting or biodegradation in soil temperature is lower (28 °C).

Biodegradability opens the way to the possibility of re-introducing carbon into nature in a sustainable and safe way.

Biodegradable material produced from renewable resources represents the third class of polymers classified as “bioplastic” and includes natural polymers like starch or polyhydroxyalkanoates (PHA).

The production of biodegradable and bio-based plastics from renewable sources represents a milestone in waste management thanks to the possibility of simultaneously valorising waste streams generated at the industrial or urban level and reducing plastic pollution.

The technical and scientific advancements in the field demonstrate the possibility of including plastic production in a more complex system called “integrated biorefinery”. An integrated biorefinery is the sustainable analogue of a petroleum refinery.

The US Department of Energy (DOE) defined biorefinery as *“an overall concept of a processing plant where biomass feedstocks are converted and extracted into a spectrum of valuable products”* [17].

A valuable potential biorefinery product is the poly(hydroxyalkanoates) (PHA) family, which represents a candidate for petroleum-based plastics substitution.

## PHA: a virtuous example of integrated biorefinery

Polyhydroxyalkanoates (PHAs) are polyesters of R-hydroxyalkanoic acid (HA) monomers (Figure 2) classified as a family of biodegradable bioplastics. PHAs are the object of several research thanks to their thermal, mechanical and gas barrier properties comparable with traditional fossil-based plastics, such as polypropylene (PP) and low-density polyethylene (LDPE), and their biodegradability. In Figure 2, the general repeating unit is reported.

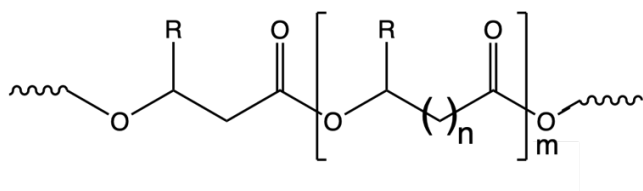


*Figure 2* General repeating unit formula of PHAs

Differently from other biobased polyester produced by polymerization of bio-sourced monomers (i.e., polybutylene succinate (PBS) from succinic acid or polylactic acid (PLA) from lactic acid), PHAs are produced from several microorganisms as intracellular carbon source starting from a carbon substrate like glucose or volatile fatty acids (VFAs). This latter prerogative allows the exploitation of renewable resources from various origins, for example, the organic fraction of municipal solid wastes (OFMSW).

PHAs are completely biodegradable to water, CO<sub>2</sub> and non-toxic compounds [18–20] producing biomasses which will be used as a feedstock for biorefinery activities.

The PHAs natural degradation in the environment, carried out by microorganisms that secrete intra- or extracellular specific enzymes like PHA depolymerase, has made them promising and interesting materials for many applications. As reported [21] PHAs can degrade in environments with high microbial activity such as soil and sewage sludge. The rate of biodegradation is significantly influenced by PHA depolymerases activity and several environmental factors such as temperature, microbial population, nutrient supply, pH, moisture level as well as the characteristics of the PHA materials, including the surface area, composition and crystallinity [22].

During the last decades, more than 150 different types of PHA monomers have been described and there is a huge variation in the composition and length of the side chains

[23,24]. PHAs are categorized into three main groups: (1) *short chain length*-PHA (*scl*-PHA), having 0-2 carbon atoms in the side chain and (2) *medium chain length*-PHA (*mcl*-PHA), with 3-11 carbon atoms in the side chain and *long chain length*-PHAs (*lcl*-PHAs) that go above C12 [25].

Additionally, PHAs may have one or more CH<sub>2</sub> in the principal chain. Classification of the most widespread PHA repeating units is reported in Table 1.

**Table 1** Classification of most widespread PHA repeating units.

R	n=1	n=2	n=3	n=4
H	Poly(3-hydroxypropionate)	Poly(4-hydroxybutyrate)	Poly(5-hydroxyvalerate)	
CH <sub>3</sub>	Poly(3-hydroxybutyrate)			
C <sub>2</sub> H <sub>5</sub>	Poly(3-hydroxyvalerate)			
C <sub>3</sub> H <sub>7</sub>	Poly(3-hydroxyhexanoate)			
C <sub>5</sub> H <sub>11</sub>	Poly(3-hydroxyoctanoate)			
C <sub>6</sub> H <sub>13</sub>				Poly(6-hydroxydodecanoate)
C <sub>9</sub> H <sub>19</sub>	Poly(3-hydroxydodecanoate)			

Depending on the type of incorporated monomers, PHAs can achieve a wide range of thermoplastic and visco-elastic properties as reported in table 2. Furthermore, the possibility to tune properties makes PHA suitable for a wide range of applications including packaging and biomedical device fabrication.

Polymers belonging to the *scl*-PHA group, mainly P3HB homopolymer and its copolymers with 3-hydroxyvalerate units P(3HB-co-3HV), are known to be highly crystalline and brittle. This high crystallinity, due to the stereoregularity, make P3HB and P3HB-co-3HV suitable materials for food packaging application since crystallinity ensure high vapor barrier properties and therefore avoid food spoilage. At the same time, crystallinity limits some applications, but it was demonstrated that the incorporation of a high amount of 3-hydroxyvalerate (3HV) or 3-hydroxyhexanoate (3HHx) units results in a more ductile material (400 % of elongation at break for P3HB-co-3HHx respect to 5 % of P3HB). Higher flexibility could enhance, as an example, processability and possibility to produce packaging films for which a higher mechanical resistance is needed, maintaining adequate barrier properties.

On the other hand, the *mcl*-PHA group is characterized by properties like that of elastomeric materials and then are appropriate for applications in biomedical field like scaffold for tissue engineering due to the ability to imitate organs with elastomeric behaviour.

**Table 2** Thermo-mechanical properties of *scl*-PHA (P3HB, P3HB-co-3HV and P(3HB-co-4HB) and *mcl*-PHA [26,27]

Parameter	P3HB	P3HB-co-3HV	P3HB-co-4HB	P3HB-co-3HHx	<i>mcl</i> -PHA
Melting temperature (°C)	177	145	150	127	40-50
Glass transition temperature (°C)	2	-1	-7	-1	-40
Crystallinity (%)	60	56	45	34	
Tensile strength (MPa)	43	20	26	21	4-2
Extension to break (%)	5	50	444	400	160-180

The wide variety of monomers and their relative properties stimulated research interest in the manipulation of microorganisms or the control of feedstock to obtain tailored copolymers. The control of monomeric composition or distribution led to the control properties and to the mitigation of each PHAs group characteristic (i.e. excessive *scl*-PHA crystallinity depression by including more co-monomeric units like 3HV or 3HHx, more strength of *mcl*-PHA by using *scl*-PHA as reinforcing additives).

In the following sections, a brief overview of PHAs biosynthesis in microbial cultures is provided.



## 1. PHAs biosynthesis

The synthesis of the PHA polymer chain takes place within the cytoplasm of the bacterial cell, within inclusions known as granules.

PHA accumulation is controlled by genes able to encode a range of enzymes directly or indirectly involved in PHA synthesis [20,24,28–31]. Eight pathways so far can be used to summarize the production of PHA [32]. First three pathways are illustrated in Figure 3.

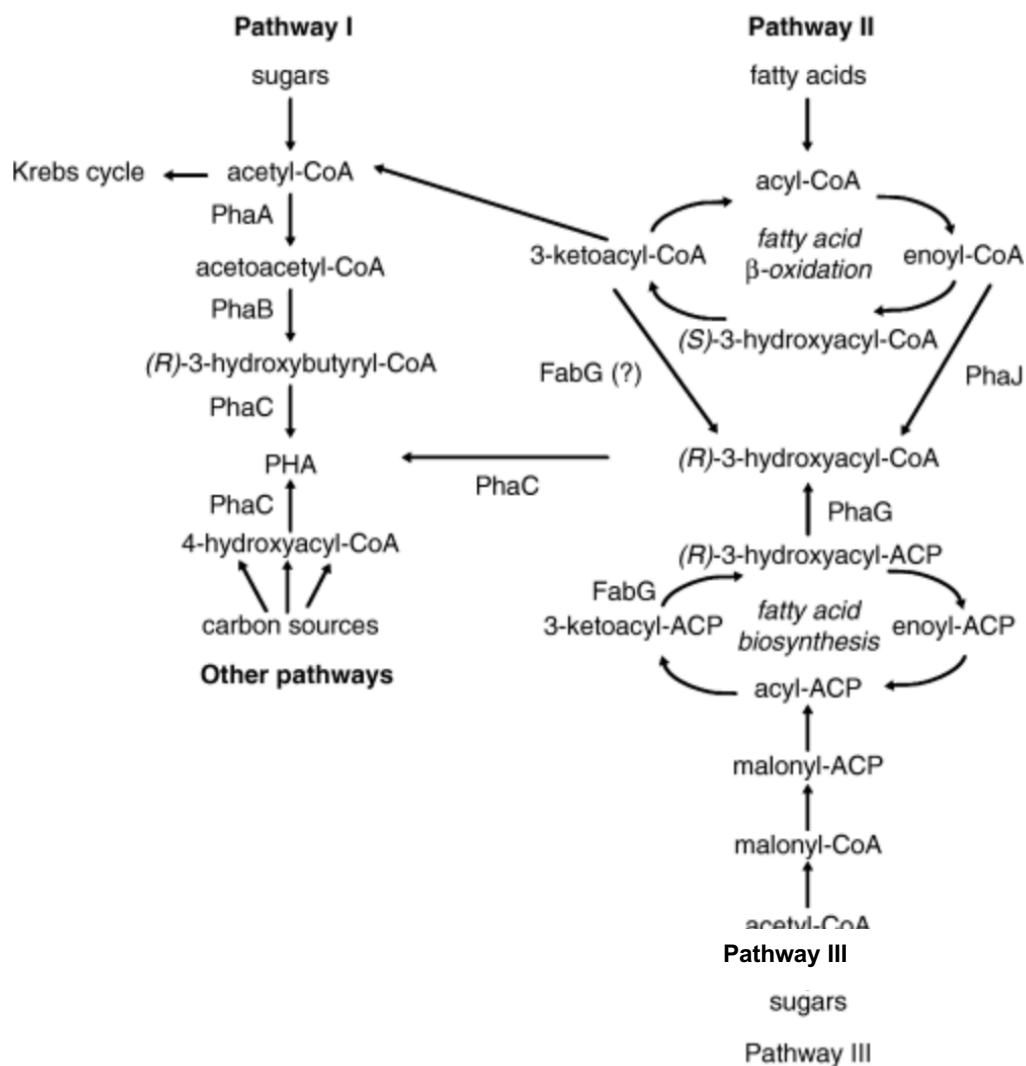


**Figure 3** First three metabolic pathways producing monomers for PHAs biosynthesis.

Pathway I involve the three key enzymes  $\beta$ -ketothiolase, NADPH-dependent acetoacetyl-CoA reductase, and PHA synthase, encoded by genes *phaA*, *phaB* and *phaC*, respectively. The carbon source (sugars) is initially converted into coenzyme A thioesters of (R)-hydroxyalkanoic acid, then two coenzyme A thioester monomers such as an acetyl-CoA and a propionyl-CoA monomer were condensed by  $\beta$ -Ketothiolase that act as a catalyst. The

condensation is followed by an (*R*)-specific reduction to give (*R*)-3-hydroxybutyryl-CoA (or (*R*)-3-hydroxyvaleryl-CoA) catalysed by acetoacetyl-CoA reductase. (*R*)-3-hydroxybutyryl-CoA (or (*R*)-3-hydroxyvaleryl-CoA) units are then converted by PHA synthase into PHA [33,34].

Four major classes of PHA synthase are being identified [35]. Class I uses fatty acids with 3–5 carbon atoms; Class II uses those with 6–14 carbons; and Classes III and IV synthesize *scl*-PHA.

Pathway II is associated with fatty acid uptake by microorganisms and is linked to the synthesis of *mcl*-PHA. Following fatty acid  $\beta$ -oxidation to give acyl-CoA, the precursor is converted to 3-hydroxyacyl-CoA and forms PHA thanks to the action of synthase catalysis. Enzymes involved in this pathway are 3-ketoacyl-CoA reductase, epimerase and (*R*)-enoyl-CoA hydratase/enoyl-CoA hydratase I.

Pathway III involves 3-hydroxyacyl-ACP-CoA transferase (encoded by PhaG) and malonyl-CoA-ACP transacylase (FabD); substrates are converted to 3-hydroxyacyl-ACP which can then form 3-hydroxyacyl-CoA and thus PHA. Pathway IV uses NADPH-dependent acetoacetyl-CoA reductase to oxidize (*S*)-(+)-3-hydroxybutyryl-CoA. The other pathways are used for the synthesis of alternative copolymers; for example, pathways V and VII are used to synthesize Poly(4-hydroxybutyrate) (P4HB).

## **2. PHA production: Pure culture vs Mixed cultures**

PHA production at an industrial scale is based on pure culture (wild-type or recombinant strains) fermentations operated in fed-batch mode. The most used microorganisms are *Cupriavidus necator* (formerly known as *Ralstonia eutropha* or *Alcaligenes eutrophus*), *Pseudomonas oleovorans*, *Protomonas extorquens*, *Alcaligenes latus*, or recombinant *Escherichia coli* [32]. The culture conditions required for polymer storage are different for the different microorganisms. Most PHA-producing bacteria require the limitation of an essential nutrient and a two-stage fed-batch process: firstly, the reactor is fed with a sterile growth media to achieve a high cellular content; secondly, growth limiting conditions are deliberately imposed with a limitation of a nutrient (nitrogen, phosphorous or oxygen) so that PHA storage is induced [36,37]. Regarding the recombinant cultures, since these can

grow and produce polymer at the same time, a nutrient-limited phase is not required to induce PHA production. However, a nutrient-feeding strategy must be developed to achieve a balance between cellular growth and polymer formation [38]. Overall, even though maximum PHA contents of up to 80-90% of the cell dry weight have been reported in literature [31] as well as substantially high volumetric productivity (up to 5 g P3HB/L h) [36,39]. This typically results in high substrate costs, expensive equipment and high energy consumption, making industrial biotechnological processes based on pure cultures unfavourable for further exploitation in PHAs production. In particular, the substrate cost accounts for about 50% of the total PHA production costs, to which the carbon source contributes most significantly [40] because substrates most used in the industrial processes are pure sugars, such as glucose or sucrose, or other sugar-based compounds, such as corn, which have a high market price.

Because of the overall high cost of PHA production, efforts have been made over the last years to turn the production into a more economical process, allowing the polymer to be used in its various applications.

During the last decade, the development of alternative low-cost processes has been the main research scope [41]. These efforts include the use of genetic engineering strategies to increase process productivity and improve PHAs extraction which requires several separation steps as they are intracellular polymers. The application of low-cost substrates based on agro-industrial wastes and by-products is of extreme interest too. Another alternative is the replacement of pure cultures with mixed microbial cultures (MMCs). MMCs are microbial populations operating in open biological systems, whose composition depends directly on the substrate mixture and operational conditions imposed on the open biological system that do not require sterile conditions or excessive operation control. MMCs have been mainly used in biological wastewater treatment plants since are able to transform a wide variety of undefined substrates into internal storage products such as PHAs. Thanks to the capacity to consume different substrates, the produced material is characterized by a broad range of compositions [42–44].

In this context, it is possible to combine the use of both MMCs [45,46] and economic feedstocks [47–51] as a promising alternative since it has the potential to decrease operation costs once they use economic substrate and save energy from the sterilization step.

### **3. PHA life cycle: from the upstream to final applications**

The combined use of waste feedstocks and MMCs is expected to decrease both investment and fermentation operating costs by simplifying equipment and saving energy (as sterile conditions are not required), as well as reducing the cost of the substrate.

The ability of MMC to convert both wastewater and synthetic VFA mixtures represents a more inexpensive procedure to synthesize the polymer in comparison to pure culture processes and poly-ethylene production [52,53].

Many efforts have been devoted to the integration, on a pilot scale, of PHA production in MMC to wastewater treatment.

As a result of this integration, the essential regional services of waste management are joined with the generation of a bio-based resource. In wastewater and solid waste management, PHA production via MMC represents an opportunity for recovering raw wastewater organic carbon by means of biological treatment, converting traditional waste treatment into an opportunity for residual bio-refineries [54].

However, some feedstock (such as some agro-industrial wastes) cannot be directly converted to PHAs and a preliminary stage is performed to convert the organic matter into appropriate substrates, such as VFA's [38]. This process occurs under anaerobic conditions and soluble organic matter is fermented into organic acids and other fermentation products such as alcohols, hydrogen and CO<sub>2</sub> [43,55].

Since MMCs are microbial consortiums, it is necessary to select PHA-storing microorganisms. This step is accomplished by using the feast and famine (F/F) regime which consists of alternating periods of substrate excess ("feast") and lack of it ("famine"). During the "feast" phase, the culture uptakes ammonia and carbon sources with simultaneous PHA synthesis. After depletion of the external carbon substrate, the intracellular PHA granules serve as carbon and energy sources used for cell growth and maintenance. As a result, the faster microorganisms to store the substrate and reuse it for growth have a greater competitive

advantage. This approach allows the selection of cultures with a high ability to produce PHA during the “feast” phase and to use it to grow during the “famine” phase [56–58]. Consequently, the proposed process for mixed culture PHA production usually comprises three stages: (I) a first acidogenic fermentation stage, (II) a successive culture selection stage (under F/F regime), and (III) a final PHA accumulation stage after which the polymer is extracted from the cells and purified. A complete scheme of integrated PHA production and life cycle is reported in figure 4.

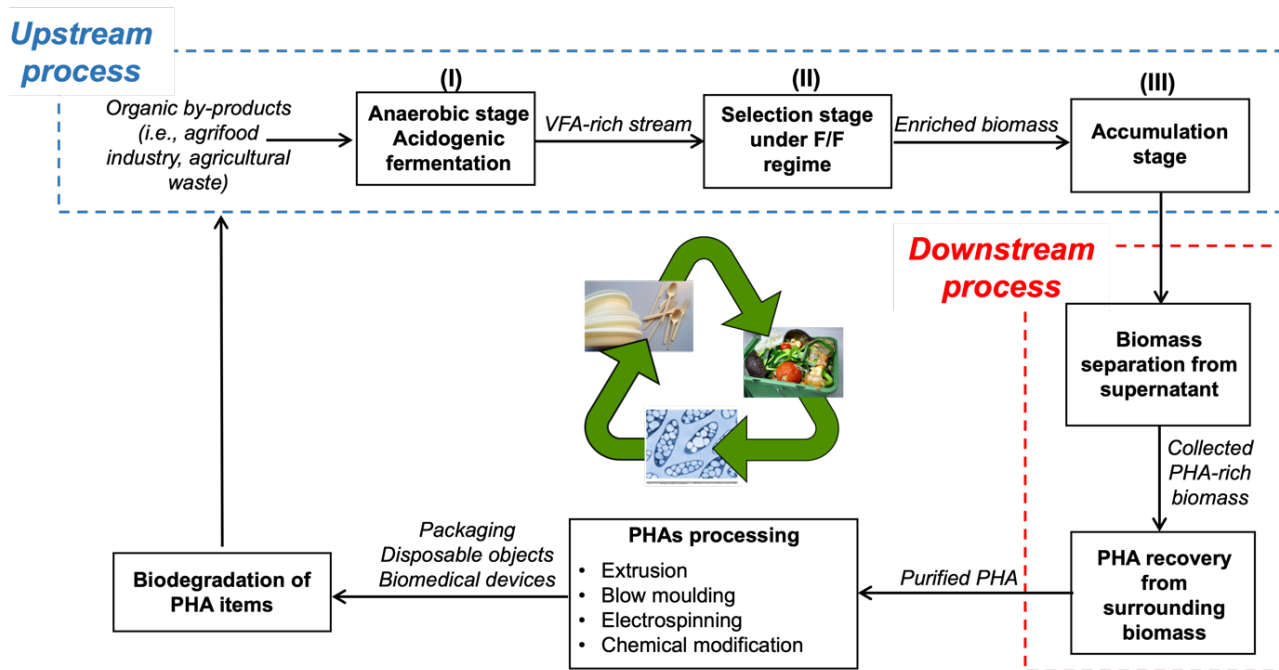


Figure 4 PHA production and life cycle scheme.

As highlighted in Figure 4, stages (I) (II) and (III) described in the above section represent the so-called upstream processing of PHAs. Subsequent steps involving biomass separation, PHA recovery and purification constitute the downstream process. After that, the purified polymer is ready for compounding step, eventual chemical modification and transformation into a consumer product. Over the last decade, PHAs applications have increased a lot in variety and specialisation. Thanks to their excellent barrier properties, the copolymer poly(3-hydroxybutyrate-co-3-hydroxyvalerate) (P(3HB-co-3HV)) is recommended for application in food packaging or plastic beverage bottles, coated paper milk cartons, plastic film moisture barriers in sanitary towels.

PHA latex can also be used to produce water-resistant surfaces to replace cardboard aluminium combination with a biodegradable option. For flexible packaging or thermoformed articles P3HB copolymers with 3-hydroxyhexanoate (3HHx) (P(3HB-co-3HHx) or *mcl*-PHA having a high number of C atoms on side chain are used due to their high elongation at break values (Table 2) [30,59].

Copolymers P(3HB-co-3HHx) and P(3HO), which have better mechanical characteristics and many more elastomers than *scl*-PHAs (table 2) have been studied for scaffold preparation. A *mcl*-PHA polymer scaffolds that can withstand and retake from several structures without damaging other surrounding tissue can be used due to the elastomeric behaviour of many organs in the body [60]

Besides their use as pure materials, PHAs have been also used as a matrix for bioactive agent encapsulation. Some evidence supports PHAs as excellent materials for packaging containing natural antimicrobial systems since PHAs can protect bioactive molecules from the environment while simultaneously providing a barrier for the food and creating a release system for the active compound [61,62]. The possibility of entrapping active molecules into a PHA matrix has been exploited for agricultural purposes. Examples of mulching films containing insecticides have been reported in the literature [63].

Besides the applications in the fields of packaging and agriculture, PHAs gained a lot of interest in the biomedical fields thanks to their bioresorbability. In fact, they are widely used in tissue engineering, drug delivery and release and dressing materials [64–66].

#### 4. PHAs limitation: how to circumvent them?

The possibility of producing them in an integrated biorefinery, the wide range of applications and their biodegradability/bioresorbability make PHAs one of the most promising biomaterials alternative to petroleum-based plastics.

Although the PHA life cycle depicted in Figure 4 appears to be ideal, there are still some critical challenges that need to be addressed, as follows:

1. PHA recovery from surrounding biomass: Although the upstream process has been optimized in the last decades thanks to the adoption of MMCs and renewable low-cost feedstocks, the PHA price is still high (1.18– 6.12 €/kg of PHA vs < 1 €/kg of oil-based polymers such as polyethylene and polypropylene [67]) limiting their competitiveness. Additionally, environmental issues also affect PHA diffusion on a large scale. The economically and environmentally limiting step is the recovery of PHA from surrounding biomass. In fact, most of PHAs are soluble only in harmful chlorinated solvents affecting their sustainability.
2. PHAs processing: The high crystallinity of many PHAs results in high melting points (about 180 °C for P3HB) close to the degradation temperature meaning that processing with common processing techniques (extrusion, moulding) is hard to achieve.
3. PHAs mechanical properties: some intrinsic macromolecular, structural, and morphological features of PHAs negatively affect their mechanical properties. For example, high crystallinity makes PHA items brittle and the slow crystallization rate affects the stability of processed material, changing its properties over time.
4. Chemical modification: The introduction of selected chemical groups on the biopolymer backbone is a common strategy often used in the biomedical field to enhance intrinsic properties or to introduce additional functionalities and features (i.e., to increase hydrophilicity to promote cell proliferation or to graft functional group able to conjugate bioactive molecules to polymer surface to increase

biocompatibility). Unfortunately, chemical modifications were usually carried out in a non-sustainable or non-safe way, using toxic solvents and reagents. PHA nanoparticles (NPs) are widely studied as drug carriers for controlled delivery systems. However, most preparation methods use toxic solvents and surfactants that can interfere with drug release or cell recognition. Therefore, thorough purification of NPs is mandatory before their use.



## **Aim and research plan**

The main purpose of the research described in this thesis is to examine and provide solutions to the aforementioned critical points (section 4) related to PHA extraction, processability, mechanical properties and application in biomedical field. The common thread that has guided all of my research activity is the use of safe, non-toxic, simple, eco-friendly, and cost-sustainable methods, as well as reactants and solvents that align with the virtues of the polymer class employed.

The illustrated research activities have been developed in the framework of interdisciplinary collaborative projects (both national and international) as well as independent ones, all aiming at proposing a valuable starting point to effectively counteract PHAs issues and accelerate the transition toward widespread sustainable materials.

### **Chapter 1: Challenges and advancements in PHA recovery.**

In this first chapter economic and environmental issues related to the extraction process will be discussed. The chapter is divided into two sections, both devoted to the research of an innovative, sustainable and eco-friendly method to recover MMC-produced P(3HB-co-3HV) copolymers from biomass. Part of this work has been conducted in the framework of the URban BIo-waSte-RES URBIS project in the European Horizon2020 (Call CIRC-05-2016) program (Grant Agreement 730349).

### **Chapter 2: Toward a new strategy for sustainable chemical modification of PHAs.**

In the second chapter, a sustainable way to chemically modify PHAs by a new aminolysis procedure, an alternative to the common one based on the use of toxic amines, is proposed and discussed. The copolymer P(3HB-co-3HHx) is used as a model. The feasibility of the proposed approach for the reaction in both heterogeneous (film surface) and homogeneous (polymer solution) conditions is illustrated in two distinct sections. This work has been conducted as an independent project.

### **Chapter 3: Exploring the role of 3HV content on properties and processability of P(3HB-co-3HV).**

In this chapter, the problem of PHA poor processability and non idoneous mechanical properties is faced. In particular, the effect of different 3HV content in P(3HB-co-3HV) copolymer on processability, miscibility with other polymers and of nucleating agent on crystallization rate are analyzed. This work has been conducted in the framework of performed in the framework of the LOOP4PACK project supported by the French National Research Agency (ANR) [Grant Agreement N#ANR-19-CE43-0006] over a six-month research period in the INRAE Centre in Montpellier.

### **Chapter 4: Rapid estimation of Poly(3-hydrpxybutyrate-co-3-hydroxyvalerate) composition by ATR-FTIR**

The possibility of having many P(3HB-co-3HV) samples characterized by a wide range of composition, stimulated the investigation of a new simple and easily accessible method to estimate P(3HB-co-3HV) composition by using Fourier-Transformed Infrared Spectroscopy.

Finally, an appendix reports other research activities carried out in the framework of side projects focused on the characterization of PHAs produced with alternative feedstocks and strategies or designed for application in the bioremediation field.

In addition, I had the opportunity to participate in a research project outside of my main topic during my PhD. This project is briefly described in the appendix.

A second appendix includes a complete list of publications, oral and poster contribution to conferences, attended seminars and courses and tutoring activities.

# CHAPTER 1

## **Challenges and advancements in PHA recovery**

Despite the advances in biomass growth and PHA accumulation achieved using MMCs and fermentable substrates, PHA commercialisation at competitive costs is still a long way off.

The PHA-rich biomass must be separated from the supernatant, which results in the spent fermentation broth, once the biotechnological PHA manufacturing process (cultivation of living cells in bioreactors) is stopped. Sedimentation, flocculation, centrifugation, or, to a lesser extent, filtration procedures are commonly used to achieve this separation.

After the separation stage, appropriate techniques are required to quickly and efficiently recover PHA from the surrounding microbial biomass. All the activities focused on biomass separation and polymer recovery and purification constitute the downstream processing of PHA.

The downstream process is a crucial stage and contributes to the entire PHA production cost. In this scenario, the choice of an appropriate extraction method strongly impacts the economy of the whole process [68]. Furthermore, the downstream process is the major factor affecting the ecological footprint of microbial polyesters [69].

To design efficient and sustainable downstream processes, issues like type, amount and recyclability of extraction solvents or other chemicals, energy input and water requirement [70] shall be considered and weighted in relation to the yield and quality of obtained PHA. The quality of extracted PHA is usually determined by the molecular weight and purity specific to a targeted application. As an example, materials for food contact or pharmaceutical applications require a high level of purity (as an example less than 0.1 %w/w of impurities for pharmaceutical grade materials).

According to this perspective, PHA recovery and purification represent the process bottleneck and the individuation of an optimal extraction method is currently the subject of extensive research. Additionally, considerations of cost-effectiveness further contribute to the complexity of these assessments. In fact, distinct feedstocks and feeding strategies can yield diverse biomasses characterized by different polymer content and cell resistance to

chemicals as well as different PHAs, in terms of molecular weight, structure and copolymer composition, all of which profoundly affect the extraction of the polymer.

Best-established PHA recovery procedures, able to produce outstanding recovery yields and product purity, are based on extraction methods employing hazardous halogenated solvents which are substances that shouldn't be used in a sustainable manufacturing chain. High amounts of solvents are produced during these operations, which are frequently detrimental to the environment and human health. The most used PHA extraction solvent, chloroform, is irritating to mucosal membranes, respiratory system, and eyes and it is supposed to be carcinogenic.

Moreover, cold precipitation is often used to further purify the extracted polymer using non-solvents such as ethanol, acetone or methanol. In this type of procedure, the non-solvent is added to a previously concentrated chloroform PHA solution. At the end of the process, the solvent mix can be recycled by separating the components through distillation or other separating techniques. However, the separation step is energy-demanding and therefore economically disadvantageous.

A solvent-free approach for PHA recovery is the solubilization of non-PHA cellular material (NPCM) that envelops polymer granules. This recovery strategy is usually carried out using oxidant substances, alkaline or acid compounds and surfactants. Among them, oxidation with NaOCl is the most widespread. It is worth noting that NaOCl is a chlorinated compound which therefore entails same environmental issues.

In light of evident safety concerns, for years the research has been increasingly directed towards exploring an alternative approach for both solvent extraction and cellular lysis. Many attempts have also been made to improve the extraction methods currently used.

Dissolution of PHA in an appropriate organic solvent [67] is an attractive procedure widely investigated, as evidenced by the great number of scientific papers, reviews or patents on this topic, mainly dealing with PHAs from pure culture [67,70–74]. Many research studies have looked at the use of green solvents as an alternative to chlorinated hydrocarbons, with low or no toxicity and possibly derived from biochemical conversion, to overcome ecological issues, worker safety restrictions, or strict regulations on solvent traces in

products for high value-added applications like food contact materials or for biomedical applications. [75]. Solvents characterized by low toxicity, including ethers [76,77], esters [75,76,78,79], carbonates [79–82] and ketones [78,83,84], have been identified as appealing alternatives to chlorinated hydrocarbons.

New alternative methods have also been developed using green and/or recyclable substances, including supercritical carbon dioxide (scCO<sub>2</sub>) treatment [85–88], ionic liquids [89,90], enzymes [91] or mechanical separation of PHA granules from biomass.

The combination of parallel or sequential methods has been also proposed to increase the recovery yields and PHA purity without compromising the original polymer features by harsh extraction conditions [92,93]. Mixed NPCM digestion or PHA solubilisation procedures, including treatment with NaOH solution and sodium dodecyl sulfate (SDS), NaClO solution and SDS, NaClO and DMC, have been reported [94–97].

Although promising results were achieved with some of the mentioned alternative extraction methods, a series of factors negatively affect their scalability. For example, scCO<sub>2</sub> is not used as the sole extraction medium because it has a different polarity than the polymer and it is therefore necessary to add a polarity modifier (i.e. chloroform, methanol or toluene) to reach high purity and yields. Similarly, even for the enzymatic and mechanical approaches the use of surfactants or oxidizing treatments is needed to purify and separate the polymer from the biomass. The use of additional chemical reagents implies the need to remove them from the polymer extracted by washing steps. The latter involves the production of waste fluids and therefore both environmental and economic impact due to any wastewater treatment interventions.

However, despite the considerable volume of literature encompassing these subjects, the comparison, evaluation, and selection of the most advantageous methodologies remain complex, challenging, and laborious.

In a recent LCIA study, Saavedra del Oso et al. [98] underlined the potential of integrating PHA recovery in biorefinery scenarios will reduce environmental impacts by up to 50%. The environmental performance of processes can be enhanced by using so-called green solvents such as ethyl acetate, fusel alcohols, ethyl lactate, or dimethyl carbonate. However, the

authors pointed out that to utilize these alternative solvents in large-scale procedures, a higher level of technical maturity in PHA extraction is necessary.

Therefore, because of the appealing possibility to use ethylic esters for the extraction of PHA from biomasses, in the next section of this chapter the possibility to use ethylic esters produced in an integrated biorefinery scenario is investigated. The EEs, in fact, can be synthesized from the fermentation products of the organic fraction of municipal solid waste (OFMSW) and sewage sludge (SS), the same feedstock used to produce PHA by mixed culture microorganisms [99,100]. Moreover, the selected EEs, ethyl acetate (EA), ethyl propionate (EP) and ethyl butyrate (EB), have very low toxicity. EA is also a suggested solvent with butyl acetate, according to all the solvent selection guides, which attribute low health and environmental scores among the whole ester class [101,102]. Nevertheless, few scientific papers deal with the use of EA for the extraction of PHA from single microbial culture and even fewer those related to MMC system.

It was considered useful a systematic analysis of the process which considers the effects of molecular weight of PHA in the biomass and of the extraction conditions on recovery yields, possible polymer fractionation according PHA composition and molecular weight as well as on the properties of the non-extracted polymer remained in the biomass. Moreover, the reported outcomes could shed some light on contradictory results reported in literature.

In the second section, thanks to the possibility of having a relatively high amount of biomass containing P(3HB-*co*-3HV) produced in a full-scale wastewater treatment plant by using MMC and thickened waste active sludge (WAS) as feedstock, a direct comparison of the performance of conventional, uncommon or innovative extraction methods were made. Aliquots of the same biomass were separately subjected to extraction and the polymer recovery yield, purity, molecular weight and thermal properties were evaluated. The conventional extraction procedures involved the solubilization of P(3HB-*co*-3HV) using chloroform and bleaching of NPCM with a NaClO and NaOH water solution. Less common chlorine-free methods included polymer solubilization in ethyl acetate and NPCM

solubilization through  $\text{H}_2\text{O}_2$  oxidation. A new sequential biomass treatment using  $\text{NaOH}$  and  $\text{H}_2\text{O}_2$  was also tested.



# Ethylic esters as green solvents for the extraction of intracellular polyhydroxyalkanoates produced by mixed microbial culture

## ABSTRACT

Taking advantage of the concept of the integrated process of a bio-refinery, in the present section a systematic investigation on the extraction of intracellular poly(3-hydroxybutyrate-co-3-hydroxyvalerate), produced by mixed microbial culture, by using ethylic esters (EEs) is reported. Among the tested EEs, ethyl acetate (EA) resulted the best solvent, dissolving the copolymer at the lowest temperature. By increasing the extraction temperature increase of recovery and a molecular weight reduction was observed. The results highlighted that the extracted polymer purity is always above 90 wt.% and that it is possible to choose the proper extraction condition to maximize the recovery yield at the expense of polymer fractionation and degradation at high temperatures or use milder conditions to maintain the original properties of polymer.

### **Adapted from:**

Alfano, S.; Lorini, L.; Majone, M.; Sciubba, F.; Valentino, F.; Martinelli, A.

*Ethylic Esters as Green Solvents for the Extraction of Intracellular Polyhydroxyalkanoates Produced by Mixed Microbial Culture.*

Polymers 2021, 13, 2789.

<https://doi.org/10.3390/polym13162789>

## 1. Materials and Methods

### 1.1 PHA production

Within the pilot platform of Treviso (northeast Italy, in the context of a full-scale municipal wastewater treatment plant), the PHA was produced from a feedstock composed by a mixture of a) the liquid slurry coming from squeezing of the OFMSW and b) SS from the treatment of urban wastewater. The main process setup (extensively described by Valentino et al., 2019 [37]) comprised of a first anaerobic fermentation reactor (380 L) for PHA-precursors production (volatile fatty acid, VFA), a second aerobic reactor (sequencing batch reactor, SBR; 100 L) for biomass cultivation, and a third fed-batch aerobic reactor (70-90 L) for PHA accumulation within cellular wall (40-50 wt %). Biomass from two different batches (Biomass1 and Biomass2), with PHA content more than 50 % w/w on dry weight, have been selected to perform polymer extraction and characterization. At the end of accumulation, the two biomasses were centrifuged and stabilized by two different procedures: Biomass1 was subjected to thermal treatment at 145 °C for 30 minutes followed by overnight drying at 70 °C; Biomass2 was acidified with H<sub>2</sub>SO<sub>4</sub> down to pH 2.0. Before the extraction, Biomass2 was washed with a 0.3 N NaOH solution up to neutral pH and dried. This step was necessary to avoid polymer acidic hydrolysis by concentrated H<sub>2</sub>SO<sub>4</sub>.

### 1.2 Preliminary dissolution tests

Before the extraction experiments, the solvent properties of selected ethylic esters (EEs), were investigated by using reference PHA samples (R-PHA), obtained from the two dry biomasses by continuous chloroform Soxhlet extraction for 8 h. This procedure brings about a nearly complete extraction of the polymer, which maintains unvaried the MW respect that of PHA inside the cells. The dissolution tests were carried out on R-PHAs by employing ethyl acetate (EA, boiling point 77 °C), ethyl propionate (EP, boiling point 102 °C) and ethyl butyrate (EB, boiling point 126 °C), all purchased from Sigma-Aldrich (Sigma-Aldrich, Milan, Italy). An amount of 100 mg of dried R-PHA was placed in 15 mL thick wall glass pressure vessel with PTFE bushing and Viton O-ring, magnetic stirrer and 4 ml of each ethylic ester. The tube was tightly closed and placed in a silicon-oil bath, preheated at the

desired dissolution temperature ( $T_s$ ), from 100 to 150 °C. It is important to take care of this procedure because high pressure could be reached into the test tube ( $P_{\max} = 7$  atm with EA at 150 °C). The minimum solubilization temperatures ( $T_{s\min}$ ) of R-PHAs were defined as the lowest temperature at which the solution became transparent within 1 h. At the end of the test, each R-PHA sample was vacuum dried at 50-70 °C to a constant weight and the average viscosity molecular weight determined. For sake of comparison, the dissolution tests were carried out also on a commercial P(3HB) homopolymer (Biomer).

### 1.3 Extraction experiments

The extraction capacity of the three EEs was evaluated on Biomass1. About 3 g of biomass and 50 mL of EE were inserted in a stainless-steel high pressure stirred mini reactor (Parr 4560), preheated at 70 °C. Then, the reactor was rapidly closed and heated at the extraction temperature  $T_E$  equal to the minimum solubilization temperature  $T_{s\min}$ , found in the abovementioned preliminary dissolution tests. After 1 h under stirring, the liquid phase was withdrawn from a dip tube endowed with a stainless still mesh to avoid biomass leakage. At room temperature, the polymer precipitated forming a stable physical gel, which was vacuum dried at 50-70 °C. The obtained solid (extracted PHA, E-PHA) was weighted and characterized by composition analysis and molecular weight determination.

Other than  $T_E = 100$  °C, the extraction of PHA from Biomass1 with EA was carried out also at increasing extraction temperatures of 115, 125, 135 and 150 °C. In the experiment carried out at  $T_E=125$  °C, a second extraction on already extracted Biomass1 was performed in the same conditions.

After the recovery of PHA solution in the three EEs, the biomass was vacuum dried and weighted. The residual non-extracted PHA remained in the biomass (NE-PHA) was solubilized in chloroform by Soxhlet extraction.

The PHA weight fraction recovered by EE extraction (recovery yield,  $f_E$ ) was evaluated by the equation (1):

$$f_E = \frac{w_s \times w_p \cdot V_0}{w_b \times f_i \cdot V_r} \times 100 \quad (1)$$

where  $w_s$  and  $p$  are the weight and purity of solid fraction in the withdrawal,  $w_b$  is the weight of the biomass and  $f_i$  the initial content of PHA in biomass,  $V_0$  and  $V_r$  are the added and recovered liquid volume, respectively.  $p$  and  $f_i$  were evaluated by the gas-chromatographic method (GC).

The weight fraction ( $f_{NE}$ ) and the polymer composition (3HB mol %) of non-extracted PHA were quantified by GC. The non-extracted PHA fraction ( $f_{NE}$ ) was calculated by taking into account the amount of polymer in non-withdrawal solvent ( $w_s \times [V_0 - V_r]$ ), according to the equation (2):

$$f_{NE} = \frac{w_r - w_s \times [V_0 - V_r]}{w_b \times f_i \times V_r} \times 100 \quad (2)$$

where  $w_r$  is the weight of non-extracted PHA.

Then, the total recovered PHA is  $f_{TOT} = f_E + f_{NE}$

A scheme of the employed stainless-steel high pressure stirred mini reactor, original dry biomass and dried extracted PHA is reported in Figure 1.1.

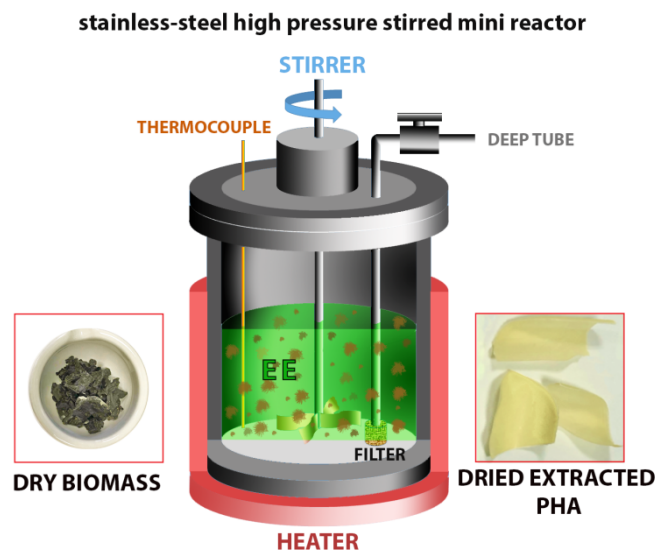


**Figure 1.1** Scheme of the employed stainless-steel high pressure stirred mini reactor, original dry biomass and dried extracted PHA

#### 1.4 Characterization methods

The PHA content in the biomass, the purity and comonomer composition (3HB mol%) of all the extracted samples were evaluated by the gas-chromatographic method according to Braunegg et al. [104]. Approximately 3.5 mg of dried biomass were suspended in 2 mL of

acidified methanol solution (at 3% v/v H<sub>2</sub>SO<sub>4</sub>) containing benzoic acid (at 0.005 %w/v) as internal standard and 1 mL of chloroform in a screw-capped test tube. Then, an acid-catalyzed methanolysis of the PHA occurred and the released methyl esters were quantified by gas-chromatography (GC-FID Perkin Elmer 8410). The relative abundance of 3HB and 3HV comonomers was determined using a commercial P(3HB-co-3HV) copolymer with a 3HV content of 5 wt. % (Sigma–Aldrich, Milan, Italy) as reference standard.

The viscosity average molecular weight ( $M_v$ ) of E-PHA and NE-PHA samples were determined by dilute solution viscosimetry in chloroform at 30 °C. The polymer intrinsic viscosity ( $[\eta]$ ) was related to  $M_v$  by Mark-Houwink equation:

$$[\eta] = k \times M_v^\alpha \quad (3)$$

The employed values of  $k = 7.7 \times 10^{-5}$  and  $\alpha = 0.82$ , suggested by Marchessault et al. [105], has been reported for P(3HB) homopolymer. Nevertheless, for comparison purposes, the  $M_v$  values of P(3HB-co-3HV) copolymer were given hereinafter, considering the nearly equal composition and the low 3HV content of PHAs in both biomasses.

All the extracted samples were characterized by FT-IR spectroscopy in attenuated total reflection mode (ATR) by using a Thermo Nicolet 6700 instrument (Thermo Scientific, MA, USA), equipped with a Golden Gate diamond single reflection device (Specac LTD, England). The spectra were collected co-adding 200 scans at a resolution of 4 cm<sup>-1</sup> in the range 4000–650 cm<sup>-1</sup>.

The extracted samples with EA at 150 °C were analysed by <sup>1</sup>H-NMR spectroscopy by a Bruker AVANCE III spectrometer (Bruker BioSpin, Karlsruhe, Germany), equipped with a Bruker multinuclear z-gradient inverse probe-head operating at the proton frequency of 400.13 MHz. The sample was solubilized in deuterated chloroform and the <sup>1</sup>H spectra were acquired at 298 K employing a spectral width of 15 ppm (6009.13 Hz), 64k data points, 32 scans and a relaxation delay of 6.55 seconds to achieve full relaxation for all the sample protons.

## 2. Results and Discussion

### 2.1 Screening of different EEs as PHA-extraction solvents

The polymer content and composition obtained by GC analyses of the two biomasses as well as the viscosity average molecular weight of PHAs extracted in Soxhlet by chloroform (R-PHA1 from Biomass1 and R-PHA2 from Biomass2), are reported in Table 1.1.

**Table 1.1** Content, composition and viscosity average molecular weight of PHAs in the two biomasses and minimum solubilization temperature ( $T_{Smin}$ ) of R-PHAs and Biomer in the tested EEs

Sample	PHA content in biomass (wt. %)	composition (3HB mol %)	$M_v$ (kg mol <sup>-1</sup> )	$T_{Smin}$ in EA (C°)	$T_{Smin}$ in EP (C°)	$T_{Smin}$ in EB (C°)
Biomass1	56	83	-	-	-	-
Biomass2	62	89	-	-	-	-
R-PHA 1	-	83	139 ± 3	100	115	120
R-PHA 2	-	89	405 ± 5	115	-	-
BIOMER	-	100	390±10	115	-	-

As expected, the chloroform extraction led to a high recovery yield (96 wt. %) and both R-PHAs showed high purity (98 wt. %) and the same composition found by GC analysis of biomasses.

PHA in biomasses are exclusively P(3HB-co-3HV) copolymers with similar chemical composition. The high 3HB monomer content was due to the fermented feedstock composition. The molar fraction of acids containing an odd number of carbon atoms (mainly propionic and valeric, precursors of HV formation) compared to total VFA was quite low and the VFA distribution was strongly oriented to the predominance of acids with even number of C-atoms (mainly acetic and butyric; 0.15-0.17 mol/mol)[103]. This parameter has been already used to characterize VFA distribution in complex mixtures and, in turn, to predict the chemical composition of PHA.

The different  $M_v$  of the two R-PHA samples is likely due to the different stabilization method [106,107]. In fact, it has been previously observed how the thermal treatment, used for the stabilization of Biomass1, led to a molecular weight reduction, due to a partial polymer hydrolysis favoured by high temperature.

At room temperature, EEs do not solubilize the P(3HB-co-3HV) and the complete dissolution occurred at temperature above (EA, EP) or close (EB) to the boiling points of the liquids. In Table 1.1, the minimum solubilization temperature ( $T_{\text{min}}$ ) of R-PHA1 in the tested EEs and R-PHA2 in EA are reported. For sake of comparison,  $T_{\text{min}}$  in EA of the commercial Biomer, a poly(3-hydroxybutyrate) homopolymer (P3HB), was also found. The dissolution tests of R-PHA1 showed that the shorter is the EE acyclic residue the lower is the  $T_{\text{min}}$  and that the EA solubilized R-PHA2 and Biomer at higher temperature than R-PHA1, presumably because of the higher molecular weight of these polymers.

According to the preliminary dissolution tests, the PHA extraction from Biomass1 was carried out initially with the three EEs at  $T_E$  equal to  $T_{\text{min}}$ .

After 1 h, at the end of the extraction, the liquid phase was withdrawn from high pressure stirred mini reactor by the dip tube at  $T=T_E$  to avoid physical gel formation and to favor the separation of the solution from the solid biomass. In this way, about 92-95 vol.% of the initial solvent volume was recovered ( $V_r$  in equation 1 and 2). Then, weight, purity, composition and molecular weight of dry extracted PHA fraction solubilized in EEs (E-PHA1) were measured. Moreover, the fraction ( $f_{NE}$ ) and composition of the non-extracted polymer (NE-PHA1) from the biomass were determined by GC. The results of the analyses are displayed in Table 1.2.

**Table 1.2** Characterization of the extracted (E-PHA1) and of the non-extracted PHA (NE-PHA1) from Biomass1 with the three EEs.

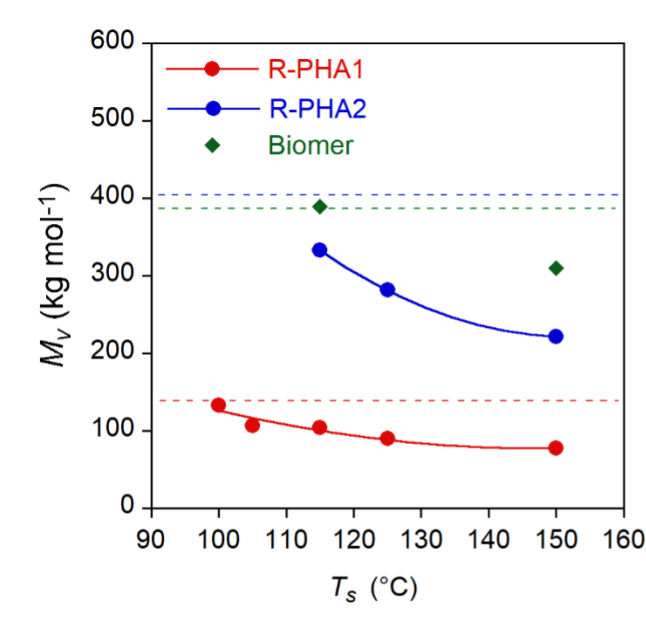
solvent	E-PHA1				NE-PHA1	
	$f_E$ (wt. %)	composition (3HB mol %)	purity (wt %)	$M_v$ (kg mol <sup>-1</sup> )	$f_{NE}$ (wt. %)	composition (3HB mol %)
EA at 100 °C	54	72	97	72	44	89
EP at 115 °C	45	74	100	38	52	88
EB at 120 °C	32	57	84	29	62	90

Table 1.2 highlights that the polymer solubilized from the biomass with the different EEs, after solvent evaporation, shows a high purity and an increase of 3HV comonomeric unit content respect to those of R-PHA1. Accordingly, in non-extracted NE-PHA, the 3HB mol % value increased. Moreover, it can be observed that all the E-PHA1s, extracted with the

three EEs, are characterized by  $M_v$  lower than that of the reference sample. Since the extraction by EA gave the best recovery yield and the lowest  $M_v$  reduction, further investigation was carried out with this solvent.

## 2.2 Evaluation of PHA extraction performances with ethyl acetate (EA)

The  $M_v$  and composition variation of extracted polymers reported in Table 1.2 could occur because of a selective solubilization of polymer according to its molecular weight and composition and/or of a degradative process taking place at high temperatures. Thus, the effect of the temperature on polymer molecular weight was investigated by dissolving the reference samples (R-PHA1 and R-PHA2) in EA also at  $105\text{ }^\circ\text{C} < T_s < 150\text{ }^\circ\text{C}$ . After 1 h, the polymer samples were recovered and dried and the molecular weights were determined. In Figure 1.2, the  $M_v$  variation as a function of solubilization temperature  $T_s$  is reported. For sake of comparison, the experiment was performed also on Biomer at  $115\text{ }^\circ\text{C}$  and  $150\text{ }^\circ\text{C}$ .



**Figure 1.2** PHA1, R-PHA2 and Biomer viscosimetry average molecular weight ( $M_v$ ) variation as a function of the dissolution temperature in EA. Dotted lines indicate the  $M_v$  values of R-PHAs and of pristine Biomer. Solids curves are guide for eyes.

Figure 1.2 shows that the R-PHA dissolution at increasing temperatures brought about a progressive molecular weight reduction of up to 44 % at  $150\text{ }^\circ\text{C}$  for both polymers. The homopolymer Biomer seems to be more stable towards degradation phenomena showing a  $M_v$  decrease null at  $115\text{ }^\circ\text{C}$  and of 20 % at  $150\text{ }^\circ\text{C}$ . Therefore, it could be inferred that the polymer in solution undergoes a progressive degradation as the temperature increases. This



phenomenon was further investigated to assess the effect of the temperature on the EA extraction of P(3HB-co-3HV) from biomass. Further experiments were carried out by extracting P(3HB-co-3HV) from Biomass1 with EA at the same temperatures of dissolution reported in Figure 1.3. As in the experiments conducted at  $T_E$  equal to  $T_s$ , the E-PHA1 and NE-PHA1 fractions ( $f_{NE}$  and  $f_E$ , respectively) as well as their compositions and molecular weights were analyzed. The results are reported in Figure 1.3, where the molecular weight of R-PHA1 obtained in the dissolution experiments, already reported in Figure 1.2, is displayed for comparison. The results at  $T_E=77$  °C are referred to the E-PHA1 extracted in Soxhlet with EA.

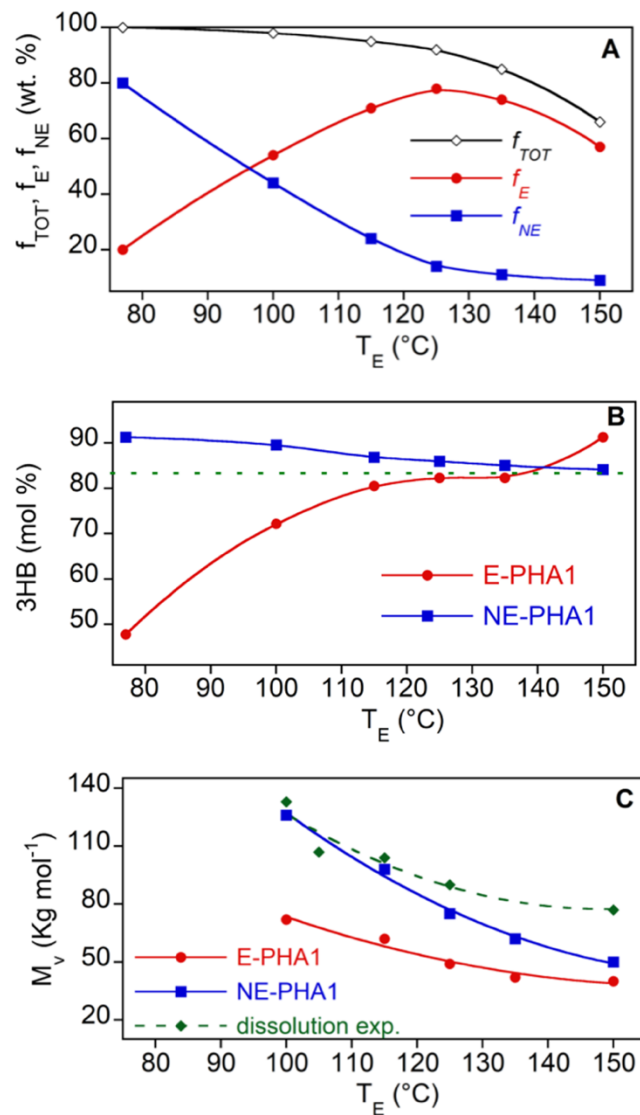


**Figure 1.3** Total ( $f_{TOT}$ ), extracted ( $f_E$ ) and non-extracted ( $f_{NE}$ ) P(3HB-co-3HV) fractions (a), composition (b) and average viscosimetry molecular weight (c) of E-PHA1 and NE-PHA1 as a function of extraction temperature  $T_E$  with EA. The dotted line in (d) is the composition of R-PHA. The green diamond marks in (c) are the molecular weight of R-PHA1 after the dissolution experiments already reported in figure 1. 2. All the lines are guides for the eyes.

Figure 1.3a shows that the P(3HB-*co*-3HV) extracted fraction ( $f_E$ ) increased by increasing temperature up to 125 °C. The decrease at higher temperature did not reflect the expected increase of the not extracted polymer fraction ( $f_{NE}$ ) remained in the biomass, leading to a total recovery  $f_{TOT}$  below 100 wt.%. Except a small amount of sample lost in the extraction and recovery procedures, this could be attributed to the formation at the highest temperatures of volatile degradation products, as shown later. On the other hand, the purity of the extracted and dried samples was always high, between 90 and 97 wt.% (not reported), also without further step of polymer precipitation with the use of an anti-solvent. Figure 1.3c shows that the increase of temperature reduced the preferred solubilization of the 3HV rich polymer fraction up to 125-130 °C, where the extracted P(3HB-*co*-3HV) has a composition similar to that of pristine polymer in biomass. Figure 1.3c highlights that the P(3HB-*co*-3HV) fraction solubilized in EA shows a lower  $M_v$  than that remained in the biomass. This let's infer a preferred degradation of the polymer in solution or a preferred solubilization of shorter chains. Moreover, at  $T_E > 115$  °C the  $M_v$  of both E-PHA1 and NE-PHA1 decreases at values lower than that of R-PHA1, heated at the same temperature (green diamond marks), evidencing an active role of the biomass on the reduction of molecular weight. This evidence could be related to the finding of Kopinke et al. [108], that, in a study on P(3HB) kept at a temperature above the polymer melting point, found a decrease of the polymer thermal stability in the presence of crude biomass. More specifically, in thermal degradation investigation on P(3HB-*co*-3HV), Xiang et al. [109] have suggested that calcium ions traces remained in the copolymer may accelerate the chain scission reaction. In fact, as shown later, the reported chain scission reaction products occurring above the melting point are the same to that observed for the polymer in EA solution at high temperature.

Ultimately, the results of P(3HB-*co*-3HV) extraction from biomass by using EA showed that the recovery yield  $f_E$  increases with temperature up to 125-135°C, but at the expense of a drastic reduction of the polymer molecular weight.

A second extraction for 1 h further at 125 °C of the already extracted biomass brought about a P(3HB-*co*-3HV) recovery of about 7 wt.%. It nearly corresponds to the polymer fraction

solubilized in EA but not withdrawn in the first experiment. Therefore, it can be concluded that longer extraction experiments did not lead to significantly  $f_E$  increase.

The extraction experiment with EA at  $T_{smin}=115$  °C was repeated by employing Biomass2. For sake of comparison, the results of the analyses on the extracted and non-extracted polymer fractions were reported in Table 1.3 together with those obtained from Biomass1 at  $T_E=T_{smin}$  (100 °C) and at  $T_E=115$  °C.

**Table 1.3** Summary of recovered fractions ( $f_{TOT}$ ,  $f_E$ ,  $f_{NE}$ ), chemical composition and molecular weight of extracted and non-extracted PHA from Biomass1 and Biomass2 with EA.

Sample	recovered fractions (wt %)			composition (3HB mol %)			$M_v$ (kg mol <sup>-1</sup> )			
	$f_{TOT}$	$f_E$	$f_{NE}$	R-PHA	E-PHA	NE-PHA	R-PHA	R-PHA $T_E=T_s$	E-PHA	NE-PHA
Biomass1 $T_E=100$ °C	98	54	44	83	69	88	139	133	72	126
Biomass1 $T_E=115$ °C	94	71	23	83	78	85	139	104	62	98
Biomass2 $T_E=115$ °C	92	66	25	89	84	92	405	333	236	358

As for Biomass1, the extraction from Biomass2 brought about the preferential solubilization of polymer fractions with 3HB content and  $M_v$  lower than those of the reference sample. Moreover, an overall reduction of P(3HB-*co*-3HV)  $M_v$  took place in all the experiments.

A slightly higher solubility of 3HV-rich P(3HB-*co*-3HV) and a decrease of  $M_v$  of the extracted P(3HB-*co*-3HV) has been observed also by Samorì et al. in extraction experiments carried out by dimethyl carbonate (DMC) [110]. Moreover, it can be observed that at  $T_E=115$  °C,  $f_E$  is lower the higher is the molecular weight of the pristine polymer in the biomass.

To the best knowledge of authors, the EA or others linear esters as P(3HB-*co*-3HV) extraction solvents are poorly reported in the literature and no examples are available on EEs use as solvent for the extraction of P(3HB-*co*-3HV) derived from MMC. As far as the P(3HB-*co*-3HV) solubility in EA, Terada and Marchessault [111], by a semi-empirical approach based on solubility parameters, have found that EA could solubilize amorphous P(3HB) but not the polymer in solvent-inaccessible crystalline regions. In general, it was observed that short-chain length PHAs, such as P(3HB) homopolymer and P3HB-*co*-3HV copolymers,

show lower solubility in non-halogenated hydrocarbon than *mcl*-PHA. In fact, EA has been successfully used as solvent for the extraction from biomass of poly(3-hydroxybutyrate-*co*-3-hydroxyhexanoate) (P3HB-*co*-3HHx) containing high levels of HHx (>15 mol %), giving a recovery yield of 99% at 100 °C [78]. More in detail, a comparison between EA and butyl acetate, both applied for extraction from *Ralstonia eutropha* pure cells at 76 wt% of PHA content, indicated EA as the best performing for the recovery yield and that both were excellent in the final PHA purity. The same study indicated the necessity to perform the extraction on dried biomass, since the presence of water had a double effect of ester hydrolysis and the reduction of the solvating power. The same extraction by EA of P(3HB-*co*-3HHx) obtained from *Aeromonas hydrophila* 4AK4 has been also employed in industrial scale production [112]. Conversely, Samorì et al. [79] have found a very low recovery (5 wt %) in the extraction of P3HB with ethyl acetate at 80°C. Similarly, the soxhlet extraction of P(3HB) with EA has been reported to give a low recovery yield of 29 wt. % [113]. However, unexpected high solubility of high molecular weight P3HB ( $1 \times 10^6$  g mol<sup>-1</sup>) in EA at temperatures below the boiling point has been found by Aramvash et al. [114], who extracted the polymer from wet biomass with surprising high yields. Also, Gahlawat and Kumar Soni [49] found a good recovery yield in the extraction of P(3HB-*co*-3HV) at high 3HV content (24.6% mol/mol) with EA, on a pure single strain (*Cupriavidus necator* DSM 545). This study reported a recovery yield of 96 %, and a purity of 93 % by using EA at 100 °C. They also observed that the extraction brought about a reduction of the pristine molecular weight of PHA in the biomass, from 150.5 to 125 kg mol<sup>-1</sup>.

However, the different results reported in literature could depend on different aspects such as the P(3HB-*co*-3HV) composition and the culture type. With specific reference to the latter, it has been generally observed that P(3HB-*co*-3HV) extraction from MMCs is more challenging in comparison to single strain cultures [67].

A possible extraction of P(3HB-*co*-3HV) at temperature above the boiling point with non-solvent or poor-solvent at room temperature, among which EEs are included, has been reported in patents but without indication on yields and possible effects on composition, chemical or physical-chemical properties of the extracted polymer [116,117].

The P(3HB-co-3HV) samples extracted from Biomass1 and Biomass2 with EA at  $T_{smin}$  were subjected to thermal characterization and compared to reference samples extracted in chloroform. TGA and DSC results are reported in Table 1.4. In the case of Biomass1 as well as Biomass2, samples extracted in EA show a decrease in  $T_d^{10\%}$  and  $T_g$  respect to those extracted in  $CHCl_3$ . This could be due to the presence of small amounts of impurities which could catalyze thermal degradation and act as a plasticizer.

**Table 1.4** TGA and DSC results of samples extracted in EA at  $T_{smin}$

Sample		$T_d^{10\%}$ (°C)	$T_d^{max}$ (°C)	%wt	$T_g$ (°C)	$T_{cc}$ (°C)	$\Delta H_{cc}$ (J g <sup>-1</sup> )	$T_m$ (°C)	$\Delta H_m$ (J g <sup>-1</sup> )
Biomass1	$CHCl_3$	265	291	100	-6	-	-	169	-
	EA	245	280	92	-10	-	-	165	37
Biomass2	$CHCl_3$	248	280	90	-5	43	58	161	53
	EA	224	282	90	-8	45	60	161	45

### 2.3 FT-IR and 1H-NMR analysis

In order to investigate the cause of the molecular weight reduction of E-PHA, mainly occurring at the higher extraction temperatures, the FT-IR spectra of the extracted samples were compared to those of relevant R-PHAs. In Figure 1.4, the spectra of R-PHA1 and E-PHA1 extracted at 100 °C as well as 150 °C are reported as an example.

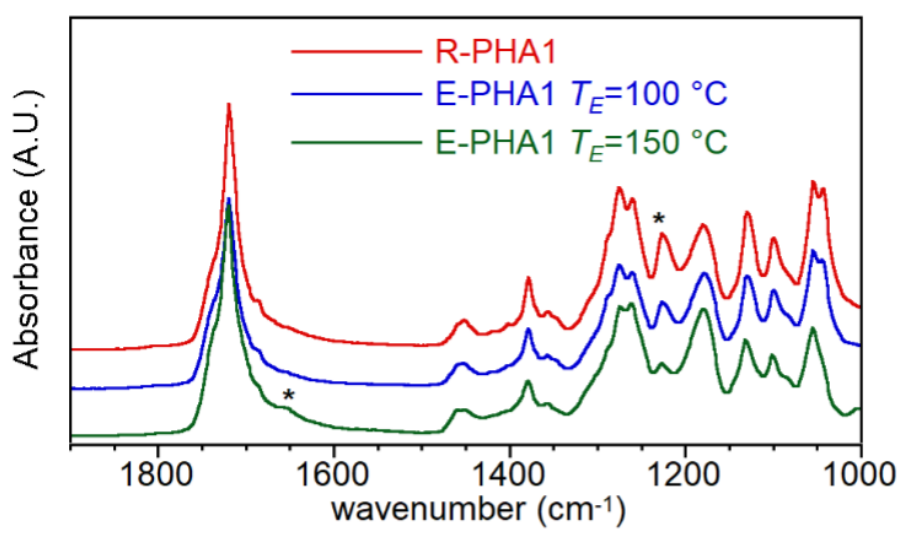


**Figure 1.4** FTIR spectra of R-PHA1 and E-PHA1 extracted with EA at 100 °C and 150 °C.

No marked differences can be observed comparing the spectra of R-PHA1 and E-PHA1 extracted at 100 °C, which showed the expected bands of P(3HB-co-3HV) co-polymer, where the strong band at 1223 cm<sup>-1</sup>, due to C-O-C stretching regular chain conformation, is indicative of high crystallinity. On the other hand, the sample extracted at 150 °C showed a clear hump at 1660 cm<sup>-1</sup>, which can be attributed to a C=C stretching, reported as possible degradation product located at one terminal of the polymer chain [118], and a drastic decrease of the band at 1223 cm<sup>-1</sup>, which was a sign of the predominant amorphous feature of the polymer.

Then, a further study on the degradation process and the macromolecule scission mechanism was carried out by analyzing the sample extracted at 150 °C by <sup>1</sup>H-NMR spectroscopy. The spectrum and the assignments of the signals are reported in Figure 1.5.

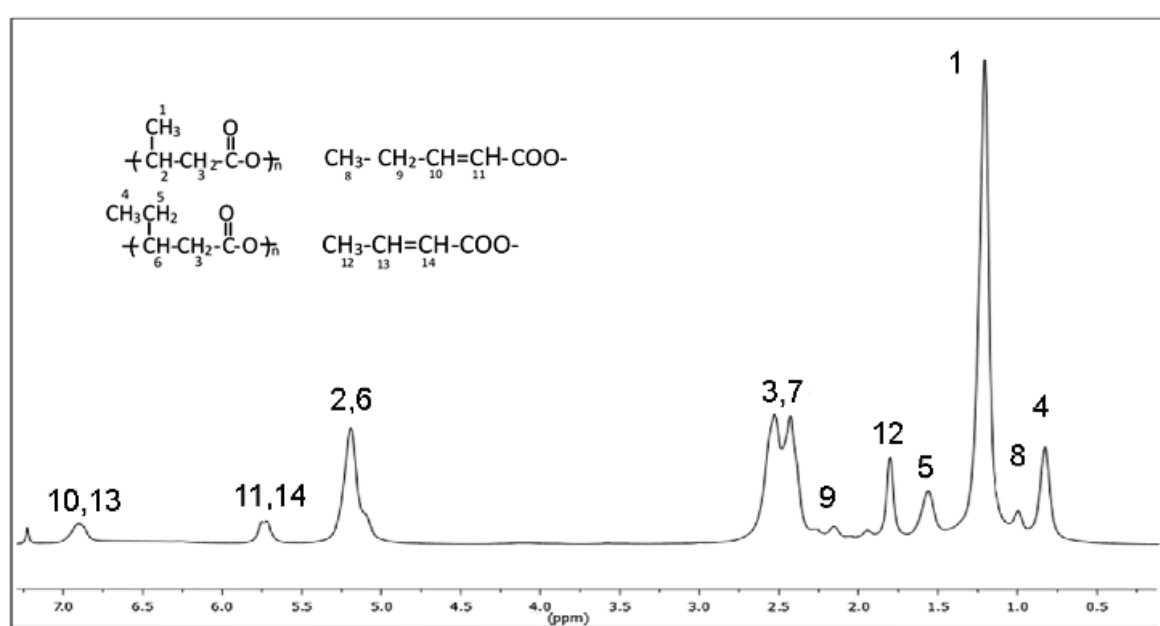


**Figure 1.5** <sup>1</sup>H-NMR of PHA extracted at 150 °C for 1 h and assignments of the peaks.

Besides the typical features of the copolymer P(3HB-co-3HV), the spectrum showed new signals assigned to unsaturated crotonate terminal groups. They were due to the random chain scission occurring through a  $\beta$ -elimination and  $\alpha$ -deprotonation mechanism, according to reported studies on thermal degradation of PHA above the melting temperature [109,119]. Then, the decrease of total polymer recovery (E-PHA1 plus NE-PHA1) recorded at temperatures higher than 125 °C (Figure 4 A) can be attributed to the scission of terminal repeating units which produced volatile low molecular weight product.

The absence of peaks of acetate or ethoxy protons lets to exclude that molecular weight reduction was caused by possible transesterification between EA and P(3HB-co-3HV) favored by high temperature. The absence of the C=C stretching absorption in the sample extracted at  $T_E < 130$  °C was due to the low concentration of terminal crotonic groups because of the higher polymer molecular weight. However, it can be presumed that the chain scission follows the same reaction mechanism also at  $T_E < 150$  °C.

### 3. Conclusions

The present study showed that the extraction of P(3HB-co-3HV) copolymers from the biomass by the selected three ethylic esters brings about polymer with high purity and that the extracted polymer composition, recovery yield and molecular weight depend on the extraction conditions as well as on the MW of pristine polymer in the biomass. The preliminary dissolution tests carried out on reference P(3HB-co-3HV), extracted from biomass with chloroform, showed that the ethyl acetate is the best solvent because it dissolves the copolymer at temperature lower than ethyl propionate and ethyl butyrate. Increasing the temperature from 100 °C to 150 °C, the P(3HB-co-3HV) dissolved in ethyl acetate underwent a progressive reduction of its molecular weight.

The results of the extraction of P(3HB-co-3HV) from biomasses showed that the higher was the molecular weight of polymer in the biomass the lower was the recovery yield. At the minimum dissolution temperature, ethyl acetate gave a recovery yield higher than the other ethylic esters, that it extracts preferentially the copolymer fraction richer in 3HV comonomer and with the lower molecular weight. Increasing the extraction temperature from 100 °C to 130 °C, the recovery yield increased from about 50 wt.% to 80 wt.% and the composition of the extracted polymer approached that of the reference sample. Pushing the extraction temperature up to 150 °C a progressive reduction of molecular weight of extracted polymer and of the polymer fraction remained into the biomass occurred.

The purity of the samples extracted with ethyl acetate was always very high, between 90 and 97 wt.%, without the need of further purification by anti-solvent precipitation.

FTIR and <sup>1</sup>H-NMR analyses, carried out on a P(3HB-co-3HV) sample extracted by the harshest condition (150 °C) showed that the chain scission occurred with the formation of

crotonic groups at the polymer ends, through the same mechanism of the P(3HB-*co*-3HV) thermal decomposition above its melting point.

In conclusion, the use of ethylic esters of VFA could be an attractive method to extract P(3HB-*co*-3HV) when the use of safe and non-toxic solvents is mandatory, particularly in the case their synthesis is included in the virtuous cycle of biorefinery. Moreover, the results highlighted that it is possible to choose the proper extraction condition to maximize the recovery yield at the expense of polymer fractionation and degradation at high temperatures or use mild conditions to maintain the original properties of polymer in the biomass.



# Chlorine-free extractions of mixed-culture polyhydroxyalkanoates produced from fermented sewage sludge at pilot scale

## ABSTRACT

In this section, various conventional and innovative methods for the recovery of poly-3hydroxybutyrate-co-3hydroxyvalerate (P(3HB-co-3HV)) produced from mixed microbial cultures (MMC) were investigated. Specifically, sustainable methods involving chlorine-free treatments using NaOH and/or H<sub>2</sub>O<sub>2</sub>, as well as polymer solubilization in non-toxic ethyl acetate, were analyzed. To evaluate the effects of the extraction procedures, the polymer purity, recovery yield, viscosity, molecular weight and thermal properties were compared with those of P(3HB-co-3HV) extracted from the same biomass using chloroform solubilization (used as a benchmark) and obtained from non-polymer biomass oxidation with sodium hypochlorite (NaClO), reported previously, as well as with results from selected existing literature.

## **Adapted from:**

Salvatori, G.; Alfano, S.; Martinelli, A.; Gottardo, M.; Villano, M.; Ferreira, B.S.; Valentino, F.; Lorini, L.

*Chlorine-free Extractions of Mixed-Culture Polyhydroxyalkanoates Produced from Fermented Sewage Sludge at Pilot Scale*

Industrial and Engineering Chemistry Research, 2023.

<https://doi.org/10.1021/acs.iecr.3c02684>

## 1 Materials and methods

### 1.1 *P(3HB-co-3HV) production*

P(3HB-co-3HV) was produced in a full-scale wastewater treatment plant (WWTP), located in Treviso (northeast Italy), by using thickened waste active sludge (WAS) as feedstock. The PHA-rich biomass production (described in previous works [120,121]) was obtained through a three stage process consisting in: *i*) a first anaerobic fermentation in a 380 L reactor for the production of volatile fatty acids (VFA), used as feedstock; *ii*) a biomass selection into PHA-accumulating consortium (enriched-MMC) in a second 100 L aerobic sequencing batch reactor (SBR) and *iii*) a PHA accumulation in a third 70-90 L fed-batch aerobic reactor. At the end of the accumulation stage, the biomass was stabilized with sulfuric acid (pH 2), in order to preserve the PHA content and properties [122], centrifuged, and stored at 4 °C until the downstream processing. The original biomass contained 62 wt.% of P(3HB-co-3HV) with respect of total dry solids, consisting in a P(3HB-co-3HV) copolymer with a 3HV content of 12.9 wt%[120].

### 1.2 *P(3HB-co-3HV) extraction*

Six different extraction experiments on aliquots of the same PHA-rich biomass were compared.

The results of the conventional extraction procedures, namely chloroform extraction in Soxhlet and NaClO oxidation, were obtained from previous papers on the same biomass [120]. These results are herein considered as reference of consolidated extraction methods.

#### 1.2.1 *Alkaline and oxidative chlorine-free treatments*

The wet acidified biomass (1.5 g with about 80 wt% of water content) was subjected to chemical digestion with NaOH or oxidative treatment with hydrogen peroxide. The stabilized biomass was suspended in a 0.2 M NaOH solution or in a H<sub>2</sub>O<sub>2</sub> (1.5 % w/v) solution. The suspensions were kept under magnetic stirring for 6 hours and 4 hours, respectively. Then, the insoluble fraction was separated by centrifugation (Multispeed centrifuge PK 131, ALC) at 8500 rpm for 15 min, washed 3 times with distilled water and, finally, dried in oven at 60 °C. Additionally, a coupled treatment was conducted on 1.5 g

and 200 g of wet biomass, by applying the chemical digestion treatment with NaOH for 4 hours, followed by centrifugation and 1 washing step. Then, oxidation with H<sub>2</sub>O<sub>2</sub>, was carried out for 1 hour on the thickened biomass. At the end of the coupled procedure, the same steps of centrifugation, washing and drying were used.

### 1.2.2 Ethyl acetate extraction

Ethyl acetate (EA) does not solubilize P(3HB-co-3HV) at room temperature and, hence, a dissolution temperature above the EA boiling point (77 °C) is used at pressure above 1 atm, as reported in a previous paper [123]. Briefly, the P(3HB-co-3HV) solubilization was carried out at 115 °C and at a pressure of about 300 KPa (3 atm). An amount of 1.5 mg of dry biomass, roughly grinded in a mortar, was placed in a 15 mL thick wall glass pressure vessel with PTFE bushing and Viton O-ring (Precision Labware), with magnetic stirrer and 4 mL of EA. The tube was tightly closed and placed in a silicon-oil bath preheated at 115 °C for 2 h. Then, the system was cooled and the physical gel, formed from solution at room temperature, was separated from the biomass and dried at 60 °C.

### 1.3 *P(3HB-co-3HV) characterization*

Extracted P(3HB-co-3HV) samples have been characterized according to procedures described in section 2.4 of the previous section.

The recovery yield, defined as the ratio between the weight of extracted polymer ( $w_e \times p$ ) and the weight of P(3HB-co-3HV) initially contained into the dry biomass ( $w_b \times f_i$ ) before the extraction procedure, was calculated according to the equation (1):

$$recovery\ yield = \frac{w_e \times p}{w_b \times f_i} \times 100 \quad (1)$$

where  $w_e$  and  $p$  are the weight and purity of extracted polymer,  $w_b$  is the weight of the biomass and  $f_i$  the initial content of P(3HB-co-3HV) in biomass. Both  $p$  and  $f_i$  were evaluated by GC analysis.

## 2 Results and discussions

### 2.1 *P(3HB-co-3HV) extraction and recovery*

In this study, the biomass containing P(3HB-co-3HV) was produced at a pilot scale by MMC and WAS as substrate. The detailed production process has been widely discussed in a recent work by Lorini et al. [120].

Table 1.5 summarizes the results of the different performed extraction experiments together with those described in other studies[120,123–128], in which conditions similar to those used in the present study were employed. All the extraction results, reported in the present or previous research, in which WAS was used as a carbon source, are referred to the same biomass [120].

The extraction methods based on the digestion of NPCM by hydrolysis or oxidation have the advantage of operating on wet biomass and, therefore, of avoiding the neutralization phase when the biomass has been stabilized with sulfuric acid. Conversely, extraction by solubilization of the polymer in water-immiscible solvents requires the neutralization of the biomass before drying to prevent P(3HB-co-3HV) hydrolysis.

Although different conditions (temperature and time) are reported in literature, the results of the conventional extractions by chloroform solubilization and NaClO oxidation usually show a high purity and recovery yield (Table 1.5). Similar results have been obtained from the biomass used in this research. Differently, the extraction carried out by using EA, a green solvent, at a temperature above the boiling point and, hence, at high pressure, brought about low recovery yield and, mainly, a polymer characterized by a very different composition with respect to the P(3HB-co-3HV) in the biomass before extraction. These findings, already investigated in a previous paper [123], are due to the preferential solubilisation of polymer fraction with higher 3HV content.

Different treatment time and temperature were also used in the extraction carried out by oxidating (H<sub>2</sub>O<sub>2</sub>, NaClO) or hydrolysing (NaOH) agents (Table 1.5). In this research, a relatively short time and room temperature were investigated to favour a possible extraction cost reduction and process scaling-up. The results show that NaOH (6 h) and H<sub>2</sub>O<sub>2</sub> (4 h) treatments brought about good (85 wt%) and very good (100 wt%) recovery yields,

respectively, and an unchanged composition of the extracted polymers, but quite low purities (79 wt% and 77 wt%, respectively). Therefore, the effect of a sequential extraction by the two methods was evaluated. The wet and not neutralized biomass was digested with NaOH solution for 4 hours followed by oxidation with H<sub>2</sub>O<sub>2</sub> for 1 hour (total 5 h). A clear increase of extracted P(3HB-co-3HV) purity was found although a reduction of the recovery yield (70 wt%) occurred. It was presumably due to a high number of washing cycles, after the first treatment with NaOH and after the oxidation with H<sub>2</sub>O<sub>2</sub>, before the final recovery of the polymer.

**Table 1.5** properties and parameters of extraction methods used to P(3HB-co-3HV) recovery.

Extraction agent	time (h)	T (°C)	P(3HB-co-3HV) purity (wt.%)	Recovery yield (wt.%)	3HV (wt.%)	Mv (kDa)	References	PHA-storing microorganism	Carbon sources
CHCl <sub>3</sub>	10	70	100.9 ± 1.3	91.5	14.3 ± 0.1	405	[120]	MMC	WAS
	24	70	92.9 ± 6.1	80.5 ± 5.3	19.2 ± 0.1	-	[124]	MMC	OFMSW-WAS mixture
	48	80	95.1 ± 7.3	-	31.2	-	[125]	MMC	fermented fruit waste
NaClO	5	25	99.8 ± 0.41	98.3	13.5 ± 0.1	396	[120]	MMC	WAS
	3	85	>80	50	-	-	[126]	MMC	synthetic effluent
	24	25	98 ± 5	100 ± 5	11 ± 0.3	-	[127]	MMC	synthetic mixture of VFA
	3.4	30	99.4 ± 4.2	-	30.9	-	[125]	MMC	fermented fruit waste
NaOH	6	25	79.4 ± 0.1	85.1	13.5 ± 0.2	461	This study	MMC	WAS
	4.8	30	56.8 ± 0.8	-	18.3	-	[125]	MMC	fermented fruit waste
	24	25	56 ± 5	80 ± 6	13 ± 0.7	-	[127]	MMC	synthetic mixture of VFA
H <sub>2</sub> O <sub>2</sub>	4	25	77.4 ± 2.5	110.5	13.3 ± 0.5	436	This study	MMC	WAS
	10	-	99.5	-	-	-	[128]	<i>C. necator</i>	-
NaOH + H <sub>2</sub> O <sub>2</sub>	5	25	92.3 ± 0.5	69.5	12.9 ± 0.2	571	This study	MMC	WAS
EA	1	115	86.6 ± 0.7	64.5	17.8	358	This study	MMC	WAS
	1	115	90 - 97	66 - 71	16 - 28	62-236	[123]	MMC	OFMSW-WAS mixture

## 2.2 Viscosity average molecular weight ( $M_v$ )

Diluted  $\text{CHCl}_3$  solution viscosity measurements of the extracted samples were conducted to evaluate the correlation between the extraction methods and the polymer molecular weight (viscosity average molecular weight,  $M_v$ ). The obtained results are reported in Table 1.5. It can be observed that the extraction method based on polymer solubilization with EA resulted in the lowest  $M_v$ . These result, together with the polymer composition data (Table 1.5), suggests that, under the adopted experimental conditions, a partial solubilization of P(3HB-co-3HV) in the biomass occurred as a function of composition and molecular weight reduction occurred. Indeed, it has been reported that the 3HV-rich polymer fractions showed higher solubility in EA and that the extraction at high temperature brought about partial degradation of the polymer [123]. For this reason, a longer time was not investigated. However, polymer solubilisation in EA resulted in high sample purity.

Differently, oxidizing ( $\text{NaClO}$ ,  $\text{H}_2\text{O}_2$ ) or hydrolysing ( $\text{NaOH}$ ) agents are cellular digesters, acting by selective solubilization of NPCM in water and releasing of P(3HB-co-3HV) (insoluble in water). Therefore, by operating in controlled and mild conditions to avoid possible P(3HB-co-3HV) degradation, the characteristics of the polymer can be preserved in terms of molecular weight and composition. As a result, the  $M_v$  obtained by dissolution of biomass were the highest and are within the range of target Mw for polymer thermal processing.

## 2.3 Thermal analysis

The P(3HB-co-3HV) samples extracted in the present research and those obtained in the previous study (i.e.  $\text{NaClO}$  and  $\text{CHCl}_3$  extraction) [54] on the same biomass, were subjected to thermal characterization by thermogravimetric analysis (TGA) and differential scanning calorimetry (DSC). Figure 1.6 displays the TGA curves of the extracted polymers.

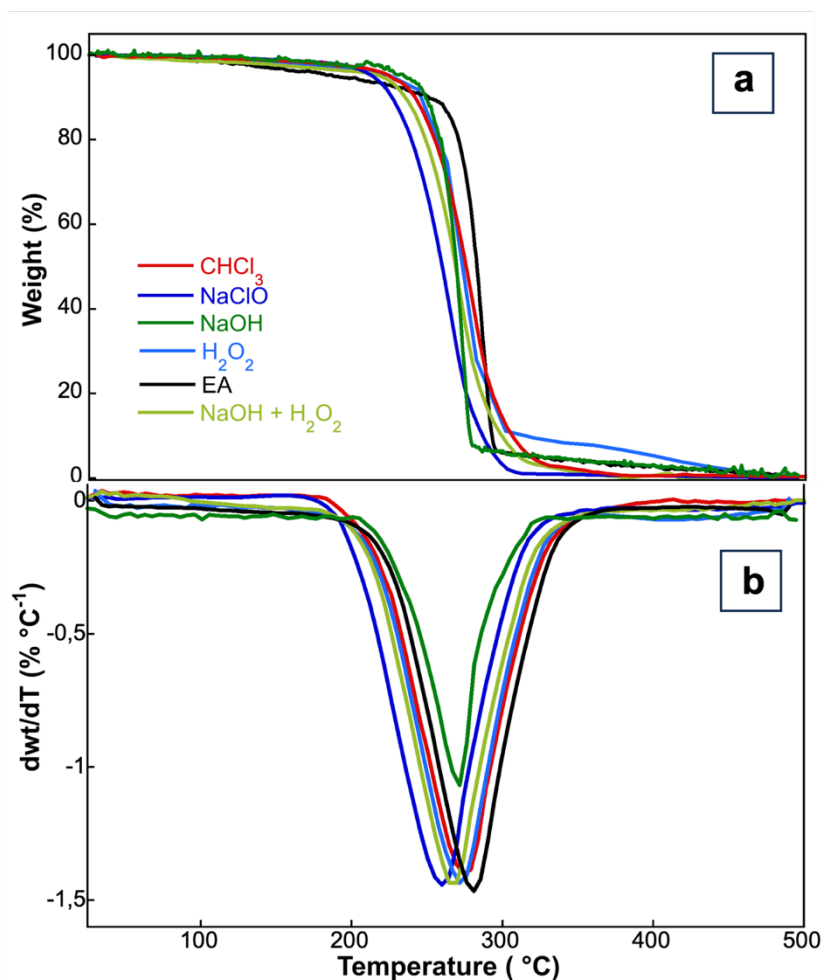


**Figure 1.6** Weight loss (a) and its derivative (b) curves of P(3HB-co-3HV) samples extracted with the different methods.

The thermal stability results, evaluated from the values of temperatures at 10 % of weight loss  $T_d^{10}$  and at the maximum decomposition rate  $T_d^{\max}$  are reported in Table 1.6.

The sample purity obtained by the thermogravimetric analyses, evaluated through the main P(3HB-co-3HV) weight loss occurring between about 200 and 320 °C [129], confirmed the data determined by GC technique (Table 1.5). The  $T_d^{\max}$  and  $T_d^{10\%}$  values are within the usually observed range for P(3HB-co-3HV) with comparable features [130] and, as expected, no significant correlation can be observed between the thermal stability of the samples and the other properties of the polymers, such as purity, composition and molecular weight [122,131].

After the first DSC heating run, during which the melting process clears the sample previous history, the samples were cooled down at 30 °C min<sup>-1</sup> and reheated at 10 °C min<sup>-1</sup> (second

heating). The thermogram of the second heating of all the extracted P(3HB-co-3HV) are reported in Figure 1.7.

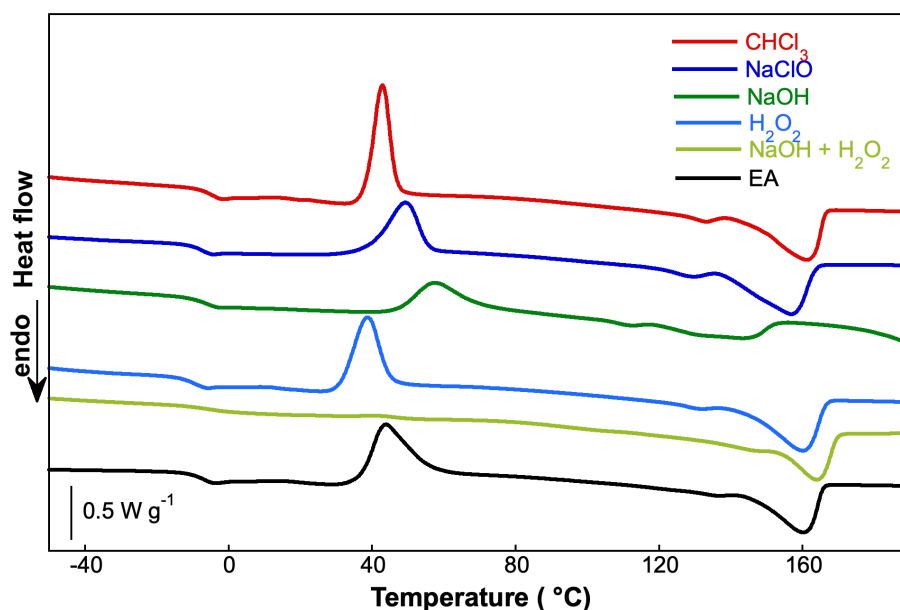


**Figure 1.7** DSC thermograms from second heating scan carried out from  $-70\text{ }^{\circ}\text{C}$  to  $190\text{ }^{\circ}\text{C}$  at  $10\text{ }^{\circ}\text{C min}^{-1}$ ) of P(3HB-co-3HV) samples extracted with alkaline and oxidative chlorine-free treatments. Samples extracted with standard methods (chloroform and hypochlorite) are also reported for comparison.

Besides the composition and molecular weight of extracted P(3HB-co-3HV), which resulted quite similar, the different thermal behaviours of the whole samples set can be related to the nature of impurities. In fact, according to their chemical and physical properties, they can act as nucleating agents or plasticizers which can promote or hamper, respectively, the melt or cold crystallization. All the samples show the glass transition ( $T_g$ ) in the  $-10 - -3.5\text{ }^{\circ}\text{C}$  temperature range. P(3HB-co-3HV) extracted by the double NaOH+H<sub>2</sub>O<sub>2</sub> treatment shows a very low specific heat capacity change ( $\Delta C_p$ ) of the amorphous phase at the  $T_g$  and lacks the cold crystallization, it being the only sample that undergoes an extensive melt-crystallization in the cooling scan. Differently, the other samples result completely or partially amorphous after cooling and cold-crystallize between about  $39\text{ }^{\circ}\text{C}$  and  $58\text{ }^{\circ}\text{C}$  ( $T_{cc}$ ). At higher temperature, the melting occurs in a wide temperature range. The enthalpy of fusion ( $\Delta H_m$ ), evaluated by the melting peak integral, is representative of the final sample crystallinity. The sample obtained by EA extraction shows the lowest  $\Delta H_m$  value because of the high fraction of 3HV monomeric unit which, as well-known, depress the polymer crystallinity [124]. On the other hand, P(3HB-co-3HV) recovered from the NaOH and H<sub>2</sub>O<sub>2</sub>



double treatments crystallized from the melt in the cooling scan and resulted to have a high crystallinity and order degree, as evidenced by the high  $\Delta H_m$  and melting temperature in the subsequent heating ramp.

**Table 1.6** Thermal properties of the whole samples set obtained by TGA and DSC analysis.

Extraction method	TGA			DSC			
	$T_d^{10\%}$ (°C)	$T_d^{MAX}$ (°C)	$T_g$ (°C)	$T_{cc}$ (°C)	$\Delta H_{cc}$ (J/g)	$T_m$ (°C)	$\Delta H_m$ (J/g)
CHCl <sub>3</sub> <sup>a</sup>	248	280	-5	43	58	161	53
NaClO <sub>a</sub>	232	266	-7	49	41	157	61
NaOH	250	273	-7	58	28	143	27
H <sub>2</sub> O <sub>2</sub>	248	278	-10	39	53	160	54
NaOH + H <sub>2</sub> O <sub>2</sub>	234	272	-3,5	-	-	164	67
EA	224	282	-8	45	60	161	45

a) Data from [132]

#### 2.4 Extraction at a pilot scale

The results of this extraction are reported in Table 1.7. Encouraged by the good results obtained by the double treatment in terms of recovery yield, purity, polymer properties and, mainly, readiness, the extraction process was repeated on larger amount of the same wet biomass (200 g). The results of this extraction are reported in Table 1.7.

**Table 1.7** Results of the extraction with the double treatment (NaOH+ H<sub>2</sub>O<sub>2</sub>) carried out on 200 g of wet biomass.

P(3HB-co-3HV) purity (wt.%)	93 ± 3
Recovery yield (wt.%)	88 ± 4
3HV (wt.%)	13.4 ± 0.5
$M_v$ (kDa)	565
$T_m$ (°C) (2 <sup>nd</sup> scan)	160
$\Delta H_m$ (J/g) (2 <sup>nd</sup> scan)	48

The extraction led to a polymer purity, composition and overall thermal properties equal to that obtained using a lower amount of biomass and, most importantly, a clear increase in the recovery yield from 70 wt% to 88 wt%. The use of larger quantities of biomass reduces

the fraction of polymer which can be possibly lost in the extraction and collection procedures. These results support the potential of coupled treatment as an alternative strategy for P(3HB-co-3HV) recovery and suggest the feasibility of this extraction method on a larger scale.

## 2.5 *Economic analysis*

In order to evaluate the feasibility and affordability of the extraction procedures presented in this study, an economic analysis has been conducted based on the calculation reported in the paper by Pagliano et al. [67].

The economic analysis has been conducted by Dr Francesco Valentino and Dr Marco Gottardo from the University Ca' Foscari (Venice, Italy).

Table 1.8 shows the main sources of costs for the studied extraction treatments, hence both aqueous-phase and solvent extractions. In detail, the overall cost for each procedure was evaluated as the operational costs (OPEX) only, since the fixed cost (CAPEX) derived from the industrial extraction apparatus resulted in non-representative evaluation at the laboratory scale. Furthermore, based on the equations reported by Pagliano and co-workers [67], the different contributions to OPEX (Eur/kgPHA) determination have been defined and calculated. Indeed, one of the most relevant costs depends on the material input (MI) which considers the commercial price of the reagents, related to the required amounts, and the maximum solvent/reagent recovery. This latter can be represented by a factor which typically ranges between 0.005 (highest solvent/reagent recovery) and 0.05 (lowest recovery) for PHA extraction. In this regard, for each inorganic reagent, a 0.05 factor was considered (taking into account the possible losses at each extraction step), while for water 0.0005 was used and for EA and CHCl<sub>3</sub> 0.005 (considering the higher recovery by solvent evaporation) [67]. Moreover, the OPEX related to the extraction reactor (ER) is mainly influenced by heating and then it has been calculated only for solvent extractions since only these treatments required high temperatures. In detail,  $\Delta T$  equal to 95 K and to 50 K, in adiabatic conditions, were considered for EA and CHCl<sub>3</sub> extractions, respectively. The last contribution comes from the solvent recovery or drying unit (SRU) which is related to the amount of evaporated solvent at the end of the extraction and then, to the required thermal

energy. In the case of EA and CHCl<sub>3</sub> extractions, SRU contribution has been calculated by considering the complete evaporation of the solvent, as reported by Pagliano et al.[67] On the other hand, in the case of aqueous-phase extraction only the residual water content in the humid pellet should be considered (since the highest volume of water was previously separated by centrifugation). In this regard, a 20 %w/w content of solids in the humid pellet recovered after centrifugation and a complete solids recovery in adiabatic conditions were considered. As a result, hydrogen peroxide is the less expensive treatment (0.35 Eur/kgPHA), followed by the EA solvent extraction (0.84 Eur/kgPHA). However, in this case, the relatively high operative pressure, the high molecular weight reduction and PHA composition change must be considered. On the other side, the highest cost is related to NaClO treatment, because of the high volume of water required. Chemical disruption by NaOH and the combined treatment are characterized by intermediate costs (1.19 and 1.52 Eur/kgPHA, respectively), comparable with that obtained for CHCl<sub>3</sub> extraction (1.33 Eur/kgPHA). Hence, the most suitable extraction method should be evaluated considering both the costs and the extraction performance. In conclusion, the combined NaOH and H<sub>2</sub>O<sub>2</sub> treatment seems to meet the criteria for choosing the best performing extraction procedure, since it allowed to obtain a very high purity of the final product (92.3 ± 0.5 % w/w) and the highest M<sub>v</sub> among the tested PHA (571 ± 25 KDa) with a competitive OPEX. As an added value, the proposed procedure reduces the amount of chemicals involved in the PHA recovery, if compared with CHCl<sub>3</sub> extraction used at industrial scale.

**Table 1.8** Sources of cost for the studied extraction treatments. MI=material input, ER=extraction reactor, SRU=solvent recovery or drying unit.

Extraction	OPEX (Eur/kg <sub>PHA</sub> )			
	MI	ER	SRU	Tot
CHCl <sub>3</sub>	0.72	0.10	0.51	1.33
NaClO	1.74	0.00	0.28	2.02
NaOH 0.2M	0.864	0.00	0.33	1.19
H <sub>2</sub> O <sub>2</sub> (1.5%)	0.069	0.00	0.28	0.35
NaOH + H <sub>2</sub> O <sub>2</sub>	1.124	0.00	0.40	1.52
Ethyl acetate	0.331	0.19	0.32	0.84

### 3 Conclusions

The PHA-extraction performances of coupled chlorine-free treatment (4h for NaOH digestion and 1h for H<sub>2</sub>O<sub>2</sub> oxidation) on the wet acidified biomass allowed to obtain high purity ( $92.3 \pm 0.5$  % w/w) and molecular weight ( $571 \pm 25$  KDa), with a recovery yield of about 70 % w/w. Moreover, this innovative extraction method led to the stabilization and crystallization of the PHA granules, which in turn positively affected its thermal stability. Furthermore, when the coupled treatment was applied to a larger amount of PHA-rich biomass (roughly 200 g), the recovery yield increased up to  $88 \pm 4$  % w/w with a purity ( $93 \pm 3$  % w/w) remained comparable to that of the sample extracted from lower mass. Also, these distinctive treatments allowed for skipping two significant steps (neutralization and drying of wet biomass), that harmed the time and cost of the entire downstream process being the contact time for the coupled treatment equal to 6 hours in total. The thermal stability of sludge derived PHAs were not influenced by the type of extraction, while its molecular weight was higher when extracted with the coupled treatment compared to the standard methods. These results attested the high potential of coupled treatment as an alternative strategy to the most cited PHA recovery methods such as chloroform or NaClO oxidation. In addition, the competitive cost quantified in the economic evaluation (OPEX = 1.52 Eur/kg<sub>PHA</sub>) was an added value to be considered in perspective of a technology scale up. Taken as a whole, the coupled treatment herein proposed can improve the environmental and economic sustainability of the entire PHA production process, by reducing operative steps, amount of reagents and total operative time involved in the extraction step.

## **CHAPTER 2**

# **Toward a new strategy for sustainable chemical modification of PHAs**

Sustainable biomass-derived materials have been extensively employed for replacing petroleum-based polymers in various fields such as energy production and accumulation, contaminants removal and food packaging [133–136]. Recently, because of their biocompatibility, biodegradability, and nontoxicity, they have found several applications in the biomedical field, including in smart drug-controlled release, tissue engineering and other areas [137,138].

In this context, there is a growing interest in polyhydroxyalkanoates (PHAs). PHAs degrade under physiological conditions via surface erosion [139,140] into natural metabolites such as 3-hydroxybutyrate and hydroxy acyl-coenzyme causing a negligible immune response. The abovementioned characteristics make PHAs a promising alternative to fossil plastics in biomedical applications, offering an environmental benefit where sustainability is often not considered a priority. Many examples of developed PHAs biomedical devices are available in soft tissue engineering [141–144], hard tissue engineering [145,146] as well as drug delivery systems [147–149].

However, the lack of polar functional groups in PHAs structure and therefore the high hydrophobicity limits their usage. In fact, the chemical composition plays a key role in the interaction between a biomaterial and extracellular matrix (ECM) since most of them occur at the interface after water adsorption and subsequent attraction of biomolecules necessary for cell attachment [150,151].

Polyester hydrophobicity represents an advantage and a disadvantage at the same time as it could be exploited to deliver poor water-soluble drugs increasing their bioavailability but hampers polymer colloidal dispersion and interaction with cells. To overcome this drawback, surfactants are commonly employed to reduce the interfacial tension between the nanoparticles and water. Commonly used NPs manufacturing processes involve the formation of a liquid/liquid stable dispersed system which consists of one substance distributed in discrete units (dispersed phase) in a second substance (continuous phase) to

produce new colloidal systems. Nanoparticles are well known to be thermodynamically unstable compared to bulk materials, due to high surface free energy causing flocculation or aggregation phenomena [152] with subsequent formation of clusters of micrometric dimensions. The maintenance of primary nanometric dimensions is a crucial aspect in biomedical applications since particles in the order of nanometers are not recognized by macrophages [153,154].

Surfactants are surface active agents able to decrease surface and interfacial energy, often used to improve dimensional stability preventing aggregation phenomena. They are amphiphilic molecules composed of a hydrophobic tail and a hydrophilic head and categorized into non-ionic, cationic, anionic, and amphoteric. The stabilization mechanism is different according to their nature, for instance, non-ionic surfactants avoid NPs aggregation by steric hindrance, ionic ones by electrostatic repulsion [155].

The effect of surfactants is not limited to nanoparticle stability but also affects biochemical processes such as cellular interaction, vectorization and pharmacokinetics [156]. Interestingly, Kreuter et al. [157] investigated the behavior of 12 surfactants coated on the nanoparticle surface, demonstrating the effectiveness of polysorbate-decorated NPs in facilitating drug delivery across the Blood Brain Barrier (BBB). Similar results were found by Wilson et al. study [158] which showed that polysorbate80-coated albumin NPs significantly enhanced gabantin concentration in the brain for epilepsy treatment.

As a result, surfactants represent an essential excipient in nanoparticle formulations. However, difficult excess removal of the most used surfactants together with environmental concerns [155,159–161] as well as cases of hypersensitivity and suspected carcinogenicity encouraged the development of more biocompatible molecules and self-surfactant systems. Bio-agents from carbohydrates, zwitterionic compounds, poly-hydroxy and bacteria-derived surfactants were largely studied [162–164]. For instance, Smulek et al. [164] have proposed long-chain alkyl glycosides as a good and inexpensive biosurfactant, while Sanjivkumar et al. [165] have suggested the potentiality of rhamnolipids from *Pseudomonas aeruginosa*. Martinelli et al. and Carrio et al. have described the use of polylactic acid and

polyglycolic acid (PLAGA) oligomers with ionized end-chain groups to form microparticles as a surfactant-free system [166,167].

Chemical functionalization is one of the most widespread strategies to enhance PHAs performance in living systems. The introduction of specific chemical groups such as amines (-NH<sub>2</sub>), carboxylates (-COO<sup>-</sup>) or hydroxyl (-OH) through aminolysis or hydrolysis [168–170] leads to the alterations of surface charge density and to the possibility of graft bioactive molecules like collagen, polypeptides, and polysaccharides able to favour cell interaction and proliferation [171–174]. Among the cited chemical reactions, aminolysis has been extensively used to functionalize PHAs [174–177]. Even though the beneficial effects of amino group introduction, some considerations about its sustainability should be appointed. The widely used di- or multifunctional amines, like hexamethylene diamine or ethylene diamine and solvents, such as chlorinated solvents, methanol, and propanol, are toxic for living systems and ecosystems. As a result, time-consuming purification steps are required to avoid the persistence of unreacted dangerous compounds. Additionally, the use of huge amounts of organic solvents for reaction and purification implies the loss of the ecological advantage of using a biomaterial.

Recently, the use of naturally occurring substances as aminolysis reagents has been investigated. Pellegrino et al. [178] studied the possibility of using the physiological amino acid taurine (Tau) for PLLA surface aminolysis transforming Tau in its corresponding salts with tetrabutylammonium (TBA), but traces of TBA could remain on PLLA surface potentially causing low cells viability. To avoid negative effects on cell proliferation, De Felice et al. [179] proposed an alternative to the use of TBA-Tau salts, replacing Tau counter anion with choline (Ch). The resulting compound is the ionic liquid choline taurinate ([Ch][Tau]) which showed no cytotoxicity and the ability to aminolyze PLLA with the obtainment of porous scaffolds.

Since it has been demonstrated that different polyesters may have different behaviour during reaction [180] the proposed work aims to investigate the feasibility of using [Ch][Tau] to achieve a sustainable and harmless PHAs aminolysis.



The study is split into two parts. In the first part poly(3hydroxybutirate-*co*-3hydroxyhexanoate) (PHBHHx) heterogenous phase aminolysis was carried out on films in non-toxic solvents by using ethanol and water, for different contact times. Also, methanol has been used as a reference. The produced functional films were characterized by Fourier Transform infrared spectroscopy (FTIR), static contact angle measurements and scanning electron microscopy (SEM).

In the second part, the reported method was exploited for the homogenous phase PHBHHx aminolysis with the scope to prepare self-surfactant systems. Usnic acid (UA), a dibenzofuran originally isolated from lichens, poorly soluble in water but well known for its antimicrobial, antiviral, antiproliferative and anti-inflammatory [181] properties was used as a drug model.

## **Sustainable surface functionalization of poly(3hydroxybutirate-co-3hydroxyhexanoate) (PHBHHx)**

### ABSTRACT

In this section, a preliminary study about surface PHBHHx aminolysis is illustrated. Aminolysis was carried out in non-toxic solvents by using ethanol and water. Functionalised films obtained at different reaction times were characterized by FTIR spectroscopy, static contact angle measurements and Scanning Electron Microscopy. Aminolyzed films in methanol were used as a reference. Characterization highlighted the occurrence of functionalization. Surprisingly, pushing the reaction to higher time does not result in a greater degree of functionalization and hydrophilicity. In fact, with a prolonged contact time, a surface etching occurs with the subsequent release of surfactant-like molecules. These kinds of structures were fractionated through selective solubilization and used for nanoparticle (NPs) production.

## 1. Materials and methods

### 1.1 Materials

Poly-3hydroxybutirate-co-3hydroxyhexanoate (PHBHHx) purchased by Kaneka (MW 550kDa, 11 % mol HHx) was purified by precipitation adding ethanol to polymer chloroform solution. The ionic liquid choline taurinate ([Ch][Tau]) was prepared according to the one-pot procedure reported in ref. [179].

### 1.2 Films preparation and functionalization

PHBHHx films were prepared by solvent casting from a 5 %w/v solution in chloroform. After the complete solvent evaporation, films were melted at 150 °C (30 °C min<sup>-1</sup>) and cooled up to 25 °C (90 °C min<sup>-1</sup>) with a hot plate Linkam TP92.

PHBHHx samples were immersed in an 8% w/v [Ch][Tau] MeOH solution for different contact times (1h, 2h, 3h, 4h, and 6h). Finally, [Ch][Tau] residues were removed by washing the films twice with fresh MeOH. The same procedures were used for reactions in ethanol and distilled water. Additionally, the effect of pH variation was investigated by using 0.1 % w/v sodium hydroxide (NaOH) aqueous solution, while the impact of a prolonged contact time was investigated in EtOH till the complete dissolution of PHBHHx film. This method has led to the formation of different products, not all soluble in the alcoholic phase and separated by selective solubilization in EtOH, ethyl acetate (EtOAc) and chloroform (CHCl<sub>3</sub>).

### 1.3 FTIR analysis

Aminolyzed films and solvent fractionated products from complete aminolysis were characterized by FTIR in attenuated total reflection mode (ATR) by using a Thermo Nicolet 6700 instrument (Thermo Scientific, Waltham, MA, USA), equipped with a Golden Gate diamond single-reflection device (Specac LTD). The ATR-FTIR spectra were collected using 200 scans in the 4000-650 cm<sup>-1</sup> range at a resolution of 4 cm<sup>-1</sup>.

#### 1.4 *Static contact angle measurements*

Static contact angle measurements were performed by dropping 5-10  $\mu\text{l}$  of distilled water on vacuum-dried samples. Photographs were acquired using a Nikon D7200 and contact angle values were obtained using the ImageJ program for digital image elaboration.

#### 1.5 *Morphological characterization*

The morphology of aminolyzed PHBHHx films were investigated by scanning electron microscopy using a field emission scanning electron microscope (AURIGA, Zeiss, Jena, Germany).

#### 1.6 *Dynamic Light Scattering (DLS)*

Size and zeta potential (PotZ) of surfactant-like structures produced during complete aminolysis were evaluated by DLS measurements using a Zetasizer Nano spectrometer (Malvern Instruments Ltd.) equipped with a 4 mW HeNe laser source (632.8 nm) at 25 °C.

## **2. Results and discussion**

### 2.1 *Study of the effect of solvents on crystallinity*

The aminolysis consists of ester bond cleavage with the formation of an amide and hydroxide groups. The most adopted reactants for heterogeneous aminolysis of solid polyesters are diamines or polyamine in which one of the two  $-\text{NH}_2$  groups reacts with the carbonyl leaving free the others on the surface. These polar groups contribute to the increase of superficial hydrophilicity of polyester materials. In the present study, the ionic liquid [Ch][Tau] has been used as a nucleophilic agent. [Ch][Tau] structure and the scheme of aminolysis reaction on PHBHHx surface are reported in Figure 2.1.

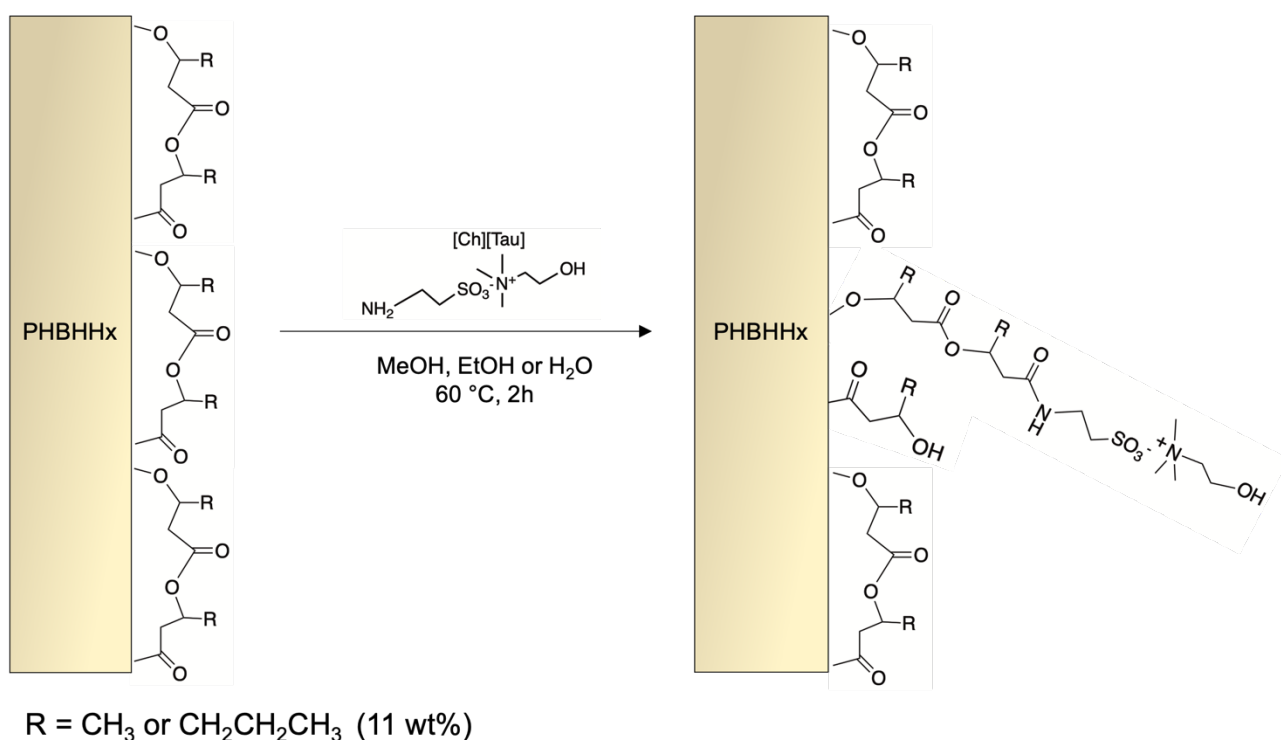


*Figure 2.1 PHBHHx surface modification scheme.*

The use of [Ch][tau] leads to the introduction of sulfonic polar moieties and, therefore, to an increased hydrophilicity as well as to the possibility to conjugate positively charged bioactive molecules (i.e., collagen) as demonstrated by De Felice et al [179].

On the other hand, the choice of solvent for aminolysis is significant to reach a beneficial contact between reactants thanks to good amine and hydrophobic surface solvation. Besides these two factors, the effect of solvent on superficial morphology is a crucial aspect to achieve a notable degree of surface functionalization. As largely reported in the literature, solvent-induced crystallization is a common feature of polyesters resulting in shrinkage and changes in morphology [182–184]. Since the aim of this work is to functionalize PHBHHx surface, the effect of the three selected solvents (MeOH, EtOH, and water) on polymer structure has been investigated before aminolysis.

To do so films of PHBHHx were soaked in each solvent for at least 6 h and FTIR spectra were acquired (figure 2.2).

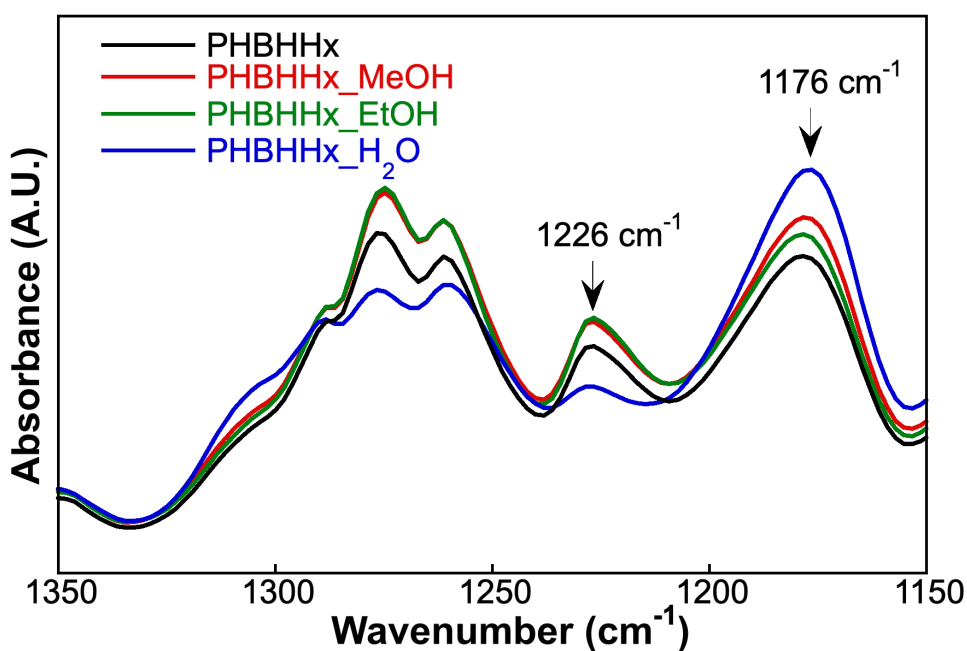


*Figure 2.2* FTIR spectra of PHBHHx films soaked in methanol (red), ethanol (green) and water (blue) for 6h. Neat PHBHHx (black) is also reported.

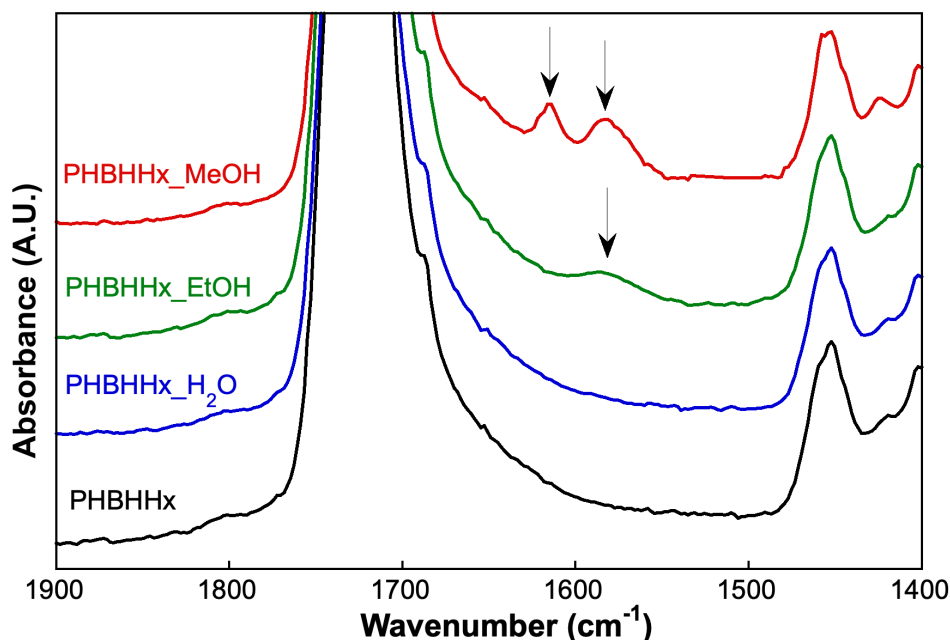
Crystallinity has been evaluated by the intensity variation of C-O-C stretching absorption at 1226 and 1178  $\text{cm}^{-1}$  related to the crystalline and amorphous phases, respectively [185]. Solvent-induced crystallization was more prevalent for PHBHHx soaked in EtOH and MeOH than in water. The different crystallinity results in different amounts of amorphous fraction on the polymer surface and therefore in different functionalization degrees. To standardize film geometry and avoid shrinkage during the reaction, thermal annealing at 60 °C for 24h was performed before aminolysis.

## 2.2 Screening of different solvents for aminolysis

Polyester aminolysis is a widely studied reaction carried out in alcoholic medium, mostly MeOH. On the other hand, some papers also reported the use of water [177,186]. The aminolysis of PHBHHx was preliminary conducted in MeOH, which was indicated as the best medium for aminolysis, and then in EtOH and water. The aminolyzed samples were called A\_PHBH\_xh, where x is the reaction time.

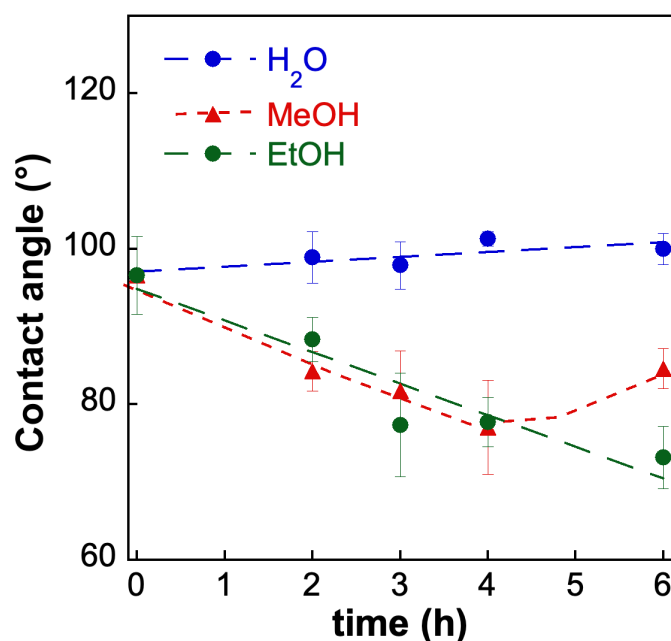
The reaction was carried out for different contact times as explained in section 1.2. ATR-FTIR spectra were collected and the results were compared to pristine PHBHHx to verify the occurrence of aminolysis (figure 2.3). The aminolysis of PHBHHx was evaluated by the

appearance of characteristic amide band at  $1650\text{ cm}^{-1}$ , due to amide carbonyl stretching (amide I), and at  $1570\text{ cm}^{-1}$ , due to N-H bending. As an example, in figure 3 spectra recorded on films aminolyzed in the selected solvents for 6 h are reported. Spectra were normalized with respect to the reference peak at  $1452\text{ cm}^{-1}$ .



**Figure 2.3** FTIR spectra of neat PHBHHx and films aminolyzed in MeOH, EtOH, and water for 6 h. The arrows at  $1650$  and  $1570\text{ cm}^{-1}$  indicate the amidic C=O stretching absorption (amide I) and the N-H bending absorption (amide II) respectively.

The spectra reported in Figure 3 highlighted the presence of the amide I and amide II peaks when MeOH is used as a solvent. When EtOH is used, only the amide II band is visible (Figure 2.3). However, films aminolyzed in water show no typical amide peaks (Figure 2.3), highlighting that water is not a good solvent for this reaction. This might be attributed to the poor wetting of hydrophobic PHBHHx films and then, to a difficult approach of amine to the polymer surface. In addition, the amino group of [Ch][Tau] may be protonated causing a reduced reactivity for the nucleophilic substitution. To preserve ionic liquid nucleophilicity, an experiment was conducted in alkaline water but also in these conditions the functionalization did not occur. Since the introduction of a polar group on PHBHHx surface leads to an increase in polymer wettability, static water contact angle measurements were carried out and taken as an indicator of surface functionalization degree. Contact angle values as a function of the reaction time are reported in Figure 2.4.



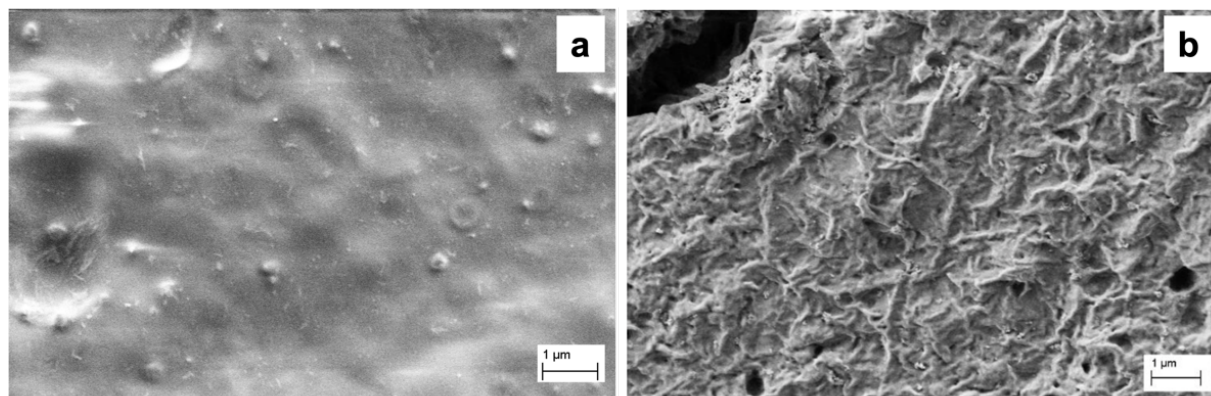
**Figure 2.4** Mean contact angle values ( $n=3\pm SD$ ) as a function of the reaction time for samples aminolyzed in MeOH, EtOH and water.

Figure 2.4 shows that the use of water did not bring about any changes in wettability because of the absence of  $SO_3^-$  polar group grafting on the film surface, in agreement with FTIR results. The use of alcoholic solvents implies a decrease in contact angle values (from  $97^\circ$  for pristine films up to about  $70-80^\circ$ ), sign of successful aminolysis. Contact angle values of films aminolyzed in MeOH decreased quickly with the increase of reaction time, reaching a minimum value at about 4 h, and then increased slightly. This could indicate that the reaction occurs at the expense of the outermost amorphous polymer layer which is progressively removed. Then, the aminolysis degree decreases on the more stable underlying crystalline phase [187]. In fact, during the initial stage of aminolysis, the erosion is not significant [188]. Prolonging the reaction time, the cleaved polyester segments were solubilized (*etching*) causing a reduction of polar group density and of wettability of the film surface.

Differently from MeOH, contact angles of EtOH-treated films reach a constant value after 3h of reaction indicating the establishment of an equilibrium between new amidic bonds and surface erosion, in agreement with Zhu et al work on PCL membranes [188]. Presumably, this is due to the lower solubility in EtOH of the highly aminolyzed products.



As a result of the etching, the surface morphology changes as shown by SEM images (Figure 2.5).



**Figure 2.5** SEM micrographs for (a) neat PHBHHx and (b) PHBHHx treated for 6 h in MeOH.

SEM micrographs highlighted the formation of irregularities due to the erosion of the amorphous surface layer and the appearance of underlying lamellar crystalline structures. Based on these results, it is possible to conclude that, by carrying out the reaction for long time, the degradative nature of aminolysis prevails and the shorter chains created were released in the reaction medium causing a surface etching with the consequent exposure of the more crystalline fraction, which is less reactive and hydrophilic (Figure 2.5).

### 2.3 Fractionation of heterogeneous aminolysis products

The aminolysis carried out using [Ch][Tau] involves the formation of shorter polymer chains functionalized on one terminal by the ionic liquid. As a result, aminolysis has the dual effect of eroding the polymer surface and making amphiphilic chains that could behave as a surfactant. In order to investigate in detail the aminolysis products, an experiment was then carried out extending the reaction time up to the polymer film disruption. The reaction was conducted in EtOH for 24 h. At the end of the reaction, the obtained products were not all soluble in ethanol. To evaluate the reaction products, after drying, the solid fraction was fractionated through selective solubilization in different solvents such as EtOH, EtOAc and CHCl<sub>3</sub>. The FTIR spectra of collected fractions are reported in Figure 2.6. For comparison purposes, the spectrum of pristine PHBHHx is also reported.

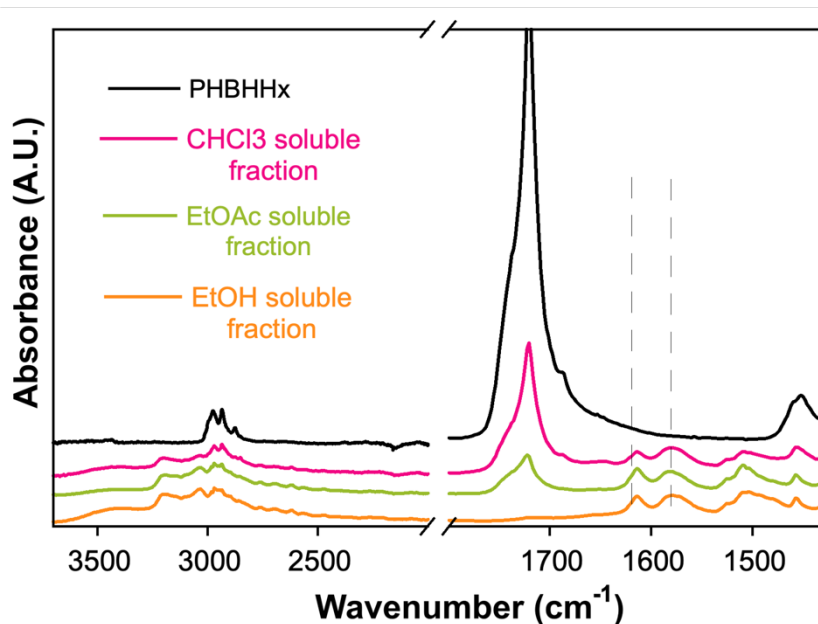


*Figure 2.6 FTIR spectra of neat PHBHHx and chloroform soluble fraction, ethyl acetate-soluble and ethanol-soluble fraction normalized with respect to 2933  $\text{cm}^{-1}$  band.*

The reported spectra refer to products which undergone different aminolysis degrees. As a result of the reaction, all collected fractions showed a lower intensity of the ester C=O stretching band at  $1720\text{ cm}^{-1}$  concerning the neat PHBHHx with respect to that of C-H stretching between  $2700$  and  $3050\text{ cm}^{-1}$ . The different degrees of aminolysis could be assessed by comparing the intensities of ester bond and amide peaks ( $1650$  and  $1570\text{ cm}^{-1}$ ). The spectrum of chloroform-soluble fraction shows a stronger absorption of ester C=O band ( $1720\text{ cm}^{-1}$ ) in relation to those of amides, a sign of low aminolysis and the high molecular weight products. In the ethyl acetate-soluble spectrum the intensity of the two amide peaks was stronger than that of the ester C=O stretching band, indicating the formation of functionalized shorter chains. The ethanol-soluble fraction spectrum, reported in orange, shows no absorption at  $1720\text{ cm}^{-1}$  meaning that there are no ester bonds, while the two amide peaks are characterized by higher intensity indicating the formation of repeating units functionalized with [Ch][Tau].

Since their potential amphiphilic nature, aminolysis product solutions in  $\text{CHCl}_3$  and EtOAc were vigorously stirred with water (1:20 v/v). The mixtures with chloroform were unstable and precipitation of the polymer occurred. On the other hand, the emulsion with water of the EtOAc-soluble fraction, characterized by a higher degree of aminolysis, resulted more

stable. After filtration, the suspension was analyzed through dynamic light scattering experiment (DLS). DLS measurements outlined the formation of a stable emulsion composed of nanostructures of about  $148 \pm 49$  nm, with a low polydispersity (PDI 0.108) and a Z-potential of  $-52 \pm 9$  mV.

### **3. Conclusions**

This preliminary work demonstrates the possibility of PHAs surface chemical modification by using non-toxic solvents and reactants opening the way to more sustainable biomedical device fabrication. Additionally, the combination of [Ch][Tau] and EtOH allows the obtainment of amphiphilic structures with surfactant activity. The possibility to prepare tailored amphiphilic molecules through sustainable procedures and their potential employment for nanoparticle preparation will be discussed in the next section.

## Preparation and characterization of PHA-based *self-surfactant* systems

### ABSTRACT

Surfactants are essential excipients in nanoparticle preparation since they ensure dimensional stability and dispersion, increased wettability of hydrophobic matrices and play a key role in cellular interaction. Recently, biosurfactants gained a lot of interest due to safety and environmental concerns. In this work poly-3hydroxybutirate-co-3hexanoate (PHBHHx) has been chemically modified using choline taurinate ([Ch][Tau]) as a non-cytotoxic and eco-friendly nucleophilic agent. Amphiphilic structures with different hydrophobic tail lengths were obtained varying the ratio between PHBHHx repeating units and [Ch][Tau]. Nanoparticles were prepared through the solvent evaporation method. Nanometric particles were successfully obtained and encapsulation efficiency has been evaluated using usnic acid as a model molecule.

## 1. Materials and methods

### 1.1 Materials

Poly(3-hydroxybutirate-co-3-hexanoate (PHBHHx, 11% mol HHx, Kaneka) was purified by precipitation adding ethanol to polymer chloroform solution. The ionic liquid choline taurinate ([Ch][Tau]) was prepared according to the one-pot protocol previously reported [47]. Usnic acid (UA, Sigma Aldrich), chloroform (CHCl<sub>3</sub>, Carlo Erba), ethanol (EtOH, Carlo Erba), ethyl acetate (EtOAc, Sigma Aldrich) were used as received.

PHBHHx is soluble in EtOAc at 65 °C and insoluble in EtOH. Vice versa, EtOH dissolves [Ch][Tau] which is insoluble in EtOAc. To conduct the aminolysis reaction in a homogeneous phase, preliminary experiments were carried out to find the right ratio between the two solvents to avoid polymer or taurine salt precipitation. An EtOAc: EtOH weight ratio of 2.5:1 was found to be the optimal mixture for the reaction. Different PHBHHx: [Ch][Tau] molar ratios were used to obtain various aminolysis degrees.

After the polymer complete solubilization at 65 °C, the [Ch][Tau] solution in ethanol was added dropwise under stirring. The reflux reaction was carried out for 2 h. Tested longer time did not bring about products with higher aminolysis degrees. For analysis purpose, the reaction medium was dried and the solid products dissolved in chloroform to eliminate unreacted [Ch][Tau] or other insoluble fractions. The product soluble in CHCl<sub>3</sub> was called S<sub>PHBHHx<sub>tot</sub></sub>. In addition, cold ethanol was added to the chloroform solution, obtaining a solid fraction (S<sub>PHBHHx<sub>prec</sub></sub>), separated by centrifugation and dried, and a fraction soluble in EtOH/CHCl<sub>3</sub> mixture (S<sub>PHBHHx<sub>sol</sub></sub>). S<sub>PHBHHx<sub>tot</sub></sub>, S<sub>PHBHHx<sub>prec</sub></sub> and S<sub>PHBHHx<sub>sol</sub></sub> samples were characterized separately.

### 1.2 Nanoparticles preparation

Nanoparticles have been obtained by solvent evaporation method. At the end of the aminolysis reaction carried out in EtOAc/EtOH mixture, the reaction medium was added dropwise to water under vigorous stirring (ULTRA TURRAX IKA® T18 basic, 10000 rpm) for 5 minutes. Then, the obtained oil-in-water emulsion (o:w=1:20 v/v) was maintained at

65 °C under magnetic stirring for 2 h to allow solvent evaporation, followed by 1h at 25 °C to stabilize the nanoparticles.

In order to prepare drug-loaded nanoparticles, UA was dissolved in EtOAc (0.5 % w/v) and added at the end of aminolysis to the reaction medium.

Sample names of both reaction products and nanoparticles are reported in Table 2.1.

**Table 2.1** Sample codification of PHBHHx surfactants and nanoparticles

PHBHHx: [Ch][Tau] (mol:mol)	$X_{[Ch][Tau]}$	Aminolysis product	Nanoparticles	Loaded nanoparticles
2.5: 1	0.29	S_PHBHHx_2.5	N_PHBHHx_2.5	N_PHBHHx_2.5_UA
5:1	0.20	S_PHBHHx_5	N_PHBHHx_5	N_PHBHHx_5_UA
10:1	0.09	S_PHBHHx_10	N_PHBHHx_10	N_PHBHHx_10_UA
20: 1	0.05	S_PHBHHx_20	N_PHBHHx_20	N_PHBHHx_20_UA

### 1.3 Fourier Transform Infrared Spectra (FTIR)

The products of the PHBHHx aminolysis reaction were evaluated by FTIR by using a Thermo Nicolet 6700 instrument (Thermo Scientific, Waltham, MA, USA). The spectra of S\_PHBHHX<sub>tot</sub>, S\_PHBHHX<sub>prec</sub> and S\_PHBHHX<sub>sol</sub> were collected in transmission by casting a CHCl<sub>3</sub> solution on a SeZn plate, co-adding 200 scans in the 4000-650 cm<sup>-1</sup> range at a resolution of 4 cm<sup>-1</sup>. The nanoparticles spectra were acquired in attenuated total reflection mode (ATR-FTIR) by using a Golden Gate diamond single-reflection device (Specac LTD).

### 1.4 Gel Permeation Chromatography (GPC)

The S\_PHBHHX<sub>tot</sub>, S\_PHBHHX<sub>prec</sub> and S\_PHBHHX<sub>sol</sub> samples were dissolved in chloroform at a concentration of 0.6 % w/v, filtered (WHATMAN 0.2 μm PTFE syringe filters) and injected in a gel permeation chromatograph equipped with a pump (JASCO PU-4180), a guard column and two linear columns in series (TSKgel®G6000-HHR TSKGel GMHHR-H), a column oven (JASCO CO-4060) and a refractive index detector (JASCO RI-4030). Chloroform was used as eluent at a flow rate of 1 ml/min. The detector was at 35 °C, whereas the columns were at 40 °C. Polystyrene standards (1.3x10<sup>3</sup>-3.05 x 10<sup>6</sup> g/mol) were used to

calibrate the system. Deconvolution of overlapped peaks was done by using the equation of a Gaussian curve:

$$G(x) = Ie^{-\frac{(x-t_{max})^2}{FWHH^2}} \quad (1)$$

where the parameters related to the sum of two curves ( $G_{tot} = G_1 + G_2$ ), intensity (I), elution time at the maximum ( $t_{max}$ ) and full width at half maximum (FWHH) were determined through a best-fit program.

### 1.5 *Dynamic Light Scattering (DLS)*

Size and zeta potential (PotZ) of PHBHHx nanoparticles were evaluated by DLS measurements using a Zetasizer Nano spectrometer (Malvern Instruments Ltd.) equipped with a 4 mW HeNe laser source (632.8 nm) at 25 °C.

### 1.6 *UV-vis spectroscopy*

UV-vis spectrophotometry has been used to quantitatively determine the usnic acid encapsulation within nanoparticles thanks to its strong absorption at 286 nm. UV spectra have been acquired using a diode-array spectrophotometer (Hewlett-Packard 8452A), in the range of 190-820 nm at a resolution of 2 nm.

Drug encapsulation efficiency was estimated through the apparent solubility ( $\Delta A\%$ ) determination according to the following formula:

$$\Delta A\% = \frac{\Delta A}{A_0} \times 100 = \frac{(A-A_0)}{A_0} \times 100 \quad (2)$$

Where A is the absorbance of UA-loaded nanoparticle suspension and  $A_0$  is the absorbance values of usnic acid in a solution obtained in the same condition used for nanoparticle preparation but without polymer.

Then,  $\Delta A\%$  represents the increase of the concentration of drug due to its encapsulation in nanoparticles suspension with respect to the concentration of the drug possibly solubilized in water during nanoparticle formation.

To remove nanostructures scattering a spectrum of the suspension of unloaded nanoparticles is subtracted from that of loaded nanoparticles.

## 2 Results and discussion

In the previous chapter, the use of eco-friendly chemicals to achieve PHBHHX superficial functionalization through heterogeneous phase aminolysis has been illustrated. The release, at high reaction time, of amphiphilic structures able to form stable oil in water emulsions, stimulated the systematic study of homogeneous phase aminolysis reaction. The proposed mechanism of the homogeneous aminolysis reaction of PHBHHx is reported in Figure 2.7.

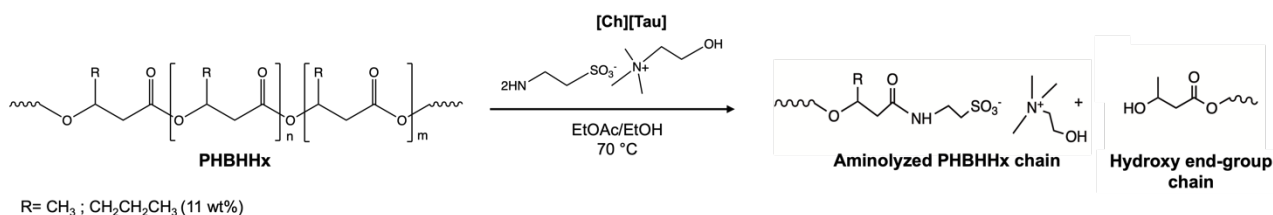


Figure 2.7 PHBHHx homogeneous aminolysis reaction scheme

The reaction is based on the nucleophilic character of the NH<sub>2</sub> group provided by [Ch][Tau], which leads to the introduction of an SO<sub>3</sub><sup>-</sup> group at one end of the cleaved chain counterbalanced by choline cation. The reaction product is then constituted by a mixture of lower molecular weight PHBHHx functionalized on the chain end by a hydrophilic group, possibly able to stabilize them in aqueous medium. Systematic studies about the influence of different reaction times and reagent ratios were conducted.

### 2.1 Evaluation of different reaction time influence

Many studies reported the strong influence of reaction time on aminolysis effectiveness. In the previous section, experiments at 2, 4 and 6 hours on films were conducted. Since the aminolysis, in this case, is conducted in a homogeneous phase, it has been necessary to explore the effect of reaction times because of the different C=O reactivity when it is on a film surface or in solution. To determine the optimal time, preliminary experiments were conducted at 1 h, 2 h and 4 h by using a PHBHHx: [Ch][Tau] molar ratio of 1:5. At the end of each experiment, FTIR and GPC measurements were acquired.

In Figure 2.8, FTIR spectra of aminolyzed samples at different times are compared with virgin PHBHHx.



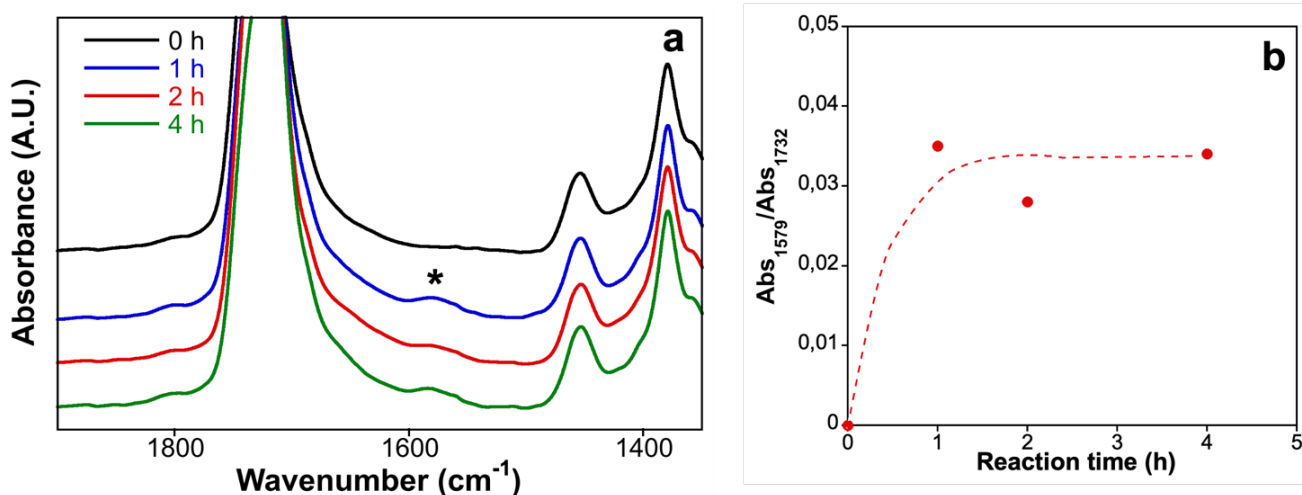


Figure 2.8 (a) FTIR spectra and (b) ratio between amidic and ester absorption peak reported as a function of reaction time. The line is a guide for the eyes.

The FTIR analysis demonstrated the functionalization of the polymer, as evidenced by the appearance of the peak at 1579 cm<sup>-1</sup> associated with the stretching of the primary amide.

To quantify the degree of functionalization, the ratio of the intensity of the amide II band at 1579 cm<sup>-1</sup> with respect to that of the ester carbonyl absorption located at 1732 cm<sup>-1</sup> was evaluated (Figure 2.8b). It is observed that after 1 h of reaction, the absorbance ratio is nearly constant.

As expected, aminolysis resulted in a lowering of molecular weight, as highlighted in Figure 2.9.

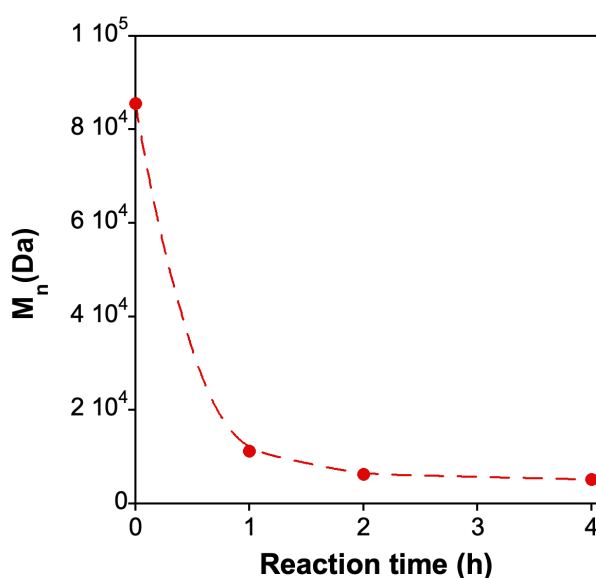


Figure 2.9 Evaluation of M<sub>n</sub> values of aminolyzed PHBHHx as a function of reaction time. The line is a guide for the eyes.

$M_n$  decrease is due to the cleavage of the ester bond and the subsequent formation of shorter chains. In accordance with FTIR data, molecular weight does not show a large decrease after 1 h of reaction. However, passing from 1 h to higher times results in a small decrease of  $M_n$  from 11200 Da (1 h) to 6300 Da (2h) and 5100 Da (4 h). Since higher reaction times does not change the degree of aminolysis, 2 hours were chosen for the further aminolysis with different reactant ratios.

## 2.2 Evaluation of different [Ch][Tau]: PHBHHx ratios effect

It was reported that the effectiveness of a surfactant in lipophilic molecule solubilization is affected by the dimension of the hydrophobic portion. The possibility of producing PHBHHx-based surfactants with different hydrophobic chain lengths by varying the ratio of the reagents has been explored. At this aim, the molar ratios between [Ch][Tau] and the repeating units of PHBHHx were selected to obtain 1 mole of ionic liquid each 2.5, 5, 10 and 20 mol of repeating units. For each condition, the reaction was carried out in duplicate.

### 2.2.1 Characterization of non-fractionated products ( $S_{PHBHHx_{tot}}$ )

At the end of the aminolysis reaction products were analysed by FTIR transmission spectroscopy and GPC. In Figure 2.10a, the FTIR spectra of  $S_{PHBHHx_{tot}}$  are reported with that of pristine PHBHHx for sake of comparison. To estimate the degree of functionalization, the values of the integral ratio of the stretching band of the amidic carbonyl, calculated between  $1610\text{ cm}^{-1}$  and  $1530\text{ cm}^{-1}$ , and that of the ester carbonyl, calculated in the range between  $1850\text{ cm}^{-1}$  and  $1732\text{ cm}^{-1}$ , were reported as a function of the molar fraction of the [Ch][Tau] (Figure 2.10b).

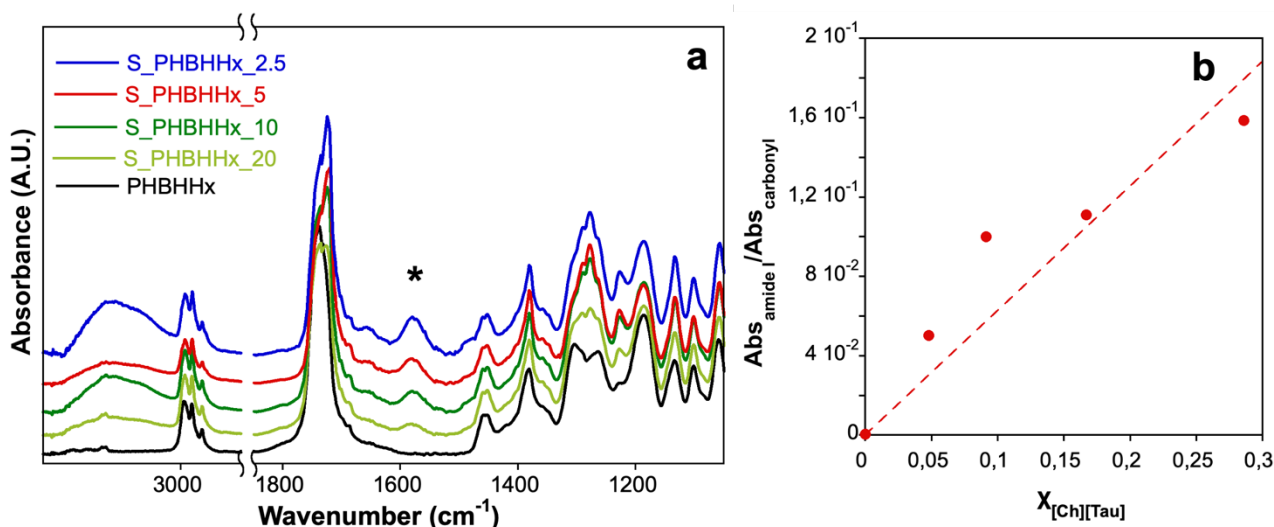


**Figure 2.10** (a) transmission FTIR spectra of  $S\_PHBHHx_{tot}$  at different reagent ratios and (b) evaluation of the degree of functionalization as a function of the  $X_{[Ch][Tau]}$ . The line is a guide for the eyes.

FTIR spectra show the appearance of the typical amide stretching peak at  $1579\text{ cm}^{-1}$  and the OH and NH stretching band at  $3250\text{ cm}^{-1}$ . Furthermore, a decrease in ester carbonyl band intensity ( $1732\text{ cm}^{-1}$ ), caused by the decrease of ester bonds, is observed. In figure 2.10b these spectral changes are quantified, clearly showing an increase in the  $Abs_{amide}/Abs_{ester}$  ratio as a function of  $[Ch][Tau]$  molar fraction. Spectroscopic results demonstrated that the PHBHHx different functionalization was successfully achieved.

GPC chromatograms and  $M_n$  values as a function of  $X_{[Ch][Tau]}$  are reported in figure 2.11.

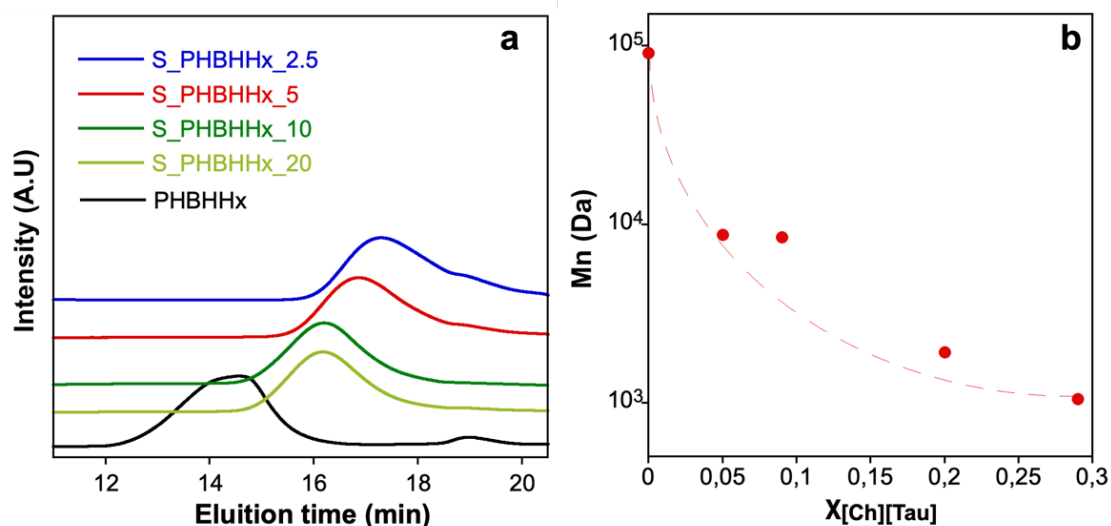


**Figure 2.11** (a) GPC chromatograms of  $S\_PHBHHx_{tot}$  obtained with different reagent ratios and (b) evaluation of  $M_n$  variations as a function of  $X_{[Ch][Tau]}$ .

It is possible to see from Figure 2.11b that  $M_n$  values decrease according to the  $X_{[Ch][Tau]}$  increase. By the analysis of the chromatograms reported in Figure 2.11a, it is possible to note that peaks are composed of an overlapping of at least of two contributions. For this reason, a deconvolution of chromatographic peaks was made as explained in section 1.5 and the elution time of single peaks was calculated. The  $M_n$  values relative to elution times of interpolated peaks were individuated through the calibration curve and indicated as  $M_n$  min and  $M_n$  max. Comparison between the  $M_n$  calculated on the whole chromatogram and  $M_n$  min and  $M_n$  max as a function of  $X_{[Ch][Tau]}$  is reported in Figure 2.12.

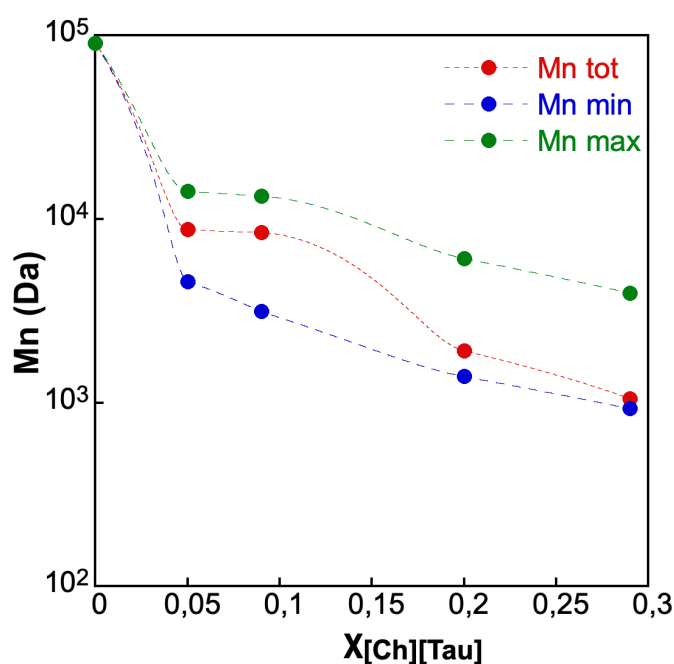


Figure 2.12  $M_{n,tot}$  values compared with those obtained from the gaussian deconvolution.

As a first approximation, these observations lead to conclude that the reaction results in the formation of at least two fractions of polymer with different molecular weights. It is worth underlining that the decrease in total  $M_n$  varies depending on the weights (integrals) of the two Gaussians. This parameter was not calculated but it seems that the  $M_n$  is more influenced by the  $M_{n,min}$  when a higher  $X_{[Ch][Tau]}$  is used for aminolysis.

The presence of at least two fractions was not evidenced by FTIR spectroscopy, which only detected the overall degree of functionalization. The presence of different molecular weight distribution suggested the fractioning of aminolysis products.

### 2.2.2 Characterization of fractionated products (*S* PHBHHx<sub>prec</sub> and *S* PHBHHx<sub>sol</sub>)

The portions collected after fractionation were characterized with FTIR and GPC.

In figure 2.13, the FTIR spectra acquired in transmission mode of *S*\_PHBHHx\_5 soluble and non-soluble fractions are compared with that of pristine PHBHHx. No marked differences can be found on the other samples.

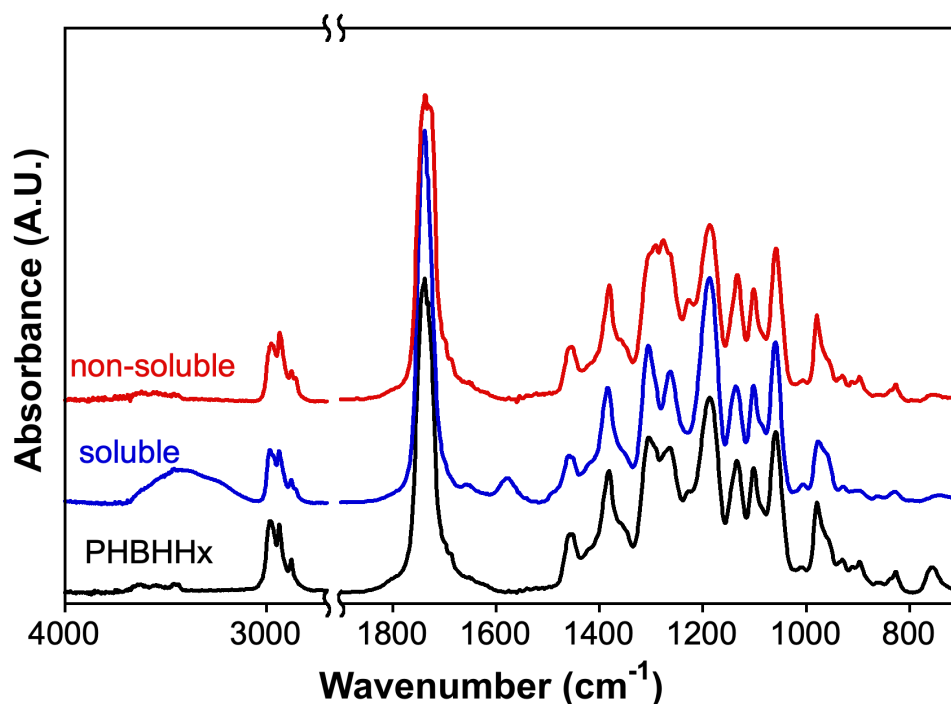


**Figure 2.13.** FTIR-ATR spectra of *S*\_PHBHHx\_5 soluble and non-soluble fractions and of pristine PHBHHx.

The spectrum of the non-soluble fraction does not display the amide II absorption at about 1570 cm<sup>-1</sup> clearly indicating that the sample is composed of polymer that did not undergo aminolysis. Differently, the soluble fraction shows the weak absorption of amide I (1650 cm<sup>-1</sup>) and medium intensity band of amide II (1570 cm<sup>-1</sup>). Then, the aminolyzed polymer solubility in CHCl<sub>3</sub>/EtOH mixture strongly depends on the presence of a sulfonic group on one chain end. The remaining non-soluble cleaved chains did not show the presence of amide groups and presumably will not have surfactant activity. To better investigate the aminolysis reaction products, the molecular weight of both fractions was determined by GPC measurements. Chromatograms of *S*\_PHBHHx<sub>sol</sub> and *S*\_PHBHHx<sub>prec</sub> are reported as a function of  $M_n$  in figure 2.14a and 2.14b.

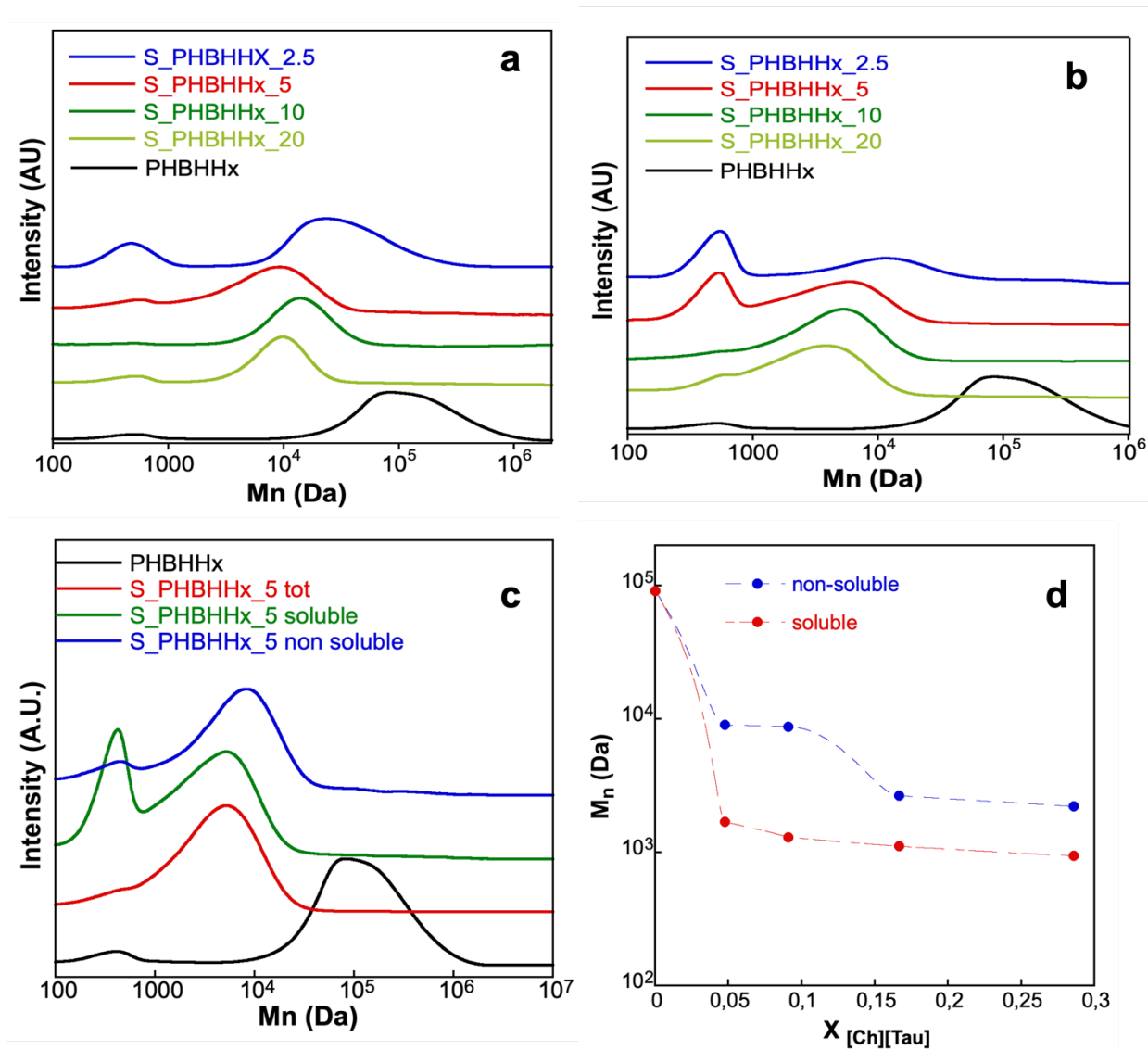


Figure 2.14 GPC chromatograms of (a) non-soluble and (b) soluble fractions. Chromatogram of pristine PHBHHx, of the whole S\_PHBHHx\_5 sample and its soluble and non-soluble fractions (c). Variation of  $M_n$  of soluble and non-soluble fractions as a function of  $X_{[Ch][Tau]}$  (d).

Figure 2.14a and b shows that, in the used experiment conditions, the fractioning did not separate completely the macromolecules according to their molecular weights. In fact, a double distribution can be observed in soluble and insoluble fractions. Moreover, in both the sample sets, the molecular weights are lower than that of the pristine polymer. At the higher [Ch][Tau] concentration, a clear increase in the contribution of the lower molecular weights fraction occurs. In Figure 2.14c, for sake of comparison, the chromatograms of pristine PHBHHx, the whole S\_PHBHHx\_5 sample and its soluble and non-soluble

fractions are reported. In Figure 2.14d, the  $M_n$  variation, evaluated considering the whole chromatogram of the two fractions, is reported as a function of  $X_{[Ch][Tau]}$ .

No noticeable variations in the  $M_n$  values of  $S\_PHBHHx_{sol}$  were detected. On the other hand,  $M_n$  of  $S\_PHBHHx_{prec}$  decreases as the  $X_{[Ch][Tau]}$  increases. The different solubility in EtOH/CHCl<sub>3</sub> mixture of the two fractions is not related only to the  $M_n$  but also to the presence of SO<sub>3</sub><sup>-</sup> moiety at the chain end, which enhances the solubility in a more polar solvent.

Then, according to the FTIR and GPC results, it is possible to infer that the aminolysis reaction brings about the formation of cleaved chains with sulfonic group at one end, characterized by a double  $M_n$  distribution. The shorter chains increase with the increase of the aminolyzing agent. It is possible to assume that the soluble fraction possesses the surfactant activity. The non-soluble fraction, with higher molecular weights, not having the amphiphilic character, could constitute the particle core in the subsequent emulsion preparation. Then, the whole product of the aminolysis reaction, without any purification step, will be used for particles formation, whose results are reported in the next section.

## 2.2 *Self-surfactant activity of $S\_PHBHHx_{tot}$*

Nanoparticles were prepared by using the emulsion drying technique in which  $S\_PHBHHx$  dissolved in the reaction medium (EtOAc/EtOH) were added dropwise to water according to the procedure reported in section 1.2. In parallel, also NPs loading with usnic acid was performed. DLS measurements were carried out to evaluate dimension and zeta potential (ZP) of the formed particles. In Figure 2.15, the distribution curves of the dimension are reported for both  $N\_PHBHHx$  (Figure 2.15a) and  $N\_PHBHHx\_UA$  (Figure 2.15b) particles.

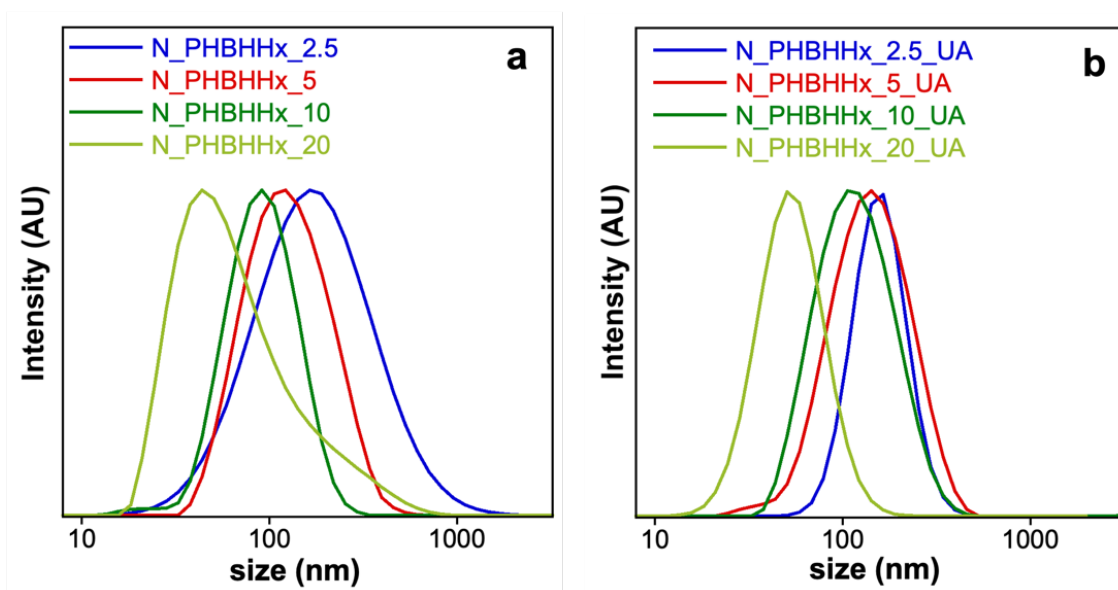


Figure 2.15 Distribution curves of dimension of (a) N\_PHBHHx and (b) N\_PHBHHx-UA particles

In general, nanoparticle sizes with and without usnic acid show a single-mode distribution excluding the N\_PHBHHx\_20 sample. In fact, although displaying the lower dimension at the maximum of the curve, it shows a tail at high size, possibly due to the formation of aggregates. However, it is important to note that the peaks related to drug-free nanoparticles are characterized by larger widths and lower mean dimensions than those without drugs. The presence of the drug favours the formation of larger nanostructures but with more uniform sizes.

Table 2.2 shows the values for the average size of nanoparticles with and without UA, expressed by mean diameter ( $d_{\text{mean}}$ ), polydispersity index (PDI) and zeta potential (ZP) values.

Table 2.2 Values of mean diameters, PDI and ZP for unloaded and loaded NPs.

Sample	$\chi_{[\text{Ch}][\text{Tau}]}$	$d_{\text{mean}}$ (nm)	PDI	ZP (mV)
N_PHBHHx_2.5	0.29	151	$0.424 \pm 0.009$	$-30 \pm 1.0$
N_PHBHHx_2.5-UA		156	$0.159 \pm 0.007$	$-59 \pm 4.9$
N_PHBHHx_5	0.20	122	$0.311 \pm 0.009$	$-26 \pm 7.9$
N_PHBHHx_5-UA		141	$0.211 \pm 0.008$	$-15 \pm 2.9$
N_PHBHHx_10	0.09	74	$0.24 \pm 0.03$	$-21 \pm 3.2$
N_PHBHHx_10-UA		114	$0.19 \pm 0.02$	$-17 \pm 1.8$
N_PHBHHx_20	0.05	43	$0.45 \pm 0.01$	$-15 \pm 1.7$
N_PHBHHx_20-UA		53	$0.162 \pm 0.008$	$-20 \pm 4.4$



In general, the  $d_{\text{mean}}$  values decrease increasing the PHBHHx: [Ch][Tau] reactant ratio.

This is because a lower  $X_{[\text{Ch}][\text{Tau}]}$  favours the formation of longer functional chains with a higher surfactant activity. Conversely, the products of the reaction at higher  $X_{[\text{Ch}][\text{Tau}]}$  lead to a high concentration of short chains, not sufficiently active in the stabilization of the emulsion.

N\_PHBHHx\_UA samples have slightly higher  $d_{\text{mean}}$  values than N\_PHBHHx samples. A similar trend has also been found in the literature [189].

The stability of the suspensions has been estimated through ZP measurements reported in Table 2.2 with the relative error.

The N\_PHBHHx\_2.5 suspension has a ZP value of -30 mV which, as reported in the literature [189] is typical of highly stable systems. When this system is used for the encapsulation of usnic acid, an increase in ZP (-60 mV) occurs suggesting a segregation of sulfonic groups on the particle surface due to its unfavourable interaction with hydrophobic drug.

The N\_PHBHx\_20 sample is the least stable (-15 mV), confirming the assumptions made about the strong tendency to aggregate. In presence of drug the value of ZP remains approximately unchanged considering the error associated with the measure (tab. 2.2).

### *2.3 Apparent solubility ( $\Delta A$ ) calculation for encapsulation efficiency evaluation*

The determination of the amount of drug loaded into the particles can be accomplished by different methods. For a direct evaluation, the nanoparticles are separated from the medium in which they are prepared. Then, they are dried, weighted, dissolved in a common solvent for polymer and drug and subject to an analysis of the drug concentration, e.g. by UV-vis spectroscopy. The nanoparticles separation is the key point of the method. In fact, it should be rapid, to avoid the start of drug release. Often, the slow dialysis is used to eliminate the drug fraction soluble in the medium in which nanoparticles are suspended. In this case it could be difficult to distinguish the purification step from the release. The centrifugation is a rapid technique to separate the nanoparticles, although its efficiency depends on their dimensions. This method was used in this research, but high centrifugation speed and time brought about an incomplete separation. With a view to using more severe centrifugation,

in alternative, the determination of apparent solubility ( $\Delta A\%$ ) was employed to evaluate drug encapsulation efficiency. It calculates the percentage increase of the concentration of the drug due to its encapsulation in nanoparticle suspension with respect to the concentration of the drug possibly solubilized in water during nanoparticle formation.

The obtained  $\Delta A\%$  values are reported in Figure 2.16.

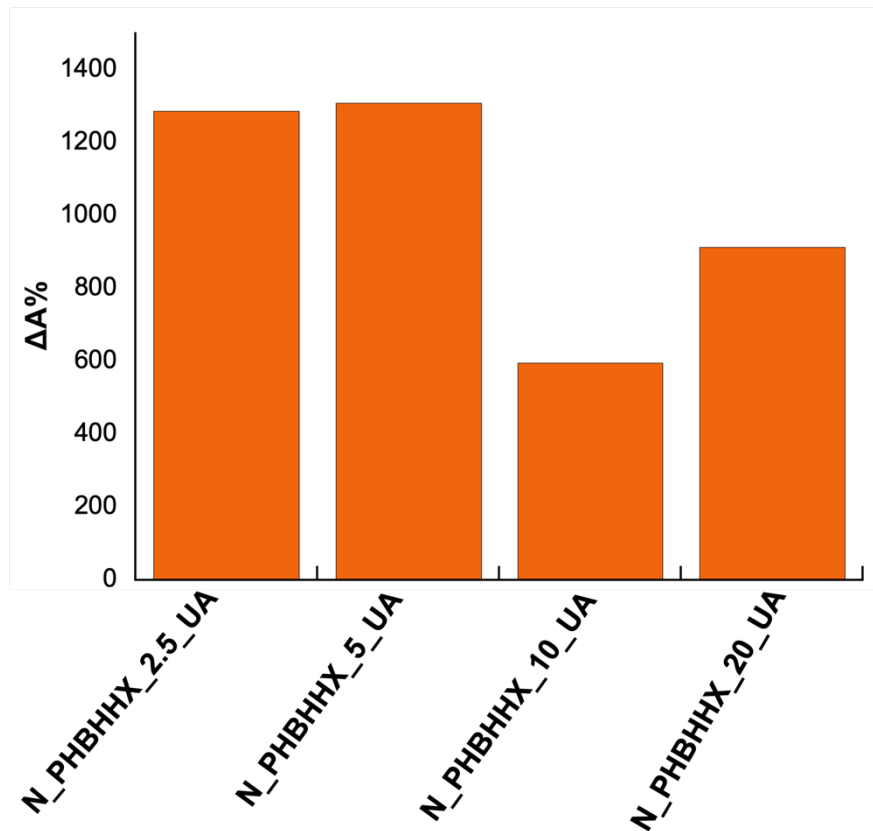


Figure 2.16 Apparent solubility values for N\_PHBHHx samples.

It can be seen from Figure 2.16, that  $\Delta A\%$  is greater for NPs pr N\_PHBHHx\_2.5 and N\_PHBHHx\_5, which are supposed to have shorter hydrophobic tails, meaning that these two formulations are more efficient for encapsulating drugs. This result is in contradiction with those reported in literature which evidenced that higher solubility is due to greater hydrophobic interaction between NPs core and drug [190,191]. On the other hand, the lower  $\Delta A\%$  values observed for N\_PHBHHx\_10 and N\_PHBHHx\_20 could be ascribed to the ability of longer polymer chains to crystallize and reject the drug causing its precipitation in the aqueous environment.

#### 2.4 *S\_PHBHHx as surfactant for PHBHHx*

An experiment was conducted to verify the possible use of the surfactant activity of S\_PHBHHx\_10 sample to prepare pristine PHBHHx nanoparticles.

Therefore, a solution of PHBHHx in EtOAc (0.5 % w/v) was added at the end of the preparation of S\_PHBHHx\_10 aminolyzed sample. Then, the same procedure to form nanoparticles was used.

The suspension was characterized by DLS, evaluating the size and ZP of the obtained nanostructures. The average diameter of the nanoparticles was  $241 \pm 8$  nm with a ZP value of - 41 mV .

In general, the amphiphilic system promotes the formation of a suspension of nanoparticles thanks to the surfactant activity that this exerts on PHBHHx.

### **3 Conclusion**

This study demonstrated the possibility of preparing self-surfactant systems by using biocompatible reactants and solvents as well as a simple procedure to form polymer nanoparticles. A future development of this work involves the optimization of the preparation process to increase the surfactant properties. The possibility to use these systems also as surfactants for pristine polymer in presence of usnic acid will be investigated. At the moment, no antimicrobial activity of nanoparticles nor drug release kinetics evaluation were carried out because the mandatory need to eliminate the non-encapsulated UA from suspension which could alter the results. At this aim, ultracentrifugation or dialysis will be tested.

## **CHAPTER 3**

# Exploring the role of 3-hydroxyvalerate (3HV) content on processability, compounding and properties of P(3HB-co-3HV)

## ABSTRACT

The aim of the present study is to bring new knowledge regarding the impact of 3HV content on processing, nucleating ability of a commonly used nucleating agent (boron nitride) as well as the ability to be blended with amorphous polymers (medium chain length- PHA). At this aim, P(3HB-co-3HV)-based films with 3, 18 and 28 mol% of 3HV have been processed through extrusion and subsequent moulding to obtain films. Characterization results indicated that increasing 3HV content from 3 to 28 mol% led not only to reduced melting points (from  $175 \pm 0$  to  $100 \pm 0$  °C) and improved mechanical properties (i.e. elongation at break from  $7 \pm 1$  % to  $120 \pm 3$  %), but also to better compatibility with mcl-PHA respect to 3HV-poor copolymers. Additionally, 3HV-rich copolymers required a slightly higher BN quantity to improve crystallization respect to 3HV-poor P(3HB-co-3HV).

## **Adapted from**

Alfano S., Doineau E., Perdrier C., Martinelli A., Gontard N., Angellier-Coussy H.

*Influence of the 3-hydroxyvalerate content on the processability, nucleating and blending ability of poly(3-hydroxybutyrate-co-3-hydroxyvalerate)-based materials*

In preparation

The homopolymer poly(3-hydroxybutyrate) (P3HB) is characterized by great stereochemical regularity resulting in a highly crystalline polymer (up to 70%). The high crystallinity contributes to excellent mechanical properties, including a high elasticity modulus of around 2.5-3 GPa and tensile strength at break of 35-40 MPa. Additionally, the lamellar structure contributes to low water vapor permeability as well as resistance to UV light, making it suitable for food packaging applications [192,193].

Despite all these desirable characteristics, P3HB competitiveness is limited due to many challenging aspects. In fact, in addition to downstream process issues illustrated in the previous chapter, P3HB suffer from poor processability, high brittleness and narrow processing window due to a melting temperature close to that of degradation.

Numerous approaches have been used to improve processability and properties of P3HB incorporating monomers with different carbon numbers. One of the most widespread copolymers of the PHAs family is poly(3-hydroxybutyrate-*co*-3-hydroxyvalerate (P(3HB-*co*-3HV))). P(3HB-*co*-3HV) is characterized by mechanical behavior dependent on the 3HV monomeric composition. In general, copolymers with low 3HV content behave like P3HB being characterized by high crystallinity and brittleness as well as melting point close to degradation temperature. Moreover, their slow crystallization rate and low nucleation density favor the formation of large spherulites leading to easier crack and fracture, evident from the low elongation at break of 2–7% [194]. In addition, both P3HB and P(3HB-*co*-3HV) undergo secondary crystallization phenomena which lead to progressive embrittlement and changes in properties over time [195]. Higher 3HV unit content led to a linear decrease of the glass transition temperature ( $T_g$ ) by increasing the 3HV content from 0 to 100 mol%, while the melting temperature ( $T_m$ ) and crystallinity are lowered by increasing 3HV content up to 45 mol% [196]. In fact, the increase of 3HV monomeric units causes the presence of defects in the crystal lattice, a more extensive amorphous region and, as a result, increases flexibility and toughness. Mainly, P(3HB-*co*-3HV) with about 40-50 mol% of 3HV units gains a lot of interest since this compositional range corresponds to the pseudo-eutectic point at which crystallinity and melting temperature reach the minimum value [197–199].

The possibility of tuning P(3HB-*co*-3HV) properties by changing the monomeric composition stimulated the development of strategies to obtain them. One is based on chemical synthesis which permits a tight control of molecular weight, monomer content and chemical composition distribution. As an example, Mai et al. [200] recently reported the synthesis of P(3HB-*co*-3HV) multiblock copolymers starting from P(3HB-*co*-3HV) blocks with different content of 3HV. The obtained copolymer showed improved elongation at break (76 %) and tensile toughness and modulus. Despite the obtained promising results, for chemical synthesis the use of chlorinated solvents (i.e., 1,2-dichloroethene) and catalysts (i.e. stannous octoate) are needed resulting in low sustainability.

Another widely investigated route to enhance 3HV content in P(3HB-*co*-3HV) copolymers is the use of microbial cultures. To vehiculate the microbial synthesis towards high 3HV contents, it is often necessary to use engineered microorganisms as the formation of 3HV portions requires the presence of the 3HV precursor propionyl-CoA. Therefore, various studies on metabolic engineering have been conducted to promote precursors-independent pathways for P(3HB-*co*-3HV) production [201–203]. These procedures obviously lead to additional costs to those generally needed for maintaining pure microbial cultures.

In recent years, a great number of studies about microbial consortium use generated enough knowledge to design P(3HB-*co*-3HV) copolymers with tailored monomeric composition by adjusting production process parameters such as microbial culture feeding strategies and circumventing the need for mutant strains.

Production of P(3HB-*co*-3HV) having tailored composition and microstructures has been achieved either using pure or mixed microbial cultures employing *ad hoc* feeding mixtures and substrate addition order. As an example, Ferre-Guell et al. [204] observed that the 3HV content of P(3HB-*co*-3HV), produced in *Haloferax mediterranei* fed with a synthetic VFA mixture, strongly depends on the composition of feeding medium. Additionally, the adoption of co-feeding results in random copolymer creation, while sequential feeding generates block copolymers or blends of P3HB and P3HV. Similarly, Laycock et al. [205] and Arcos-Hernández et al. [206] achieved 3HV-rich copolymer production with controlled microstructure with mixed microbial cultures fed with combined or alternated

administrations of VFAs. These studies demonstrated that manipulating the biomass selection and/or the accumulation strategies could influence copolymer properties such as morphologies, which in turn govern microstructure, thermal behaviour and resulting mechanical properties.

Despite the extensive work done to understand the correlation between the biosynthesis process and the properties of obtained materials, there are some crucial aspects of 3HV-rich copolymer processing still not been explored.

During any transformation process, it is important to achieve a rapid solidification of the material to minimize production cost and time. It has been observed that increasing 3HV content causes slow crystallization rates [207,208], not suitable for industrial applications. The lower crystallization rate is a bottleneck in P(3HB-*co*-3HV) applications. The inclusion of nucleating agents in polymer formulations is a usual approach to ensure rapid crystallization, controllable and homogeneous spherulite dimension and to limit secondary crystallization. The effect of additives on P(3HB-*co*-3HV) crystallization and mechanical behaviour has been assessed in several studies [209–212]. Among the tested additives there are boron nitride (BN), organoclays and cellulose nanocrystals (CNCs).

However, such studies have been exclusively performed on commercially available P(3HB-*co*-3HV) characterized by a low 3HV content (i.e. 3HV content of about 0-8 mol%) causing a lack of knowledge about the performances of filled 3HV-rich copolymers.

Besides the use of fillers, another frequent practice is blending polymers to enhance inherent properties, biodegradability and reduce costs.

Examples of PHAs blends with other synthetic and natural polymers, including polysaccharides such as starch [213], natural rubber [214,215] and other polyesters like polylactic acid (PLA) [216,217] have been reported in the literature. P(3HB-*co*-3HV) copolymers have also been blended with other PHAs like poly(3-hydroxybutyrate-*co*-3-hydroxyhexanoate) (PHBHHx) [218,219] or amorphous *mcl*-PHA [219].

For instance, Godbole et al. have shown an improvement in mechanical properties, thermal stability, and cost reduction by blending P3HB with starch. Blends of P3HB and polylactic acid (PLA) at different ratios have been studied by Zhang et al., who demonstrate the



establishment of molecular interactions between components with a consequent improvement in tensile properties [220]. Toughening with natural rubber (NR) has also been considered as a simple and economical route to reach good properties of a thermoplastic matrix thanks to the role of NR as a stress concentrator [214].

Nevertheless, to obtain significant improvements in the physical-chemical and mechanical properties, great attention must be paid to the formulation and the processing conditions to avoid phase segregation phenomena, which could lead to a decrease in the general performance of the material. Quite all studies about blending demonstrate the necessity of using a compatibilizer or a cross-linker like grafting with glycidyl methacrylate [221] or dicumyl peroxide [222] to allow the miscibility of P3HB or P(3HB-*co*-3HV) (< 8 mol% 3HV) with other polymers [221,222].

A valid approach to encourage miscibility could be the use of 3HV-rich copolymers exploiting the presence of an extensive amorphous fraction that may limit phase segregation phenomena. However, no study on 3HV-rich P(3HB-*co*-3HV) copolymers blending has been yet conducted, causing a lack of knowledge.

In this chapter, the role of 3HV content on common processing aspects such as compounding, use of fillers and blend preparation is shown trying to fill the gap of knowledge about 3HV-rich copolymers by answering the following three questions:

- How can the process impact the final mechanical properties of P(3HB-*co*-3HV)-based materials with increased 3HV content?
- How the increased 3HV content impacts the nucleating effect of BN (which is already well known for P3HB and P(3HB-*co*-3HV) with low 3HV content)?
- How the increased 3HV content impacts the ability of P(3HB-*co*-3HV) to be blended with a toughening additive such as *mcl*-PHAs?

## 1. Materials and methods

### 1.1 Materials

P(3HB-*co*-3HV) containing about 1-3 mol% of 3-hydroxyvalerate units (3HV), was purchased from NaturePlast under the reference PHI003 in the form of a very fine powder. It is noted PHBV3 in the present study. P(3HB-*co*-3HV) copolymers with 18 and 28 mol% of 3HV units (noted respectively PHBV18 and PHBV28) were produced by UMR IATE (Montpellier, France) in the frame of the ANR LOOP4PACK project, as reported in [223] and extracted using a solvent-free high-pressure homogenization (HPH) based method [208]. Boron Nitride (BN) purchased from Sigma Aldrich was used as a nucleating agent. The *mcl*-PHA, containing 70 wt% of 3-hydroxynonanoate (3HN), 29 wt% of 3-hydroxyheptanoate (3HHp) and 1 wt% of 3-hydroxyvalerate (3HV) units, was purchased from Versamer in the form of a single sticky block under the reference PHN970. Before compounding, *mcl*-PHA was reduced in a powder by crushing the block in liquid nitrogen. The resulting powder was further dried at 25 °C in vacuum oven for 24 hours. Intrinsic physical-chemical characteristics of all used polymers are summarized in Table 3.1.

**Table 3.1** Physical-chemical characteristics of the materials used in this study: purity, molecular weight (MW), melting temperature ( $T_m$ ), glass transition temperature ( $T_g$ ) and crystallinity degree.

Sample	Purity (%)	MW (Kg mol <sup>-1</sup> )	$T_m$ (°C)	$T_g$ (°C)	Crystallinity degree (%)
PHBV3	n.p.	1124	$174.3 \pm 0.2^{**}$	$1.2 \pm 0.1^{**}$	$69 \pm 3^{**}$
PHBV18	95	$935 \pm 25^*$	$120.8 \pm 0.0^*$ $174.4 \pm 0.0^*$	$1.0 \pm 0.2^*$ $64.5 \pm 0.1^*$	$63 \pm 1^*$
PHBV28	98	$1075 \pm 14^*$	$94.5 \pm 0.5^*$ $173.5 \pm 1.2^*$	$-4.4 \pm 1.4^*$ $52.8 \pm 0.4^*$	$55 \pm 1^*$
<i>mcl</i> -PHA	n.p.	104	46	-40	0

n.p. non provided

\*From Doineau et al. [208]

\*\*From Bossu et al. [224].

## 1.2 Methods

### 1.2.1 Preparation of P(3HB-co-3HV)-based films

P(3HB-co-3HV) powders were mixed with 5 wt% of *mcl*-PHA and either 0.5, 1, and 2 wt% of BN, by manual agitation for 2 min. The codification of samples is given in Table 3.2. Before compounding, the mixtures were dried at 25 °C under vacuum for 24 hours to eliminate traces of humidity and limit thermodegradation phenomena during processing. In the case of virgin P(3HB-co-3HV), samples were dried at 50 °C. The compounding step was carried out by melt extrusion using a Process 11 thin screw extruder (Thermo Scientific, Germany) with an L/D of 40, a screw diameter of 11 mm, and a 3 mm rod die. The temperature profile has been adjusted according to the melting point of P(3HB-co-3HV)<sub>s</sub>, *i.e.* 130-160-180-180-180°C for PHBV3 and 130-130-160-160-160 °C for PHBV18 and PHBV28 from the feeder to the die. The polymer was fed manually and the screw speed was 150 rpm. The extruded rods were cooled at room temperature and pelletized using a granulator (Thermo Scientific, Germany). Resulting compounds were dried at 25 °C under vacuum for 24 hours before being pressed in films using a heating hydraulic press (20T, Pinette Emidecau Industries, Chalon-sur-Saône, France). For that purpose, 2.2 g of pellets were heated between two Teflon coated films in a 100 µm thick mold to obtain films of 12x12 cm<sup>2</sup> following 4 processing steps: contact with plates at heating temperature for 5 min, then pressing from 50 bar to 100 bar at heating temperature during a period time of 1 minute, then applying a pressure of 150 bar for 1 minute and finally cooling during 10 minutes under a constant weight of 1 kg. Different heating temperatures have been used for the preparation of the films, depending on the sample formulation. PHBV3 was pressed at 180 °C while PHBV18 and PHBV28 were pressed at both 160°C and 170 °C, to evaluate the impact of the heating temperature on final material properties.

In the case of virgin polymers, films were also produced directly from powders, by skipping the compounding step. Non-extruded samples were noted PHBV3<sub>ne</sub>, PHBV18<sub>ne</sub> and PHBV28<sub>ne</sub>.

All the films were stabilized for 14 days at 25 °C and 50 % HR before further characterization.

**Table 3.2** Codification of samples.

Neat polymer	+0.5 wt% BN	+1 wt% BN	+2 wt% BN	+ 5 wt% <i>mcl</i> -PHA	+0.5 wt% BN + 5 wt% <i>mcl</i> -PHA
PHBV3	PHBV3_0.5BN	PHBV3_1BN	PHBV3_2BN	PHBV3_5mcl	PHBV3_0.5BN_5mcl
PHBV18	PHBV18_0.5BN	PHBV18_1BN	PHBV18_2BN	PHBV18_5mcl	PHBV18_0.5BN_5mcl
PHBV28	PHBV28_0.5BN	PHBV28_1BN	PHBV28_2BN	PHBV28_5mcl	PHBV28_0.5BN_5mcl

### 1.2.2 Thermal characterization

Differential Scanning Calorimetry (DSC) analyses were carried out using a TA Instruments (Q200 modulated DSC, TA Instruments, New Castle, USA) calorimeter under a nitrogen atmosphere with a flow rate of 50 mL min<sup>-1</sup> and at a heating rate of 10 °C min<sup>-1</sup>. Around 12 mg of sample was used for each analysis. Melting enthalpies have been used as an indicator of crystallinity, because of the lack of  $\Delta H_m^0$  for P(3HB-*co*-3HV) copolymers with higher 3HV content making impossible to calculate the crystallinity %. The shifting in melt crystallization has been calculated according to equation (1) and has been taken as an indication of BN nucleation ability in P(3HB-*co*-3HV) nucleated samples.

$$\Delta T_{mc} = T_{mc}(\text{nucleated PHBV}) - T_{mc}(\text{neat PHBV}) \quad (1)$$

TGA was carried out using a Mettler TGA2 device (Schwerzebbach, Switzerland) equipped with an XP5U balance. Samples were heated from 25 °C to 600 °C at 10 °C min<sup>-1</sup> under nitrogen flow of 50 mL min<sup>-1</sup>. Results were analyzed using STARe software. The maximum degradation temperature ( $T_d$ ) corresponded to the temperature at which the degradation rate was maximum. The onset temperatures ( $T_d^{\text{onset}}$ ) were measured respectively when the first derivative of the weight loss became higher than 0.1 % °C<sup>-1</sup> and lower than 0.1 % °C<sup>-1</sup>. Analyses were done at least in triplicate. Simulated TGA traces of PHBV/*mcl*-PHA blend have been plotted by applying the additive rule and used for compatibility evaluation. The used equation (2) is the following:

$$W_{A-B} = (1 - x)W_A + xW_B \quad (2)$$

where  $W$  is the TGA curve,  $A$  and  $B$  are the component of the blend and  $x$  is the weight fraction of component  $B$ .

### 1.2.3 Tensile tests

Tensile properties were measured on stabilized samples using an Instron 68SC-5 machine, equipped with a 50N cell, at a crosshead speed of 10 mm min<sup>-1</sup>, on samples cut in dumbbell shape with a width of 4 mm, an effective length ( $L_0$ ) of 22 mm and a distance between jaws of 45 mm. Ten replicates were characterized for each formulation.

### 1.2.4 Polarized optical microscope measurements (POM)

Polarized optical microscopy (POM) analysis was performed by an Optiphot2-Pol light microscopy (Nikon) equipped with a Linkam HFS 91 hot stage (Linkam, Tadworth, UK) driven by a Linkam TP 92 temperature controller. The images were acquired by a Nikon D7200 camera. Nucleated and neat PHBV films were melted and cooled to room temperature. Pictures were acquired after 2 weeks of stabilization at 25 °C.

### 1.2.5 Scanning electron microscopy (SEM)

The morphology of the PHBV\_5mcl and virgin PHBVs liquid nitrogen fractured pellets was investigated by scanning electron microscopy using a field emission scanning electron microscope (AURIGA, Zeiss, Jena, Germany). Prior to measurements samples were gold sputtered.

### 1.2.6 Water Vapor Permeability

Water vapor permeability of films (mol·m<sup>-1</sup>·s<sup>-1</sup>·Pa<sup>-1</sup>) was determined at 23°C using a gravimetric method. Films (five repetitions) were hermetically sealed with Teflon seal in glass permeation cells containing distilled water. These cells were placed in a desiccator containing silica gel (RH around 3%). They were weighed using a four-digit balance (BALCO – Type LX 220A, Switzerland) at regular intervals for 7 days. Water vapor permeability was calculated from the following equation:

$$WVP = \frac{S \times e}{3600 \times A \times \Delta P \times M_{H_2O}} \quad (3)$$

where  $S$  is the slope of the weight change from the straight line (g·h<sup>-1</sup>),  $A$  is the permeation area (m<sup>2</sup>),  $e$  is the average specimen thickness (m),  $\Delta P$  is the water vapor pressure differential (Pa), and  $M_{H_2O}$  is the molar mass of water (g·mol<sup>-1</sup>).

## 2. Results and discussion

### 2.1 Effect of 3HV content on processability and mechanical properties

It is largely described in literature that increasing 3HV content results in higher ductility due to the formation of smaller and homogeneous spherulites [37,225]. Recently, an in-depth DSC analysis of HPH-recovered P(3HB-co-3HV)s combined with mechanical testing allowed identifying an optimal processing temperature for each grade of P(3HB-co-3HV) [208]. Such results were gathered on films prepared using a simple thermopressing step of the polymer powders, so without considering the possible shearing effects that may occur during a preliminary compounding step by melt extrusion. In this context, the aim of this work was to assess if an additional compounding step impact the final mechanical properties of P(3HB-co-3HV)-based materials with increased 3HV content.

Regardless of the monomeric composition, it was possible to obtain continuous rods of P(3HB-co-3HV) thanks to their high molecular weight (Table 3.1). However, the ability to pelletize the rods depended on the 3HV content. In fact, unlike PHBV3, which crystallizes rapidly, PHBV18 and PHBV28 were sticky upon exiting the die and required stabilization for at least 30 min before the granulation. This behaviour is the consequence of the different crystallization rates of copolymers, which are very low for PHBV18 and PHBV28 samples as evidenced by Doineau et al. [208]. The thermograms relative to the first and second heating scans of pellets are displayed in Figure 3.1 and the temperature and enthalpy of the observed transitions are reported in Table S3 (table S3 is reported in supporting file at the end of the chapter).

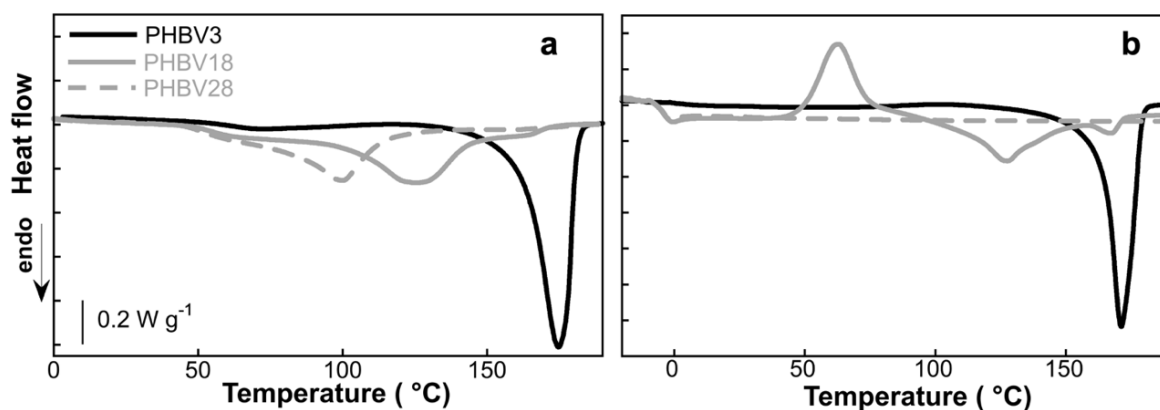
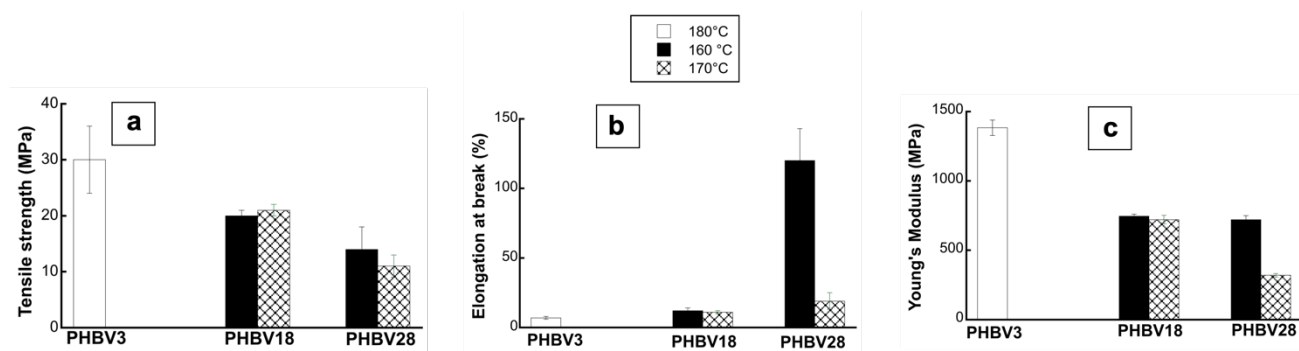


Figure 3.1 First (3.1a) and second (3.1b) heating scan of PHBV3, PHBV18 and PHBV28 pellets.

The first scan confirmed that the melting temperature decreased with increasing the 3HV content, from 174°C for PHBV3 to 94°C for PHBV28 (Table S3, Figure 3.1a). When polymers were heated up to 190 °C, melt crystallization was hindered for P(3HB-co-3HV) with increased 3HV content due to the difficulty for P(3HB-co-3HV) to reach a new ordered system when all the nuclei are eliminated, especially because of a drop of viscosity that hinders heterogeneous nucleation [208]. In fact, PHBV18 pellets melt crystallize partially at  $T_{mc}= 39$  °C with a very low enthalpy ( $\Delta H_{mc}= 1.3 \pm 0.4$  J g<sup>-1</sup>) and underwent a further substantial cold-crystallization ( $\Delta H_{cc}= 36$  J g<sup>-1</sup>) only in the following heating at about  $T_{cc}=62$  °C (Figure 3.1b). PHBV28 showed no melting nor cold crystallization, remaining amorphous at the end of the cooling, as revealed by the absence of melting peak during the second heating (Figure 3.1b). The crystallization process of PHBV18, occurring in two stages (melt and cold crystallization), implies the formation of spherulites in different conditions, characterized by different morphologies and dimensions. Differently, PHBV3 completely crystallized upon cooling, not showing further crystallization in the subsequent heating scan.

The thermal stability of pure copolymers was evaluated by TGA experiments, which showed that the main thermal degradation temperature of the P(3HB-co-3HV) pellets decreased from 264°C for PHBV3 down to 223 °C and 234°C for PHBV18 and PHBV28, respectively (Table 3.3). Worth to note that the increase in the temperature of thermodegradation together with the decrease in melting temperatures for PHBV28 contribute to widening the processing window.

Since the processing temperature, and thermal history in general, is known to influence crystallization mechanisms, and thus resulting micro-crystalline structure and mechanical properties, PHBV18 and PHBV28 films were prepared at the optimum processing temperatures (160 and 170 °C) that were identified in a previous work [208]. In this way, the effect of thermopressing temperatures on mechanical properties of P(3HB-co-3HV) films submitted to a double thermal treatment (first melt extrusion step to obtain compounds, followed by a thermopressing step to obtain films) has been established (Figure 3.2).



**Figure 3.2** a) Tensile strength (MPa), b) elongation at break (%) and c) Young's Modulus (MPa) of PHBV3, PHBV18 and PHBV28 films prepared from compounded pellets and thermopressed at 160, 170 and/or 180 °C.

Due to their high crystallinity, films made of PHBV3 exhibited a low elongation at break ( $7 \pm 1$  %), together with high tensile strength ( $30 \pm 6$  MPa) and Young's Modulus values ( $1383 \pm 55$  MPa). Increasing the 3HV content from 3 to 18% resulted in a general decrease of tensile strength ( $20 \pm 1$  MPa and  $21 \pm 1$  MPa for PHBV18 thermopressed respectively at 160 °C and 170 °C), a slight improvement of the elongation at break ( $12 \pm 2$  % and  $11 \pm 1$  % for PHBV18 thermopressed respectively at 160 °C and 170 °C) and a decrease of the Young's modulus ( $746 \pm 15$  MPa and  $721 \pm 31$  MPa for PHBV18 thermopressed at 160 °C and 170 °C). For PHBV28 thermopressed at 160°C, a huge increase of the elongation at break up to  $120 \pm 23$  %.

The thermopressing temperature, i.e. 160°C or 170°C, did not significantly affect the mechanical properties of PHBV18 films, while all the mechanical characteristics of PHBV28 films experienced a huge drop as the thermopressing temperature increased by only 10°C. Thermodegradation could occur with the consequent production of oligomers, which make PHBV28 films more brittle. This observation led to the conclusion that the beneficial effect of increasing the 3HV content can be negatively counterbalanced by an inappropriate choice of processing temperature.

Data collected for films thermopressed at 160 °C were compared with those produced at the same temperature but by a simple thermopressing of powders (without a preliminary compounding step), to evaluate the effect of additional thermal treatment and shearing stresses caused by the melt extrusion step (Figure 3.3). Interestingly, both the tensile strength and elongation at break of films obtained by thermopressing compounded pellets were globally higher than that of films directly obtained from powders (Figure 3.3a and



3.3b). The increase in elongation at break was very low for PHBV3 (from  $2 \pm 1\%$  to  $7 \pm 2\%$ ) and PHBV18 (from  $7 \pm 1$  to  $12 \pm 1\%$ ), while it was huge for PHBV28 (from  $27 \pm 4$  to  $120 \pm 23\%$ ). The Young's modulus was decreased for PHBV3 (from  $2285 \pm 57$  to  $1383 \pm 67$  MPa), while it was slightly increased for PHBV18 (from  $695 \pm 224$  to  $721 \pm 29$  MPa) and PHBV28 (from  $334 \pm 6$  to  $371 \pm 31$  MPa). The improvement of ductility observed for extruded samples was ascribed to favoured chain entanglement induced by shear forces occurring during extrusion.

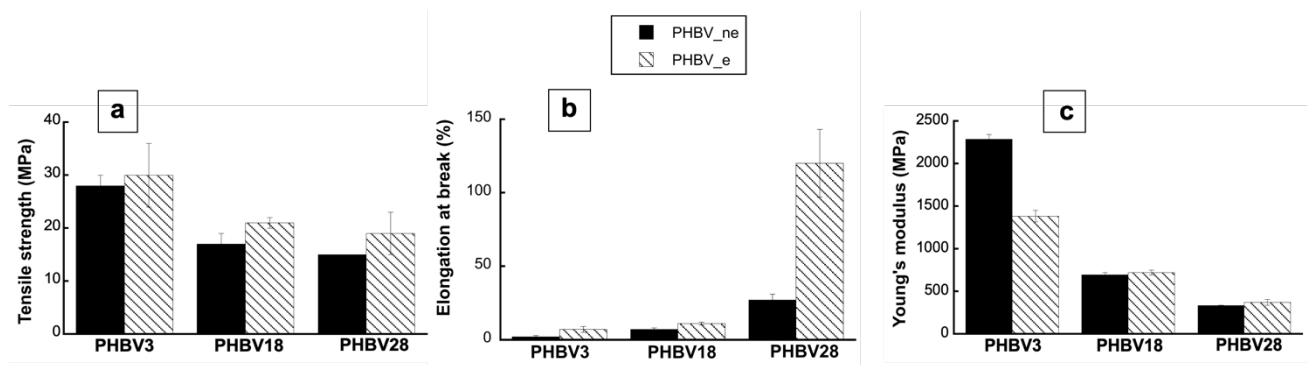


**Figure 3.3** a) Tensile strength (MPa);,b) elongation at break (%) and c) Young's modulus (MPa) of P(3HB-co-3HV) films obtained by thermopressing at 160°C either powders (PHBV\_ne) or compounded pellets (PHBV\_e)

Although the increase in the 3HV content displays the advantage to reduce the brittleness and enlarge the processing window, it has the side effect to decrease crystallization rate and, hence, the rapid material solidification in processing stages. The low crystallization rate also implies that materials crystallize for a long time after the melt processing, possibly through different and uncontrollable stages. This could favour the formation of different crystal structures and morphology, which make the properties of P(3HB-co-3HV) manufactures unpredictable and unstable. The next section therefore deals with the addition of boron nitride as nucleating agent, which has already been widely used for P3HB and P(3HB-co-3HV) with low 3HV content, and aims to assess how the increased 3HV content impacts the nucleating effect of BN.

## 2.2 Effect of BN addition

One of the main challenges in P(3HB-co-3HV) processing is to produce compounds with improved processability by accelerating melt crystallization. To do so PHBV3, PHBV18, and

PHBV28 were mixed with various concentrations of BN, used as nucleating agent. Thermal properties were evaluated through DSC and TGA measurements (Tables 3.3).

Nucleation efficiency (NE) is usually evaluated based on the self-nucleating theory [226,227]. In this work, NE of different BN amounts has been estimated by considering only the shifting of melt crystallization temperature towards higher temperature (named  $\Delta T_{mc}$ ) as an indicator of nucleation ability.

**Table 3.3** Melting enthalpies from first heating scan ( $\Delta H_m$ ), nucleation efficiency ( $\Delta T_{mc}$ ) and onset thermal degradation temperatures ( $T_d^{onset}$ ) of virgin and nucleated P(3HV-co-3HV)s.

Sample	$\Delta H_m$ (J.g <sup>-1</sup> )	$\Delta H_{mc}$ (J.g <sup>-1</sup> )	$\Delta T_{mc}$ (°C)	$T_d^{onset}$ (°C)
PHBV3	87.22±0.74	75.83±0.84	-	264 ± 1
PHBV18	29.60±0.72	1.26±0.42	-	223±1
PHBV28	21.13±1.59	0.36±0.19	-	234±3
PHBV3_0.5BN	96.71±0.66	87.05±1.17	24	280±0.7
PHBV18_0.5BN	28.70±0.06	41.69±1.00	30	242±9.9
PHBV28_0.5BN	20.45±0.44	0.34±0.20	0	263±2
PHBV18_1BN	27.08±0.42	41.48±1.10	33	225±5.7
PHBV28_1BN	15.66±2.50	1.56±0.53	9	263±0.7
PHBV28_2BN	19.1±1	0.60±0.06	6	259±6.4

As already reported for P(3HB-co-3HV) with low 3HV content [209,228], the addition of only 0.5 wt% of BN in PHBV3 resulted in an increase of the melt crystallization for PHBV3 and PHBV18 while it has not significant effect on PHBV28 (Table 3.3). For PHBV3 and PHBV18, such a BN content was sufficient to avoid two-stage crystallization since no cold crystallization was observed (Figure 3.4).

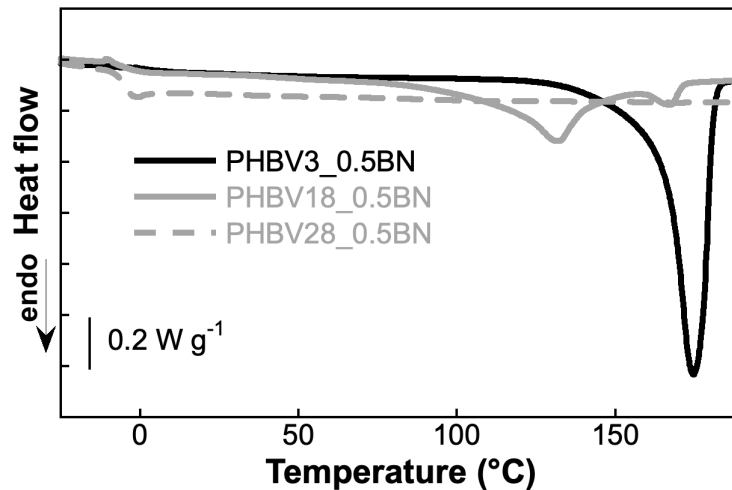


**Figure 3.4** Second heating scan for PHBV3\_0.5BN, PHBV18\_0.5BN and PHBV28\_0.5BN. The second heating scan was recorded from -30 °C to 190 °C at 10 °C min<sup>-1</sup>

In case of PHBV3, the addition of BN also resulted in a higher crystallinity, as shown by the increase in melting enthalpy ( $\Delta H_m$ ) of PHBV\_0.5BN has been compared to neat PHBV (Table 3.3). It was not the case for PHBV18. POM observations reported in Figure 3.5 confirmed the efficiency of the addition of a low amount of BN to reach smaller spherulites in the case of PHBV3, passing from 140  $\mu\text{m}$  for neat PHBV3 to about 10  $\mu\text{m}$  for PHBV3\_0.5BN. Conversely, morphology and dimensions of PHBV18 and PHBV28 spherulites were not affected. The lower dimension of neat PHBV18 and PHBV28 spherulites (figures 3.5c and 3.5e), around the order of magnitude of 13 and 9.5  $\mu\text{m}$  respectively, makes it difficult to notice changes in dimension and structures. Worth to note that the lower dimension of virgin PHBV18 and PHBV28 spherulites could be ascribed to the presence of impurities deriving from the extraction process which could act as nucleating agents themselves [208]. Since 0.5 wt% BN was not enough to ensure shorter crystallization times for P(3HB-co-3HV) enriched in 3HV units, additional formulations with increasing BN amounts were prepared.  $\Delta T_{mc}$  values demonstrated a greater ability of 1 wt% BN to allow for faster crystallization in PHBV28 ( $\Delta T_{mc} = 9^\circ\text{C}$ ), while PHBV18 showed quite a constant value. PHBV28 was mixed with even more BN (2 wt%) but no noticeable change was detected. The obtainment of constant  $\Delta T_{mc}$  values for PHBV18\_1BN and PHBV28\_2BN may be caused by the aggregation of BN particles. Despite the addition of higher content of BN as 1 wt% improve

crystallization when 3HV content increase, PHBV28 still show a slow crystallization form the melt.

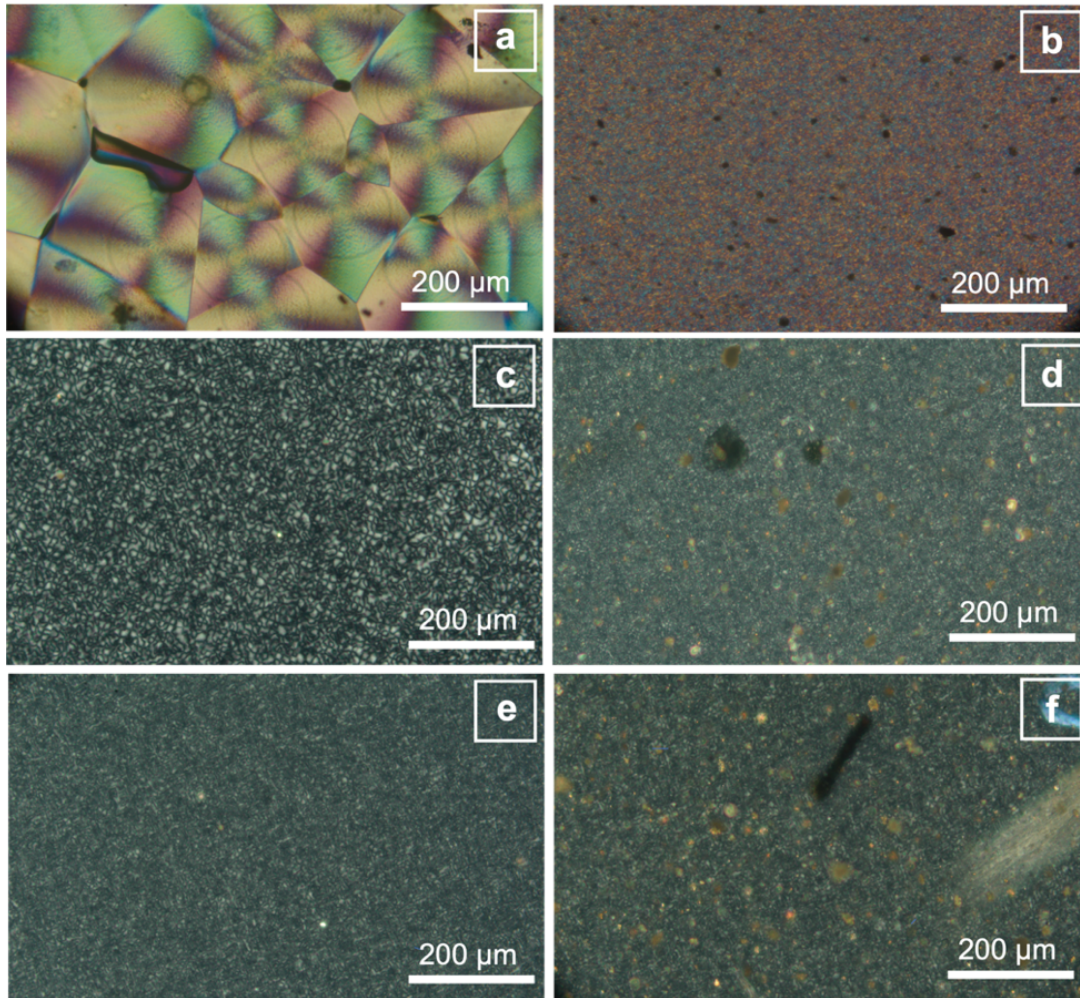


**Figure 3.5** POM images (mag 20x) of virgin and nucleated P(3HB-co-3HV)s with 0.5 wt% of BN. a) PHBV3 b) PHBV3\_0.5 c) PHBV18 d) PHBV18\_0.5 e) PHBV28 f) PHBV28\_0.5

PHBV3 thermal stability was not affected by the presence of BN since there was no shift in thermal degradation temperatures, according to the results shown in Miao et al [210] work. In contrast, PHBV18 and PHBV28  $T_d^{\text{onset}}$  values increased according to added BN amount, reaching a quite constant value at higher %wt BN because of filler aggregation as in the case of PHBV/clay nanocomposites in Chen et al work [229], confirming DSC results. Improvement in thermal stability may be attributed to BN's strong thermal conductivity[230,231] and capacity to prevent local heat accumulation, which delays the generation of degradation by-products and protects the polymeric matrix from thermodegradation. Additionally, according to Yu et al research, the inclusion of BN may limit the thermal motion of polymer chains and enhance thermal stability [232].



The impact of BN addition on mechanical properties was assessed through uniaxial tensile tests, the obtained stress-strain curves are shown in Figure 3.6.

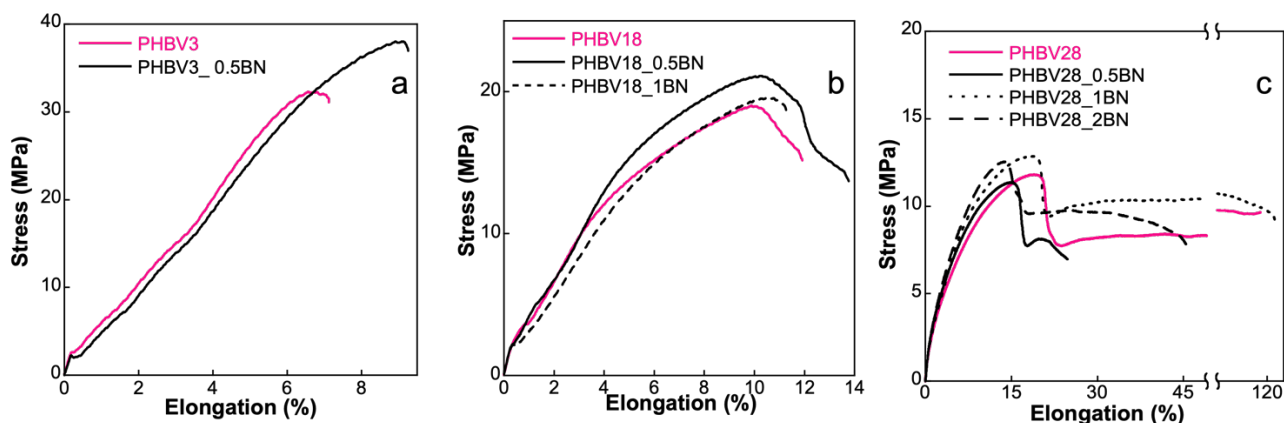


**Figure 3.6** Stress-elongation curves of virgin and nucleated PHBV3 (a), PHBV18 (b) and PHBV28 (c) films.

Although PHBV3 crystallinity degree did not change when 0.5 wt% BN was added, a slight increase in tensile strength (from  $30 \pm 6$  MPa to  $38 \pm 2$  MPa) and elongation at break (from  $7 \pm 2$  % to  $9 \pm 1$  %) occurred. The toughening may be related to greater nucleation density, resulting in a more homogeneous crystalline morphology, as highlighted in Figure 3.5. BN addition had no relevant effect on mechanical properties of PHBV18 films, with tensile strength and elongation at break values comprised in the range of 18–20 MPa and 10–13%, respectively. However, the BN addition to PHBV28 led to a more contrasted results depending on the amount of added BN. In fact, a reduction of tensile strength and elongation at break values was observed for PHBV28\_0.5BN and PHBV28\_2BN. However, the addition of 1 wt% BN induced higher tensile strength, stress at break and similar elongation at break values. This observation agreed with DSC and TGA results and corroborated that PHBV28\_1BN might be the optimal formulation to ensure the best thermal and mechanical performances. The addition of lower or higher BN amount (0.5 or 2 wt%) to PHBV28 led to worst polymer elongation at break. This could be due to a series of factors including polymer matrix viscosity and specific parameters of the filler such as percolation threshold ( $\phi$ ). In the case of 0.5 wt% BN addition the amount of filler is not enough to reach a good mixing in the PHBV28 matrix respect to PHBV18 and PHBV3 due to hypothetical differences in viscosity and melt flow behavior. On the other hand, the addition 2 wt% of BN to PHBV28 lead to a better filler distribution but probably this value

is close to the percolation threshold and the formation of network between BN particles starts. Agglomerates could be disrupted and filler redispersed by shear forces during mixing processes, but maybe the screw speed used for this work is not enough to ensure filler redispersion.

### 2.3 Effect of *mcl*-PHA addition

One of the drawbacks of P3HB and P(3HB-*co*-3HV)s with low 3HV content is the high crystallinity, which limits first mechanical performance but also miscibility with other polymers, particularly with amorphous ones. In fact, different crystallinity levels and crystallization kinetics cause phase separation and therefore poor mechanical properties. Modulating P(3HB-*co*-3HV) crystallinity by varying monomeric composition is a potential solution to immiscibility. Blends of P(3HB-*co*-3HV)s and *mcl*-PHA were prepared and characterized aiming at the investigation of the effect of monomeric composition on miscibility with other polymers and the obtainment of more flexible films suitable for food packaging applications.

Thermal properties are in general unchanged with respect to the neat PHBV (Table S3), but DSC analysis highlighted a plasticizing effect of *mcl*-PHA on PHBV18. In fact, PHBV18\_5mcl showed a drop in cold crystallization temperature and melting point, which may be associated with enhanced chain mobility causing a lowering of the activation energy required for cold crystallization. DSC measurements are usually carried out to verify miscibility in binary blends through the presence of a single glass transition (as well as crystallization and melting) [233–235].

Interestingly, there was no multiple thermal transitions in all PHBV\_5mcl blends. To clarify if this might be ascribed to miscibility or not, TGA analysis has been conducted and data were analysed using the additive rule according to the equation reported in section 1.2.2. The additive rule consists of a simulation of TGA curve starting from the weighted contribution of each component of a blend [219,236] considering the hypothesis of the interaction and miscibility absence, between components.

Comparison between simulated and experimental TGA curves is illustrated in Figure 3.7.

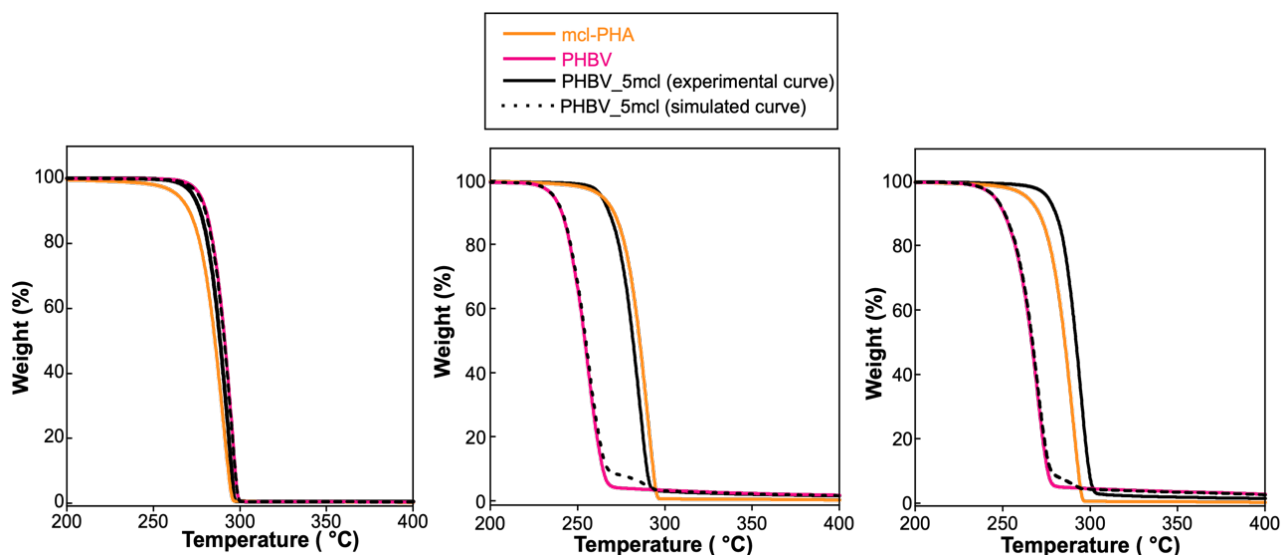


**Figure 3.7** Comparison between experimental and simulated TGA curves of PHBV\_mcl blends and pure components a) PHBV3 b) PHBV18 c) PHBV28.

In all cases, experimental curves of both single components and blends exhibited only one weight loss.

Regarding thermal stability, it is worth to note that mcl-PHA thermodegradation starts at lower temperature than PHBV3 (261 °C for mcl-PHA respect to 270 °C of PHBV3) while it is more thermally stable than PHBV18 (223 °C) and PHBV28 (234 °C). Mixing PHBV3 and mcl-PHA does not result in noticeable changes of thermal stability. No difference between experimental and simulated curves was observed for PHBV3\_5mcl, meaning that, according to the additive rule, PHBV3 and mcl-PHA were not miscible. The reason for such behavior could be the independent crystallization of two phases after consecutive cooling which results in macrophase separation. On the other hand, PHBV18\_5mcl and PHBV28\_5mcl experimental curves show that degradation start respectively at 254 °C and 264 °C. Thus, the addition of 5 wt% mcl-PHA to PHBV18 or PHBV28 led to the obtainment of blends with high thermal stability than PHBVs alone (degradation starts at 223°C and 234 °C for PHBV18 and PHBV28 respectively). Comparing experimental and simulated curves it emerges that blend are more thermally stable since degradation started at higher temperatures than those predicted (229 °C and 238 for PHBV18 and PHBV28). The discrepancy between experimental and simulated findings suggests that mcl-PHA and PHBV with a greater 3HV concentration could interact. Crystallization rate is lower in PHBV copolymers with larger

3HV unit contents, which means insufficient time for a melted blend to demix favouring miscibility with a more amorphous polymer, as is the case of PHBV18\_5mcl and mainly PHBV28\_5mcl.

Regarding Figure 3.8, it appears that the immiscibility implies a worsening in morphology and mechanical properties, i.e. tensile Young's modulus and strength, of all P(3HB-co-3HV) / mcl-PHA blends.

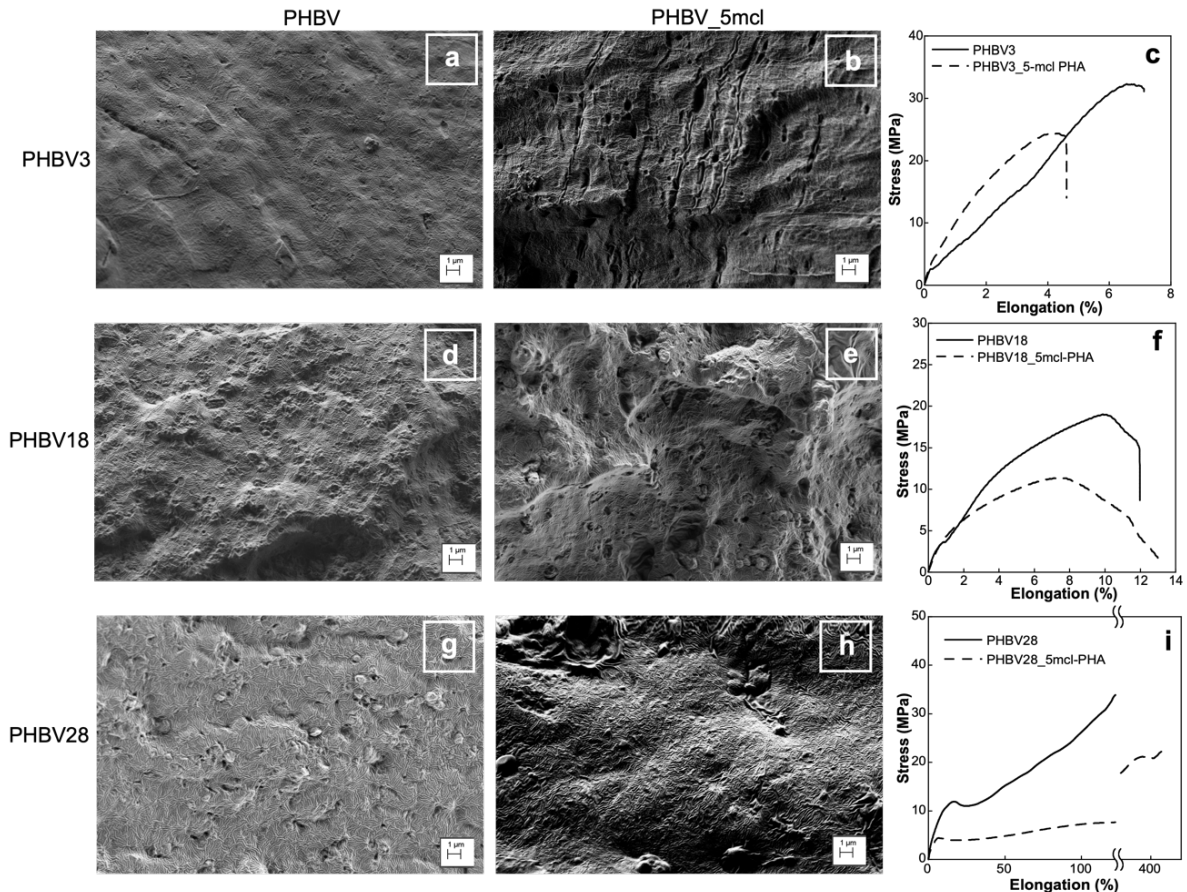


**Figure 3.8** SEM micrographs (mag 10k x) and stress-strain curves of PHBV3 (fig 3.8a-c), PHBV18 (fig 3.8d-f) and PHBV28 (fig 3.8g-i) blend with 5 wt% of mcl-PHA.

Morphological analysis carried out by scanning electron microscopy confirmed the hypothesis that, according to their monomeric composition, P(3HB-co-3HV)s are characterized by different compatibility with *mcl*-PHA. PHBV3 (Figures 3.8a and 3.8b) had a droplet-matrix-like morphology, typical of immiscible blends. The holes are caused by the segregation of amorphous polymer, leading to the creation of two macrophases and therefore to the formation of interfaces which may act as preferential planes of fracture causing the reduction of elongation at break values (Figure 3.8c). Even though TGA results, PHBV18\_5mcl exhibits an irregular morphology (Figures 3.8d and 3.8e) and a tensile



strength drop by almost 50% (Figure 3.8f) behaving like an immiscible binary blend. On the other hand, increasing 3HV to 28 mol% results in a more regular morphology and different mechanical properties as in the case of PHBV28\_5mcl. The latter shows no droplet-matrix-like structure (Figures 3.8g and 3.8h) and an improvement in elongation at break which increases from  $120 \pm 23$  % to  $400 \pm 200$  % (Figure 3.8i).

It is worth to note from the images reported in Figure 3.9 that PHBV18\_5mcl and PHBV28\_5mcl films are transparent. Transparency is a key factor when selecting food packaging materials that permit to the consumers see the product inside and control its physical condition.

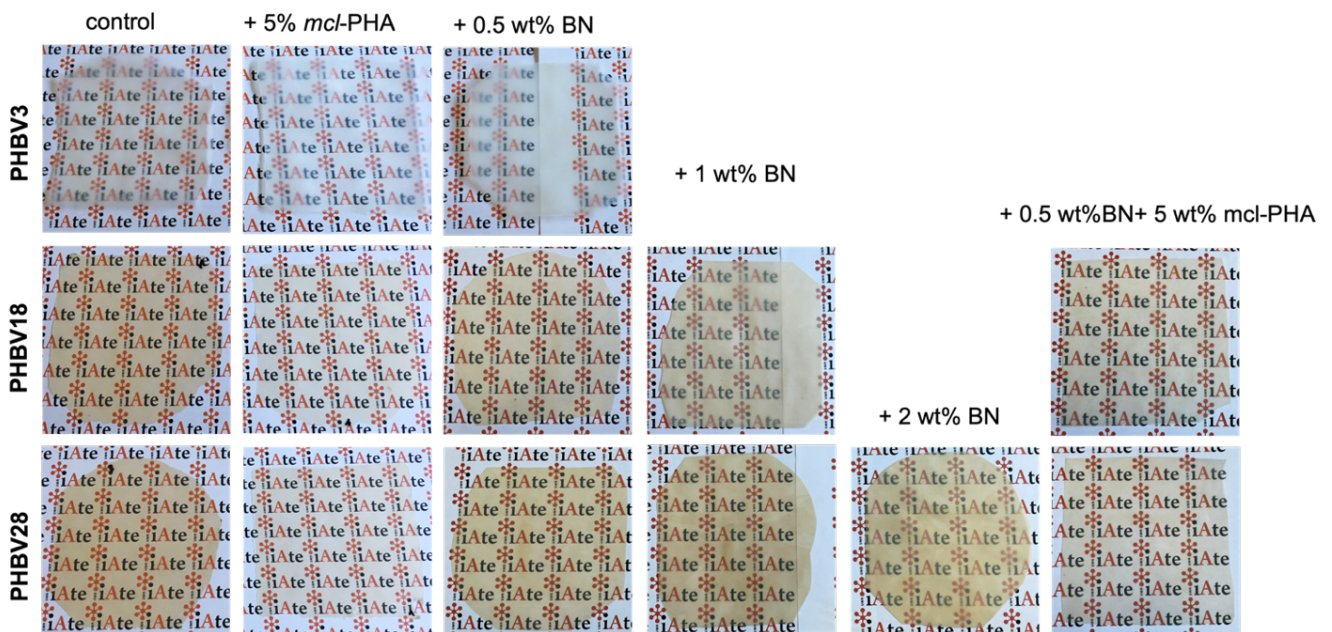


**Figure 3.9** Comparison between neat PHBV and PHBV-based formulations visual aspect. It is worth noting that PHBV\_5mcl are more transparent than neat copolymers.

Mechanical and morphological results are therefore in good agreement with thermal characterization outcomes which evidence different degrees of compatibility PHBV / mcl-PHA depending on the 3HV unit content. PHBV28 is compatible with a more amorphous copolymer (*mcl*-PHA) and combining these two PHAs enables the creation of a material with improved flexibility and qualities suited for food packaging, according to all the data. A higher concentration of *mcl*-PHA could have a stronger plasticizing effect, but it is known that a higher concentration of the second component results in a severe lack of miscibility

and significant phase separation, both of which have an adverse impact on the final characteristics.

#### 2.4 Synergistic effect of BN and *mcl*-PHA addition

The results illustrated in previous sections highlighted the effectiveness of BN addition in reducing melt crystallization time and enhance processability, while *mcl*-PHA thanks to its compatibility with 3HV-rich P(3HB-*co*-3HV) contributed to improve elongation at break and transparency. Considering all the above, synergistic reinforcement of PHBV18 and PHBV28 by adding both the BN and *mcl*-PHA was assessed by preparing ternary compounds of P(3HB-*co*-3HV) with 0.5 wt% BN and 5 wt% *mcl*-PHA. BN quantity has been decided to limit filler segregation. PHBV3 has not been tested because its excessive crystallinity did not allow to produce a miscible blend, the simultaneous addition of both BN and *mcl*-PHA could result in higher immiscibility and worse properties.

The positive effects of BN and *mcl*-PHA on thermal stability illustrated in the previous section were maintained also when added simultaneously, as the increasing of  $T_d^{\text{onset}}$  respect to neat polymers demonstrates (PHBV18 passes from  $223 \pm 0.7$  to  $250 \pm 5$  °C, while PHBV28 from  $234 \pm 3$  to  $262$  °C) (Table S3). On the other hand, no effect on thermal properties analysed by DSC (Table S3) were detected, For example PHBV18 melting temperature is  $125 \pm 2$  °C (1<sup>st</sup> peak) and  $164 \pm 1.01$  °C (2<sup>nd</sup> peak) and it is comparable to PHBV18\_0.5BN\_5mcl ( $123.74 \pm 1.03$  °C 1<sup>st</sup> peak,  $162.52 \pm 0.11$  °C 2<sup>nd</sup> peak).

The production of a ternary compound had a slight impact on mechanical properties (Figure 3.10), particularly visible on PHBV18\_0.5BN\_5mcl.

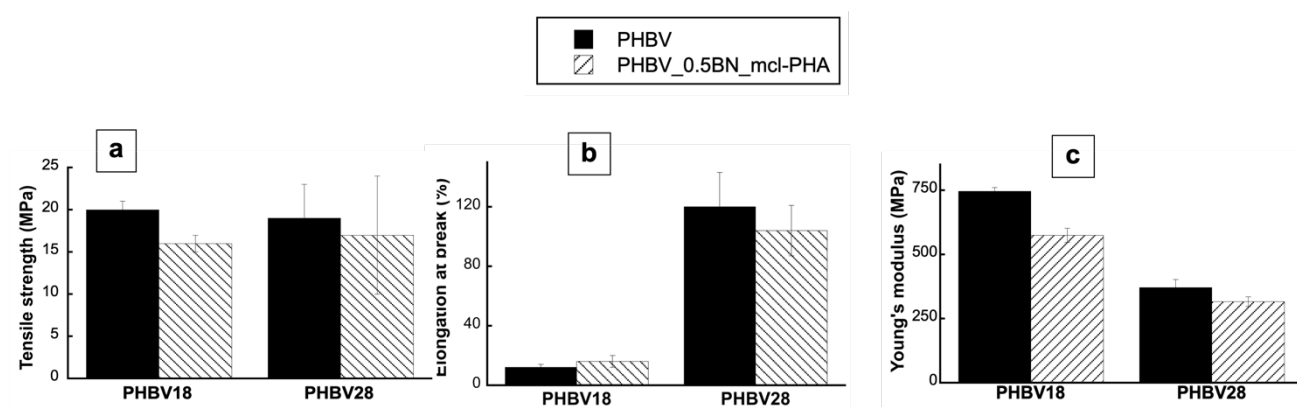


Figure 3.10 Mechanical properties of PHBV\_0.5BN\_5mcl ternary compounds

PHBV18 became slightly more ductile and less rigid, as the elongation at break increased from  $12 \pm 2$  % to  $16 \pm 4$  % and Young's Modulus and tensile strength decreased from  $746 \pm 15$  MPa to  $575 \pm 27$  MPa and from  $20 \pm 1$  to  $15 \pm 1$  MPa respectively. Despite a lowering in elongation at break from  $120 \pm 23$  to  $104 \pm 17$  %, PHBV28 mechanical properties remained high, attesting that the inclusion of a nucleating agent and amorphous polymer did not degrade native properties with the advantage of greater thermal stability. Mechanical properties are affected by high standard deviation values, which reveals a certain heterogeneity within materials. This was ascribed to a bad distribution of mcl-PHA and BN when added simultaneously to the P(3HB-*co*-3HV) matrix.

## 2.5 WVP measurements

WVP measurements were carried out on both neat and formulated PHBV-based films (Table 3.4) to assess if the monomeric composition as well as the formulation can affect one of the main barrier properties of a primary packaging, i.e. the water vapor barrier. Despite the correlation between 3HV content and crystallinity, which in turn affected other properties as discussed in section 2.1, it is worth noting that WVP was not significantly impacted by the different monomeric composition nor by the addition of BN or *mcl*-PHA (or both). This agrees with the study of Miguel and Irui's work [237] about the characterization of water sorption and transport in P3HB and its copolymers with various 3HV content. The constancy of WVP demonstrates that it is possible to improve P(3HB-*co*-3HV) thermal and mechanical properties without affecting significantly the originary barrier property.

**Table 3.4** WVP values of PHBV-based films

Sample	WVP (mol m <sup>-1</sup> s <sup>-1</sup> Pa <sup>-1</sup> )		
PHBV3	7.3 × 10 <sup>-13</sup>	±	1.9 × 10 <sup>-13</sup>
PHBV3_0.5BN	5.1 × 10 <sup>-13</sup>	±	9.4 × 10 <sup>-14</sup>
PHBV3_5mcl	4.4 × 10 <sup>-13</sup>	±	1.2 × 10 <sup>-13</sup>
PHBV18	6.8 × 10 <sup>-13</sup>	±	1.5 × 10 <sup>-13</sup>
PHBV18_0.5BN	7.1 × 10 <sup>-13</sup>	±	1.5 × 10 <sup>-13</sup>
PHBV18_1BN	5.3 × 10 <sup>-13</sup>	±	9.6 × 10 <sup>-14</sup>
PHBV18_5mcl	6.8 × 10 <sup>-13</sup>	±	8.5 × 10 <sup>-14</sup>
PHBV18_0.5BN_5mcl	6.5 × 10 <sup>-13</sup>	±	1.1 × 10 <sup>-13</sup>
PHBV28	6.5 × 10 <sup>-13</sup>	±	1.1 × 10 <sup>-13</sup>
PHBV28_0.5BN	6.7 × 10 <sup>-13</sup>	±	7.1 × 10 <sup>-14</sup>
PHBV28_1BN	6.7 × 10 <sup>-13</sup>	±	1.0 × 10 <sup>-13</sup>
PHBV28_2BN	8.7 × 10 <sup>-13</sup>	±	1.2 × 10 <sup>-13</sup>
PHBV28_5mcl	6.4 × 10 <sup>-13</sup>	±	1.5 × 10 <sup>-13</sup>
PHBV28_0.5BN_5mcl	6.6 × 10 <sup>-13</sup>	±	1.3 × 10 <sup>-13</sup>

## Supplementary files

**Table S3** Thermal properties of neat and formulated P(3HB-co-3HV)s. Values are reported as  $n \pm SD$  ( $n = 3$ )

Sample	1 <sup>st</sup> heating				Cooling				2 <sup>nd</sup> heating				TGA		
	T <sub>g</sub> (°C)	T <sub>m</sub> (°C)	ΔH <sub>m</sub> (J/g)	T <sub>mc</sub> (°C)	ΔH <sub>mc</sub> (J/g)	T <sub>g</sub> (°C)	T <sub>cc</sub> (°C)	ΔH <sub>cc</sub> (J/g)	T <sub>m</sub> (°C)	ΔH <sub>m</sub> (J/g)	T <sub>d<sup>onset</sup></sub> (°C)	T <sub>d<sup>max</sup></sub> (°C)	T <sub>d<sup>offset</sup></sub> (°C)	T <sub>d<sup>max</sup></sub> (°C)	T <sub>d<sup>offset</sup></sub> (°C)
PHBV3	-	175±0	87.22±0.74	95±0	75.83±0.84	4±1	-	-	171±0	92.73±1.42	264 ± 1.4	295±0.7	300±0.7	295±0.7	300±0.7
PHBV3_0.5BN	-	175±0	96.71±0.66	119±0	87.05±1.17	5	-	-	175±0	92.02±7.30	280±0.7	298±1.4	301.5±2.1	298±1.4	301.5±2.1
PHBV3_5mcl	-	176±0	82.77±0.69	99±0	72.65±0.97	4±1	-	-	172±0	88.44±1.01	261±1.4	295±0.7	298±0.7	295±0.7	298±0.7
PHBV18	-4±2	125±2 164±1.01	29.60±0.72 0.87±0.04	39±0	1.26±0.42	-4±1	62±2	36.43±4.62	149±31 167±1	60.21±43.92 3.08±0.04	223±0.7	258±1.4	270±2	258±1.4	270±2
PHBV18_0.5BN	-7±2	123±0 164±1	28.70±0.06 0.83±0.09	70±0	41.69±1.00	-5	-	-	128±6 166±2	29.21±0.76 1.97±1.37	242±9.9	268±9.2	284±4.2	268±9.2	284±4.2
PHBV18_1BN	0.11±3.1 0	122±0.26 153±0.62	27.08±0.42 1.09±0.10	73.38±1.15	41.48±1.10	-	-	-	-	-	225±5.7	263±2	285	263±2	285
PHBV18_5mcl	-5±3	125±0 163±1	27.87±0.58 0.62±0.20	33	1.18±0.08	-3±1	53±2	36.58±0.15	124±0 167±0	31.50±0.83 2.93±0.00	254	286±1.4	294	286±1.4	294
PHBV18_0.5BN_5mcl	1.51 ±2.78	123.74±1.03 162.52±0.11	27.64±0.33 0.57±0.03	55.46±2.11	25.36±7.57	-	-	-	-	-	250±5	284±2.8	292±3	284±2.8	292±3
PHBV28	-2±1	100±1 161±1	21.13±1.59 1.01±0.17	33	0.36±0.19	-6±1	-	-	-	-	234±3	267±3.5	278±3.5	267±3.5	278±3.5
PHBV28_0.5BN	-3±2	100±1	20.45±0.44	33	0.34±0.20	-6	-	-	109±2 168±1	0.31±0.06 0.16±0.03	263±2	292±2.1	302±2.1	292±2.1	302±2.1
PHBV28_1BN	4.08±1.5 0	100.41±0.35 162±2.22	15.66±2.50 1.21±0.01	42.45±1.32	1.56±0.53	-	-	-	-	-	263±0.7	294	304	294	304
PHBV28_2BN	-4 ±0.01	100.68±0.04 161.8±0.51	19.1±1 1±0.02	38.46±2.22	0.60±0.06	-	-	-	-	-	259±6.4	291± 4.2	302±2.1	291± 4.2	302±2.1
PHBV28_5mcl	-2±1	100±1	22.15±1.12	32±1	0.30±0.11	-5±1	-	-	110	-	264.5±0.7	295	395	295	395
PHBV28_0.5BN_5mcl	-4.24 ±0.42	100.16±0.45 173.89±0.12	18.22±1.13 1.22±0.03	29.65 ±14.26	0.40±0.05	-	-	-	-	-	262	294	394	294	394

### 3. Conclusions

The present work investigated the influence of 3HV content on processability and final properties of P(3HB-co-3HV)-based films. In view of improving ductility, it was shown that a 3HV content of 28 mol% was the optimal composition and that the compounding step by melt extrusion was necessary to favour polymer chain entanglement. An elongation at break of 120 % was thus achieved for PHBV28 films obtained by thermopressing compounded pellets.

However, since the increase of 3HV unit content causes a decrease in the crystallization rate, the nucleating effect of BN added in different quantities has been investigated. A threshold limit of 1 wt% BN has been individuated for PHBV28. By adding this amount of BN, a quite good but still low nucleation efficiency ( $\Delta T_{mc} = 9^{\circ}\text{C}$ ) was noticed. It was also a way to strengthen thermal stability ( $T_d^{\text{onset}}$  increases from  $234 \pm 3$  to  $263 \pm 0.7^{\circ}\text{C}$ ). For PHBV28\_1BN the optimal mechanical properties have been individuated, more in particular values of tensile strength of  $13 \pm 1$  MPa, Young modulus of  $393 \pm 13$  and elongation at break of  $122 \pm 16$  % have been estimated.

PHBV28 also shows a good ability to be blended with mcl-PHA. The compatibility between PHBV28 and mcl-PHA could be ascribed to the slow crystallization of PHBV which means insufficient time for a melted blend to demix favouring compatibility. However, the preparation of PHBV ternary compounds did not produce noticeable improved properties. Finally, worth to note that barrier properties of all tested formulations were not affected.

This work provides clarification about 3HV-rich copolymers, proposing interesting solutions to overcome drawbacks related to low processability and ductility and to obtain a potential bio-based and biodegradable material for packaging application.

## **CHAPTER 4**

## **Rapid Estimation of Poly(3-hydroxybutyrate-co-3-hydroxyvalerate) Composition by ATR-FTIR**

### **ABSTRACT**

PHAs thermal and mechanical properties could be tuned by varying their monomeric composition through the proper selection of microorganism feedstock and bioreactor operative conditions. Hence, a rapid and facile determination of the PHA chemical structure by a widely available instrumentation is useful. In alternative to the standard gas-chromatographic method, a new procedure for the composition determination of poly(3-hydroxybutyrate-co-3-hydroxyvalerate) (P3HBV), the most common PHA copolymer, by attenuated total reflection FTIR (ATR-FTIR) is presented. It is based on the linear dependence of selected normalized absorption band intensity with the molar fraction of repeating units. The proposed method proves to be useful for an easy and rapid estimation of P3HBV composition.

### **Adapted from:**

Alfano, S.; Pagnanelli, F.; Martinelli, A.

*Rapid Estimation of Poly(3-hydroxybutyrate-co-3-hydroxyvalerate) Composition by ATR-FTIR.*

Polymers, 2023, 15, 4127

<https://doi.org/10.3390/polym15204127>



The knowledge of the copolymer composition is of utmost importance to control the production process operating conditions and predict the copolymer features required for specific applications.

Nowadays, there are two main methods for determining the P3HBV composition: <sup>1</sup>H-NMR and gas chromatography (GC) [238]. However, the absolute <sup>1</sup>H-NMR method is not used routinely due to the obvious reasons of instrument availability and cost, even though it provides the most precise results. On the other hand, GC is the most commonly used method, despite it is somewhat laborious and requires calibration and instrumentation. This method was initially proposed by G. Braunegg et al. in 1978 [104] and has undergone minor variations since then [238]. It is based on the methanolysis of PHA in the presence of sulfuric acid followed by the GC determination of the obtained monomer methyl ester. The relative abundance of 3HV and 3HB comonomers is calculated using a standard P3HBV of known composition. The proposed procedure offers the advantage of allowing direct analysis without the need for prior extraction of polymers from the cells and the quantification of the total amount of polymer in the biomass. Then, GC method is routinely used to characterize the extracted P3HBV composition and purity.

In the 1986, Bloemberg et al. have suggested an alternative method based on FTIR spectroscopy [239]. The study reported a good correlation between the composition of P3HBV copolymers, as determined by <sup>1</sup>H-NMR, and FTIR absorption band intensities. In particular, it has been observed that the ratio between the integrate absorbance of the C-H stretching region (3130-2770 cm<sup>-1</sup>) and the C=O stretching region (2000-1580 cm<sup>-1</sup>) is linearly related to the 3HV molar fraction. Meanwhile the relationship holds well with the FTIR results acquired from chloroform polymer solution, it is linked to polymer crystallinity when the spectra were recorded from P3HBV solid film casted on KBr pellets. The authors have argued that the composition of solid copolymer can be evaluated if the samples have quite similar level of crystallinity. Specifically, this rare feature has been resulted from the same isolation process carried out by solution precipitation of the P3HBVs. Actually, PHA spectra, as for other semi-crystalline polymers, are closely related to crystallinity which

brings about band shift, sharpening, intensity variation as well as the appearance of bands of regular helical conformation [240–242].

Another alternative method to determine PHAs composition has been proposed by Jos et al. [243] that used Raman spectroscopy and relied on the linear relationship between the ratio of the band integrals at  $844\text{ cm}^{-1}$  ( $\nu$  C-COO) to that at  $1101\text{ cm}^{-1}$  ( $\nu_s$  C-O-C,  $\rho\text{CH}_3$ ) and the 3HV molar fraction. However, the model has been tested within a limited composition range ( $0 \leq 3\text{HV mol}\% \leq 12$ ) and the coefficient of determination obtained ( $R^2=0.90$ ) was relatively low.

Stimulated by these studies and the evidence that FTIR instruments are more common in industrial laboratories and more easily accessible in academic laboratories than GC or Raman apparatus, as well as the frequent need for rapid analysis, this paper describes a new procedure to evaluate P3HBV composition based on infrared spectroscopy. In particular, the intensity of selected absorption bands was related to the copolymer composition. Furthermore, to circumvent the unpredictable crystallinity of pristine real samples, attenuated total reflection FTIR (ATR-FTIR) spectra were obtained from samples immediately quenched from the melt onto the internal reflection element surface of the ATR device at room temperature. The data analysis demonstrates that the proposed method has proven effective for the rapid and easily accessible preliminary quantification of P3HBV composition.

## **1. Materials and Methods**

### *1.1. Materials*

The opportunity afforded to our research group for conducting physical-chemical characterizations on numerous P3HBV samples, extracted from biomasses obtained through various polymer production and extraction processes, has yielded a substantial collection of copolymers spanning a wide and representative composition range. All the analyzed samples have been obtained by soxhlet extraction with chloroform to reach high recovery yields and purities. However, any other extraction procedures that ensure sufficiently low impurity content that does not affect the PHA FTIR spectrum can be used.

The samples were implemented by commercial P3HB (Biomer ® powder, Krailling, Germany). The samples were in form of films, powders or pellets.

### 1.2. *Sample Preparation and Characterization*

The copolymer composition, expressed as molar fraction of 3-hydroxybutyrate repeating unit ( $X_{3HB}$ ), were determined by GC method, described elsewhere [104,244]. Briefly, approximately 3 mg of extracted PHA were suspended in 2 mL of acidified methanol solution (at 3% v/v  $H_2SO_4$ ) containing benzoic acid (at 0.005% w/v) as internal standard and 1 mL of chloroform in a screw-capped test tube. Then, an acid-catalyzed methanolysis of polymer took place and the formed methyl esters were quantified by gas-chromatography (GC-FID Perkin Elmer 8410). The relative abundance of 3HB and 3HV comonomers was determined using a commercial P3HBV copolymer with a 3HV content of 5 wt% (Sigma-Aldrich, Milan, Italy) as a reference standard. A maximum error in monomeric unit concentration of  $0.02 \text{ mol mol}^{-1}$  was evaluated by repeated GC experiments. In this research, 14 different PHA with  $X_{3HB}$  spanning from  $0.15 \text{ mol mol}^{-1}$  to  $1 \text{ mol mol}^{-1}$  were analyzed. The adopted sample code is P3HBV-X, where X is the 3HB molar fraction in the copolymers.

The ATR-FTIR spectra were acquired by Nicolet 6700 instrument (Thermofisher) by coadding 200 scans at a resolution of  $4 \text{ cm}^{-1}$ . The ATR devices are a Golden Gate (Specac) endowed with a diamond single internal reflection element (IRE) at  $45^\circ$ . The polymer sample were melted over a Kapton foil (about  $1 \text{ cm} \times 1 \text{ cm}$ ) at  $180^\circ \text{C}$  by using a Linkam HFS 91 hot stage (Linkam) driven by a Linkam TP 92 temperature controller. Alternatively, a heating plate (ArgoLAB M3-D) set at about  $200^\circ \text{C}$  was used for some samples randomly selected. In both experiments, the molten samples were rapidly transferred on the IRE surface and the spectrum collected in 30 s, according to adopted conditions. P3HBV-0.15, P3HBV-0.60 and P3HBV-0.92 samples were kept on IRE surface for further 1 h at  $25^\circ \text{C}$ . During this period the cold crystallization occurred, allowing for the acquisition of polymer spectra in the semi-crystalline phase.

For each sample at different composition, at least two independent experiments comprising quenching, spectrum acquisition and elaboration were carried out. No variation of the spectra was found by melting the polymer on heating plate and hot stage nor clear

indication of possible oxidation phenomena were evidenced. Spectra elaborations, performed by Omnic software (version 1.70, Thermo Fisher Scientific Inc.) comprises a baseline correction between 1510  $\text{cm}^{-1}$  and 848  $\text{cm}^{-1}$ . The wavelengths were carefully selected in correspondence of spectrum valleys which showed no or negligible variation according sample composition. Then, the intensities of the selected bands at 968  $\text{cm}^{-1}$ , 1004  $\text{cm}^{-1}$ , 1050  $\text{cm}^{-1}$  and 1084  $\text{cm}^{-1}$  were normalized with respect the intensity of the band 1453  $\text{cm}^{-1}$ , used as internal standard. The absorbance ratios were named  $R_{\bar{\nu}}$ , where  $\bar{\nu}$  is the wavelength of the absorption band.

### 1.3. Data analysis

Data analysis was performed in collaboration with prof. Francesca Pagnanelli from research group of Theory of the Development of Chemical Processes (Sapienza University of Rome). Experimental data reported as absorption ratios ( $y$ ) vs  $X_{3HB}$  ( $x$ ) have been compared by statistical discrimination evaluating the confidence intervals for model parameters, the adequacy of linear models, and the prediction intervals for inverse regression. Confidence intervals on parameters are evaluated according to usual formulas [245].

$$\hat{\beta}_0 \pm t_{\alpha/2, m-2} \sqrt{MS_E \left( \frac{1}{m} + \frac{\bar{x}^2}{S_{xx}} \right)} \quad (1)$$

$$\hat{\beta}_1 \pm t_{\alpha/2, m-2} \sqrt{MS_E / S_{xx}} \quad (2)$$

Where  $\hat{\beta}_0$  is the estimated value of the intercept,  $\hat{\beta}_1$  is the estimated value of the slope,  $t_{\alpha/2}$  is the value of the  $t$  distribution corresponding to  $\alpha=0.05$  and  $m-2$  degree of freedom, where  $m$  is the number of points used for calibration,  $MS_E$  is the sum of square due to random errors evaluated in regression analysis,  $\bar{x}$  is the mean of  $x$  values used in the calibration phase,  $S_{xx}$  is the sum of squares of  $x$  values used in calibration phase.

Adequacy of linear models was assessed by regression analysis and the Lack Of Fit (LOF) test estimating the pure error variance ( $PE$ ) by replicated measurements of  $y$  at fixed  $x$  and comparing it with  $MS_{LOF}$  term by an  $F$  test of hypotheses [245].

Prediction intervals for inverse regression (i.e. confidence intervals on the predicted  $x$  by measuring the  $y$  variable) were estimated considering two replicates of  $y$  measurement according to the following formula [246]:

$$\hat{x}_h \pm t_{\frac{\alpha}{2}, m-2} \cdot \sqrt{S_{xh}^2} \quad (3)$$

with

$$S_{xh}^2 = \frac{MS_E}{\beta_1^2} \cdot \left( \frac{1}{n} + \frac{1}{m} + \frac{(\hat{x}_h - \bar{x})^2}{S_{xx}} \right) \quad (4)$$

where  $\hat{x}_h$  is the  $x$  predicted value by inverse regression for a measured  $y_h$  value replicated two times,  $n$  is the number of replicated  $y$  in the measurement phase.

## 2. Results

### 2.1. ATR-FTIR analysis

It is well-known that P3HBV copolymers crystallize at low rate, mainly at high 3HB content [247]. So, the adopted quenching directly on ATR crystals allows to obtain nearly amorphous samples with the exception of P3HB and P3HBV-0.97, as shown later. For sake of clarity, the spectra of only three representative P3HBV samples with different composition are reported in Figure 4.1. The results acquired immediately after the quenching and after 30 min, during which the crystallization process has taken place, are superimposed. For sake of comparison, all the spectra were normalized with respect of the absorption band at 1453  $\text{cm}^{-1}$ .

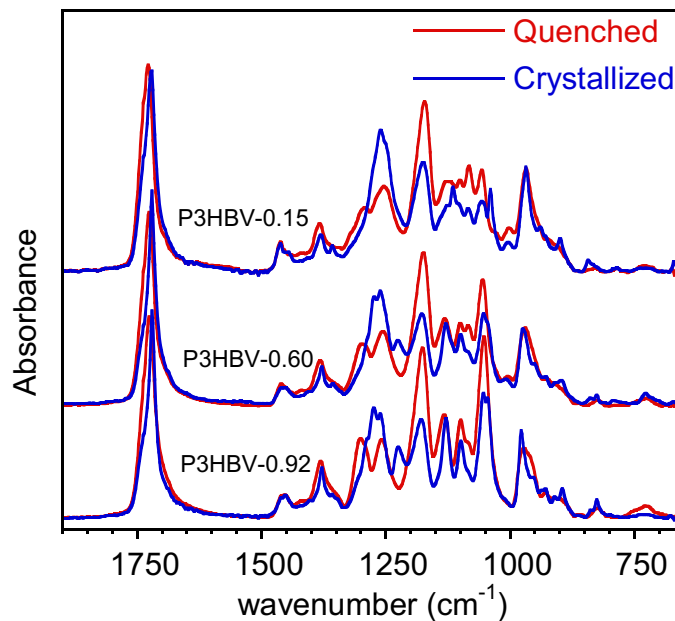
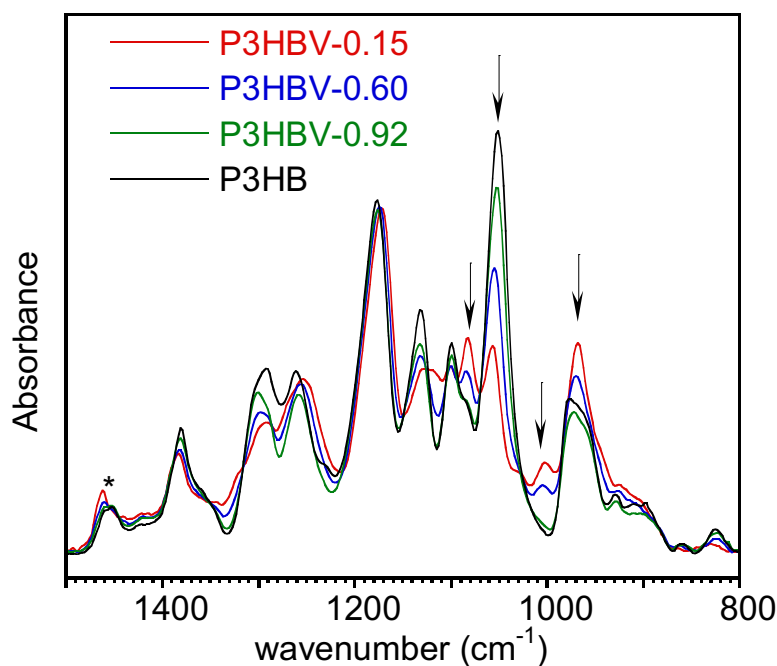


**Figure 4.1** ATR-FTIR spectra of quenched and crystalline P3HBV representative sample at different 3HB molar fractions.

The assignments of vibrational mode of all the absorption bands of PHAs spectra is a challenging task because there are limited systematic studies and a lack of unequivocal spectral interpretation in the literature. Several papers are focused on deep investigations to the thermally induced phase transition [240–242] or to the evaluation of inter-chain hydrogen bond formation [248,249] and are often limited in the analysis of small spectral ranges where C-H (3100-2800  $\text{cm}^{-1}$ ) and C=O stretching (1800-1700  $\text{cm}^{-1}$ ) resonate.

Figure 4.1 shows that, except for a few bands that are consistent across the samples with varying compositions, the spectra exhibit significant dissimilarity. The main differences are situated in the 1300  $\text{cm}^{-1}$ -1200  $\text{cm}^{-1}$  spectral range, where the bending of CH, CH<sub>2</sub>, CH<sub>3</sub> groups resonate, and between 1150  $\text{cm}^{-1}$  and 1000  $\text{cm}^{-1}$ , where the multiple absorption bands are due to C-O-C stretching and C-CH<sub>3</sub> bending [250,251]. Furthermore, as described in numerous studies reported in the literature, there are notable spectral differences between amorphous and semi-crystalline polymers. These complex changes encompass variations in band intensity, position shifts and the emergence of new bands. As a result, in a preliminary study poor correlations and large data scattering were identified between band intensities and the sample composition when comparing as received extracted P3HBV samples, characterized by different and unknown crystallinity.

In Figure 4.2, overlaid representative ATR-FTIR spectra of quenched P3HB and of three selected P3HBV samples with varying 3HB content are displayed. They have been normalized with respect to the intensity of the band at 1453  $\text{cm}^{-1}$  ( $\delta_{\text{as}}$  CH<sub>3</sub> [251]). This absorption has been used as an internal standard in previous studies as it is not significantly affected by crystallinity [241]. Furthermore, the band intensity is not influenced by nearby absorptions that are lightly sensitive to composition. Additionally, baseline correction was applied between 1510  $\text{cm}^{-1}$  and 848  $\text{cm}^{-1}$ , wavenumbers where the spectral characteristics were not influenced by the polymer composition.



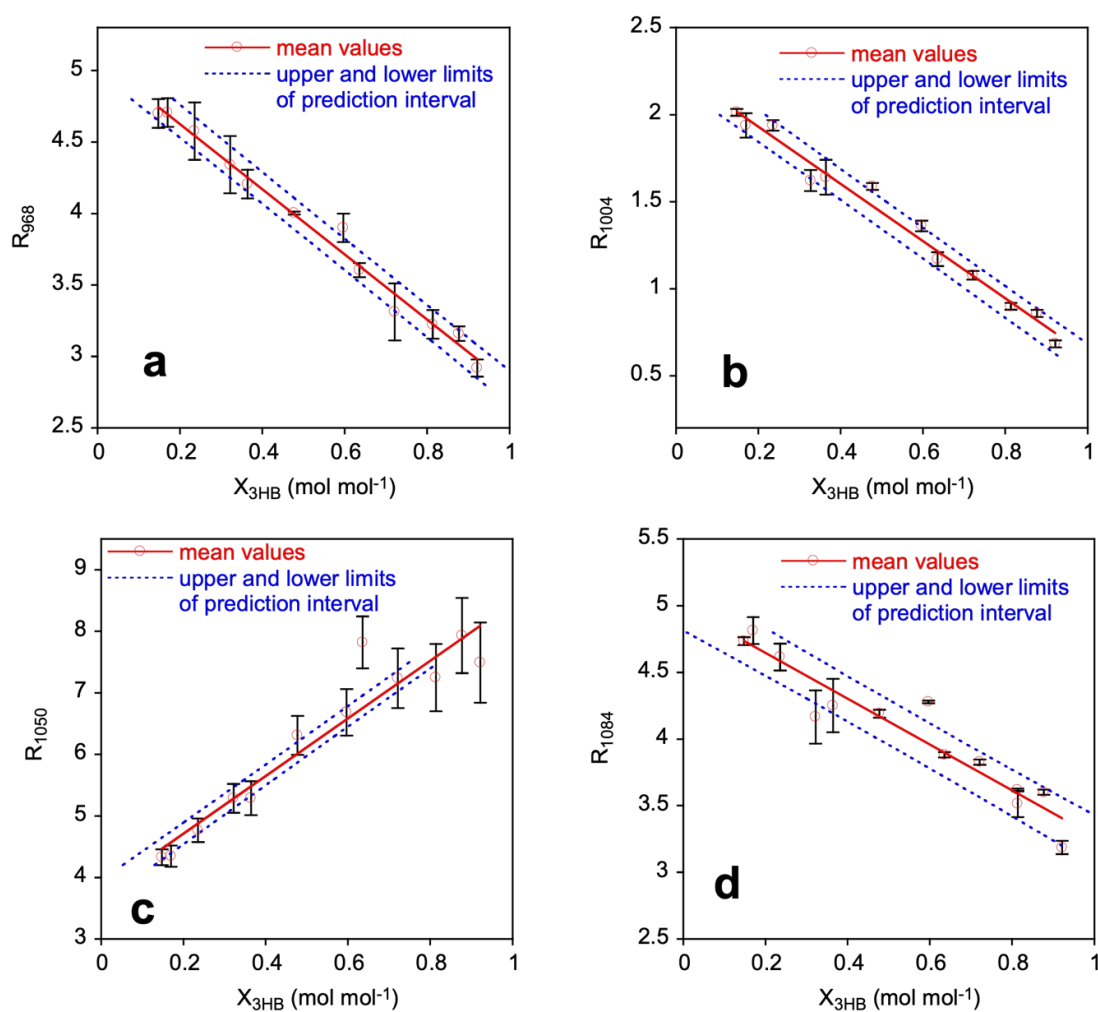
**Figure 4.2** Baseline corrected ATR-FTIR spectra of representative quenched P3HBV and P3HB samples with different 3HB repeating unit molar fractions. The absorbance values were normalized with respect the intensity of the band at  $1453\text{ cm}^{-1}$ , marked with an asterisk. The arrow indicates the bands used for the correlation with polymer composition.

Figure 4.2 shows that the intensity of the absorption bands at  $1084\text{ cm}^{-1}$ ,  $1050\text{ cm}^{-1}$ ,  $1004\text{ cm}^{-1}$  and  $968\text{ cm}^{-1}$  (marked with arrows) markedly changes as function of the P3HBV composition. According to the spectra interpretation reported in literature, the absorption at  $1050\text{ cm}^{-1}$  was attributed to C-O symmetric stretching [252] or to C-CH<sub>3</sub> bending [251] while that at  $968\text{ cm}^{-1}$  to C-H bending [253] or C-C stretching [251,254] or to C-O-C stretching [255]. In the samples with high 3HB concentration, the band at  $1084\text{ cm}^{-1}$  is observed as a shoulder of the medium intensity band at  $1100\text{ cm}^{-1}$ , assigned to C-O stretching, [255,256] and turn in a resolved band by increasing the 3HV content in copolymers. The weak absorption at  $1004\text{ cm}^{-1}$ , located in the valley between the two medium-strong bands at  $1050\text{ cm}^{-1}$  and  $968\text{ cm}^{-1}$ , has been never described in literature and is not yet attributed to a specific vibration. In a diagnostic perspective, it was considered interesting as it is entirely absent in P3HB homopolymer and evolves from a hump into a well-defined band in P3HBV as the 3HV content increases.

Then, the intensity of these selected absorptions was normalized with respect to that of the band at  $1453\text{ cm}^{-1}$  to obtain  $R_{\bar{\nu}}$  data. The quenched samples with  $X_{3\text{HB}} = 1$  and  $X_{3\text{HB}} = 0.97$  showed the presence of an absorption peak at  $1225\text{ cm}^{-1}$ , either as a well-defined band or as

a hump (Figure 4.2, PHB spectrum). This arises from the partial crystallization [239–241] occurring during the transfer of samples from the heating device to the IRE surface or during spectrum acquisition, since P3HB and P3HBV with low 3HV content crystallize rapidly. Consequently, in subsequent data analysis, samples with  $X_{3HB}=1$  and  $X_{3HB}=0.97$  were excluded from consideration because of the high scattering of values and associated errors.

The mean  $R_{\bar{\nu}}$  values as a function of the P3HB molar fraction in the  $0.15 < X_{3HB} < 0.92$  range are reported in Figure 4.3 a-d with the linear interpolation and the prediction interval on  $X_{3HB}$  described in the next section 1.3. The error bars correspond to the half-difference between the maximum and minimum values of the data acquired on at least two independent measurements.



**Figure 4.3** Variation of normalized intensity of the bands at  $968\text{ cm}^{-1}$  (a),  $1004\text{ cm}^{-1}$  (b),  $1050\text{ cm}^{-1}$  (c) and  $1084\text{ cm}^{-1}$  (d) as a function of 3HB molar fraction. The solid lines are the regressed linear models and the dotted lines are the lower and upper limits of the prediction intervals.



## 2.2 Data analysis

As far as the parameter estimates and confidence intervals (95%) (Table 4.1), intercepts present similar relative errors except  $R_{1050}$  with the confidence interval corresponding to 26% variability with respect to estimated value.

**Table 4.1** Coefficients (intercept and slope), upper and lower limits for the confidence intervals, and relative errors for the investigated normalized band intensities.

	Intercept	lower limit (95%)	upper limit (95%)	relative error* (%)	slope	lower limit (95%)	upper limit (95%)	relative error* (%)	$R^2$
$R_{968}$	5.11	4.95	5.26	6	-2.33	-2.58	-2.07	22	0.930
$R_{1050}$	3.77	3.29	4.25	26	4.75	3.95	5.55	34	0.851
$R_{1084}$	5.00	4.82	5.18	7	-1.75	-2.05	-1.45	34	0.848
$R_{1004}$	2.27	2.18	2.36	8	-1.68	-1.83	-1.53	18	0.953

\* The relative error was calculated as the half-difference between the upper and lower limit divided by intercept or slope value.

This is due to the great variability of data due to random errors, as evidenced by the high values of  $MS_E$  and  $MS_{PE}$  (Table 4.2).

**Table 4.2** Variances related to residual error (MSE), Pure error (MSPE) and Lack of Fit error (MSLOF), F values for the LOF test and related p values.

	$MS_{PE}$	$MS_{LOF}$	F value	p value
$R_{968}$	0.0198	0.0423	2.1350	0.0850
$R_{1050}$	0.1243	0.5191	4.1772	0.0056
$R_{1084}$	0.0289	0.0527	1.8246	0.1367
$R_{1004}$	0.0074	0.0131	1.7587	0.1514

As far as the slopes, they are all negative except again for  $R_{1050}$  data which present a positive correlation with  $X_{3HB}$  along with high % relative errors (34%), as in the  $R_{1084}$  case (34%). Both  $R_{1050}$  and  $R_{1084}$  regressions present the highest  $MS_E$  values thus determining the highest variation of the confidence band. The high relative errors evidenced by confidence intervals for  $R_{1050}$  and  $R_{1084}$  are also accompanied by the lowest values of the coefficient of determination ( $R^2$ ) representing the ratio of total variability accounted by the linear model

with respect to the total variability of data. Then, when  $MS_E$  is high the coefficient of determination tends to decrease.

In order to assess the goodness of the linear model the Lack of Fit test was performed: the  $p$  values reported in the table evidenced that, for  $R_{1050}$  case, the linear model is not a good approximation of data, while in all the other cases the data can be adequately represented by linear models ( $p > 0.05$ ). Then according to both large confidence intervals on parameters, low coefficient of determination and Lack of Fit tests, the data calculated by using the normalized intensity at  $1050\text{ cm}^{-1}$  cannot be considered as an optimal choice for the investigate calibration method.

Finally, prediction intervals for the  $X_{3HB}$  ( $x$ ) in the measurement phase were estimated considering two replicates of  $R_{\bar{y}}$  ( $y$ ): the prediction intervals on  $X_{3HB}$  were reported in the figure 3 along with experimental data and calibration lines. In order to visualize in a better way, the variability of these prediction intervals, the associated error bands have been evaluated as upper  $X_{3HB}$  limit minus lower  $X_{3HB}$  limit and displayed in figure 4.4. As expected, the error band for prediction intervals are non-monotonic with a minimum around mean  $X_{3HB}$  of standard samples.

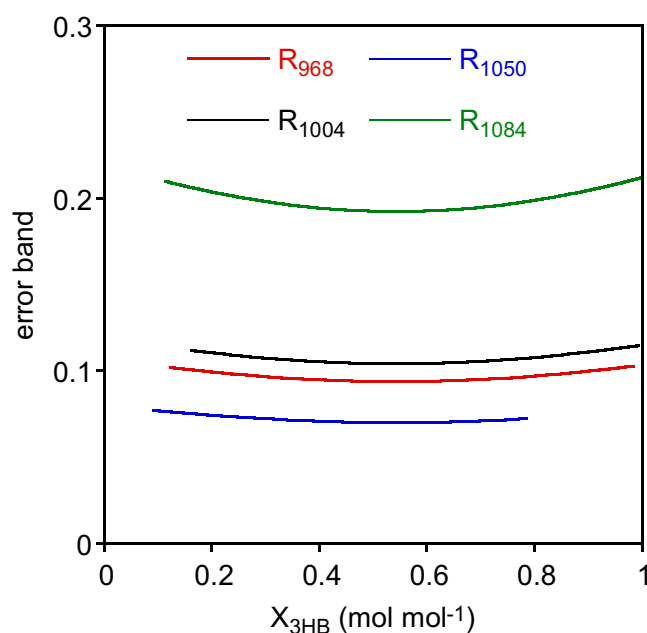


**Figure 4.4** Error bands for the four cases evaluated as the difference between the upper limit and the lower limit of the prediction interval.

Considering the comparison among the different cases, we should exclude  $R_{1050}$  data as linear calibration is not an adequate representation of data even if this case presents the lowest error band. This can be explained considering the formula for estimating the prediction intervals on  $X_{3HB}$ : the  $R_{1050}$  case presents the lowest error band because the high error variability ( $MS_E$ ) is compensated by the highest slope.

On the other side  $R_{1084}$  presenting the second largest error variability does not benefit by such "compensation" having a low value for the slope: accordingly, the error bands are the largest ones.

$R_{968}$  and  $R_{1004}$  presents similar values of the error bands and also considering previous statistical analysis about confidence intervals on parameters, coefficient of determination and the lack of fit tests these are the best correlations to be considered for assessing the composition of the mixture.

### 3 Conclusions

Fourier transform infrared (FTIR) spectroscopy is a widely used technique for the preliminary qualitative characterization of extracted PHAs or, more commonly, for the initial estimation of PHA content in biomass [257,258]. However, the standard gas chromatography analysis is required to determine the polymer composition, the exact amount of polymer in the biomass, and the purity of the extracted polymer. On the other hand, it can be useful to use a more rapid and facile method to assess the composition of PHAs of unknown origin or to check the extraction procedure using a readily accessible instrument such as FTIR. In an early paper, a method to determine P3HBV composition by FTIR spectroscopy has been proposed [239]. It was based on the evaluation of the integral intensity ratio of the stretching bands of C-H and C=O. The sample preparation consisted in polymer dissolution in chloroform and casting on KBr disks for the spectra acquisition in transmission mode. In this way, the authors stated that, since all the sample reached the same crystallinity upon solvent evaporation, the relationship between integral intensity ratio and composition of standard samples was linear. Actually, the crystallinity that P3HBV can reach strongly depends on copolymer composition even in the same sample preparation conditions. This is especially true when a wide composition range is considered.

Then, the key point of the method proposed in this paper is the analysis of quenched polymer samples. This approach ensures that the initial state of the sample does not influence the measurement, enabling a rapid and straightforward sample preparation and spectrum acquisition by ATR-FTIR. In fact, the ATR device is nowadays very common for its ease of use and is often included into the FTIR apparatus; a heating plate is the only supplementary tool needed; the amount of sample for the analysis is about 5-10 mg and, in the adopted instrument set-up, the sample melting, quenching and spectra acquisition take about 1-2 min. This allow to build a custom calibration curve rapidly with few standard samples, necessary, for example, whenever a different IRE or incident angle of ATR device is used.

The data analysis showed that the normalized band intensity at  $968\text{ cm}^{-1}$  and  $1004\text{ cm}^{-1}$  are the most reliable to predict P3HBV composition.

## CONCLUDING REMARKS

In this work of thesis, PHAs critical aspects have been explored. Starting from downstream processing-related issues to chemical functionalization, sustainable methodologies have been proposed to mitigate ecological and economic drawbacks. A scalable, economically competitive and sustainable method to recover the copolymer P(3HB-*co*-3HV) from biomass has been identified. Additionally, a greener and more efficient method for chemical functionalization of PHAs has been presented. Based on the use of an ionic liquid as a reactant, it represents a novel and promising approach to increase hydrophilicity and, then, PHAs performances in living systems. As far PHAs limited processability and mechanical properties, a systematic study demonstrated the positive effect of incorporating high 3HV units amount, up to 30 mol%.

Besides the promising scientific results, this work demonstrated the importance of collaborative work as an effective tool to accelerate the transition toward sustainable materials.

## **APPENDICES**

# APPENDIX 1- Side research activities

In the following appendix, side research activities conducted in collaboration with other research groups will be illustrated.

## PHAs production

### 1) Pure cultures: halophiles microorganism

frontiers | Frontiers in Microbiology

TYPE Original Research  
PUBLISHED 21 September 2022  
DOI 10.3389/fmicb.2022.1000962

Check for updates

#### OPEN ACCESS

EDITED BY  
Yinglong Su,  
East China Normal University, China

REVIEWED BY  
Steven Pratt,  
The University of Queensland, Australia  
Manish Kumar,  
National Environmental Engineering  
Research Institute (CSIR), India  
Sangay Kumar Singh Patel,  
Konkuk University, South Korea

\*CORRESPONDENCE  
Carlo Giuseppe Rizzello  
carlogiuseppe.rizzello@uniroma1.it

SPECIALTY SECTION  
This article was submitted to  
Microbiotechnology,  
a section of the journal  
Frontiers in Microbiology

RECEIVED 22 July 2022  
ACCEPTED 31 August 2022  
PUBLISHED 21 September 2022

## Exploitation of wasted bread as substrate for polyhydroxyalkanoates production through the use of *Haloferax mediterranei* and seawater

Marco Montemurro<sup>1</sup>, Gaia Salvatori<sup>2</sup>, Sara Alfano<sup>2</sup>,  
Andrea Martinelli<sup>2</sup>, Michela Verni<sup>1</sup>, Erica Pontonio<sup>1</sup>,  
Marianna Villano<sup>2,3</sup> and Carlo Giuseppe Rizzello<sup>4\*</sup>

<sup>1</sup>Department of Soil, Plant and Food Science, University of Bari Aldo Moro, Bari, Italy, <sup>2</sup>Department of Chemistry, Sapienza University of Rome, Rome, Italy, <sup>3</sup>Research Center for Applied Sciences to the Safeguard of Environment and Cultural Heritage (CIASC), Sapienza University of Rome, Rome, Italy, <sup>4</sup>Department of Environmental Biology, Sapienza University of Rome, Rome, Italy

The use of the halophile microorganism *Haloferax mediterranei*, able to synthesize poly(hydroxybutyrate-hydroxyvalerate) (PHBV), is considered a promising tool for the industrial production of bioplastic through bioprocessing. A consistent supplementation of the growth substrate in carbohydrates and minerals is overall necessary to allow its PHBV production. In this work, wasted bread was used as substrate for bioplastic production by microbial fermentation. Instead of the consistent and expensive minerals supplement required for *Hfx. mediterranei* DSM1411 growth, microfiltered seawater was added to the wasted bread-derived substrate. The suitable ratio of wasted bread homogenate and seawater, corresponding to 40:60, was selected. The addition of proteases and amylase to the bread homogenate promoted the microbial growth but it did not correspond to the increase of bioplastic production by the microorganism, that reach, under the experimental conditions, 1.53 g/L. An extraction procedure of the PHBV from cells, based on repeated

washing with water, followed or not by a purification through ethanol precipitation, was applied instead of the conventional extraction with chloroform. Yield of PHBV obtained using the different extraction methods were  $21.6 \pm 3.6$  (standard extraction/purification procedure with  $\text{CHCl}_3$ :  $\text{H}_2\text{O}$  mixture),  $24.8 \pm 3.0$  (water-based extraction), and  $19.8 \pm 3.3$  mg PHAs/g of wasted bread (water-based extraction followed by ethanol purification). Slightly higher hydroxyvalerate content (12.95 vs 10.78%, w/w) was found in PHBV obtained through the water-based extraction compared to the conventional one, moreover, the former was characterized by purity of 100% (w/w). Results demonstrated the suitability of wasted bread, supplemented with seawater, to be used as a substrate for bioplastic production through fermentation. Results moreover demonstrated that a solvent-free extraction, exclusively based on osmotic shock, could be used to recover the bioplastic from cells.

See more at <https://doi.org/10.3389/fmicb.2022.1000962>

## 2) Mixed microbial cultures at a pilot scale

Journal of Cleaner Production 354 (2022) 131728

Contents lists available at ScienceDirect

 **Journal of Cleaner Production** 

journal homepage: [www.elsevier.com/locate/jclepro](http://www.elsevier.com/locate/jclepro)

---

**Sewage sludge as carbon source for polyhydroxyalkanoates: a holistic approach at pilot scale level** 

Laura Lorini<sup>a</sup>, Gianluca Munarin<sup>b</sup>, Gaia Salvatori<sup>a</sup>, Sara Alfano<sup>a</sup>, Paolo Pavan<sup>c</sup>, Mauro Majone<sup>a</sup>, Francesco Valentino<sup>c,\*</sup>

<sup>a</sup> Department of Chemistry, "La Sapienza" University of Rome, P.le Aldo Moro 5, 00185, Rome, Italy  
<sup>b</sup> Department of Biotechnology, University of Verona, Strada Le Grazie 15, 37134, Verona, Italy  
<sup>c</sup> Department of Environmental Sciences Informatics and Statistics, "Ca' Foscari" University of Venice, Via Torino 155, 30170, Mestre-Venice, Italy

In the present study, polyhydroxyalkanoates (PHA) production by mixed microbial cultures (MMC) has been carried out using thermally pre-treated excess thickened waste-activated sludge (WAS), applying the feast-famine approach at a pilot scale. The preliminary results of WAS fermentation conducted both in mesophilic and thermophilic conditions, in combination with a thermal pre-treatment at 70 °C for 48 h, highlighted how the thermal



hydrolysis has a crucial role in the solubilization of the chemical oxygen demand (COD), which allows a significant increase of the final volatile fatty acid (VFA) concentration (roughly 8.5 g CODVFA/L). Since thermophilic fermentation after thermal pre-treatment was the best performing condition, it has been applied at a pilot scale in order to routinely produce VFA as precursors for the following PHA synthesis. The selection and enrichment of PHA-producing biomass was successfully established and maintained in a Sequencing Batch Reactor (SBR) during the whole experimentation period, under short hydraulic retention time (HRT; 2 days) and medium-low organic loading rate (OLR; 2.0–2.2 g COD/L d). At the end of the production process, an average PHA content of  $53 \pm 3$  %w/w was achieved. The polymer was finally extracted and recovered from the biomass using traditional chloroform and sodium hypochlorite extraction and then characterized for the quantification of thermal properties ( $T_m = 156.8\text{--}160.9$  °C) and molecular weight ( $M_v = 396\text{--}405$  kDa). A final overall mass balance, usually poorly reported in the literature, has been also assessed, resulting in an overall yield of 56 g PHA per kg of volatile solids (VS).

See more at <https://doi.org/10.1016/j.jclepro.2022.131728>

# PHAs applications

## 1) PHAs and Biochar combination for bioremediation purposes



Article

### **A Polyhydroxybutyrate (PHB)-Biochar Reactor for the Adsorption and Biodegradation of Trichloroethylene: Design and Startup Phase**

Marta M. Rossi <sup>1,\*</sup>, Sara Alfano <sup>1</sup>, Neda Amanat <sup>1</sup>, Fabiano Andreini <sup>2</sup>, Laura Lorini <sup>1</sup>, Andrea Martinelli <sup>1</sup> and Marco Petrangeli Papini <sup>1</sup>

<sup>1</sup> Department of Chemistry, Sapienza University of Rome, Piazzale Aldo Moro 5, 00185 Rome, Italy; sara.alfano@uniroma1.it (S.A.); neda.amanat@uniroma1.it (N.A.); laura.lorini@uniroma1.it (L.L.); andrea.martinelli@uniroma1.it (A.M.); marco.petrangelipapini@uniroma1.it (M.P.P.)

<sup>2</sup> Ecotherm s.r.l., Via Vaccareccia, 43/D, 00071 Rome, Italy; fabiano.andreini@ecothermspa.it

\* Correspondence: martamaria.rossi@uniroma1.it

In this work, polyhydroxy butyrate (PHB) and biochar from pine wood (PWB) are used in a mini-pilot scale biological reactor (11.3 L of geometric volume) for trichloroethylene (TCE) removal (80 mgTCE/day and 6 L/day of flow rate). The PHB-biochar reactor was realized with two sequential reactive areas to simulate a multi-reactive permeable barrier. The PHB acts as an electron donor source in the first “fermentative” area. First, the thermogravimetric (TGA) and differential scanning calorimetry (DSC) analyses were performed. The PHB-powder and pellets have different purity (96% and 93% w/w) and thermal properties. These characteristics may affect the biodegradability of the biopolymer. In the second reactive zone, the PWB works as a *Dehalococcoides* support and adsorption material since its affinity for chlorinated compounds and the positive effect of the “coupled adsorption and biodegradation” process have been already verified. A specific dechlorinating enriched culture has been inoculated in the PWB zone to realize a coupled adsorption and biodegradation process. Organic acids were revealed since the beginning of the test, and during the monitoring period the reductive dichlorination anaerobic pathway was observed in the first zone; no chlorinated compounds were detected in the effluent thanks to the PWB adsorption capacity.

See more at <https://doi.org/10.3390/bioengineering9050192>

## 2) Antimicrobial surfaces

Surfaces and Interfaces 39 (2023) 102924



Contents lists available at ScienceDirect

Surfaces and Interfaces

journal homepage: [www.sciencedirect.com/journal/surfaces-and-interfaces](http://www.sciencedirect.com/journal/surfaces-and-interfaces)



### Surface modification of polyester films with polyfunctional amines: Effect on bacterial biofilm formation



Gianmarco Mallamaci<sup>a</sup>, Benedetta Brugnoli<sup>a</sup>, Alessia Mariano<sup>b</sup>, Anna Scotto d'Abusco<sup>b</sup>, Antonella Piozzi<sup>a</sup>, Valerio Di Lisio<sup>c</sup>, Elisa Sturabotti<sup>a</sup>, Sara Alfano<sup>a</sup>, Iolanda Francolini<sup>a,\*</sup>

<sup>a</sup> Department of Chemistry, Sapienza University of Rome, Piazzale Aldo Moro, 5, Rome 00185, Italy

<sup>b</sup> Department of Biochemical Sciences, Sapienza University of Rome, P.le A. Moro, 5, Rome 00185, Italy

<sup>c</sup> Donostia International Physics Center, Paseo Manuel de Lardizabal, 4, San Sebastian 20018, Spain

The development of materials with antifouling properties is crucial in many areas, including medicine and food packaging. In this study, 2D-matrices made of polylactic acid (PLA), polyhydroxybutyrate (PHB), or polyhydroxybutyrate-co-valerate (PHB-HV) were surface functionalized through aminolysis with three poly-functional amines, 1,6-hexamethylenediamine (HDA), tetraethylenepentamine (TEPA), and polyallylamine hydrochloride (PAH). The aminolysis procedure was thoroughly studied to ensure a high amount of amine groups while preserving the structural properties of the films. Interestingly, PHB and PHB-HV were found to be more sensitive to aminolysis than PLA, and the highest amino group density was achieved in surfaces etched with PAH. A decrease in the contact angle from ca. 85° to ca. 70° was revealed for polymers functionalized with HDA and TEPA and a drastic reduction in *Staphylococcus epidermidis* adhesion was observed for PHB-HV functionalized with the polymeric amine PAH. Polymer antimicrobial activity was found to be related to the degree of surface functionalization. The functionalized, cationic polymer surfaces were supposed to act upon contact with bacteria, without releasing any antimicrobial agent. The developed bioactive surfaces may have potential applications as flexible films for food packaging.

See more at <https://doi.org/10.1016/j.surfin.2023.102924>


## 1) Vitrimers

Received: 1 October 2021 | Revised: 26 January 2022 | Accepted: 4 March 2022  
DOI: 10.1002/app.52408

**ARTICLE**

Applied Polymer SCIENCE WILEY

### **Transamidation-based vitrimers from renewable sources**

Luca Pettazoni  | Francesca Leonelli | Andrea Martinelli |  
Luisa Maria Migneco | Sara Alfano | Daniele Di Luca | Lorenzo Celio |  
Valerio Di Lisio

*Vitrimers* are polymeric materials that behave as thermosets at room temperature but, when heated, they exhibit a plastic flow similar to thermoplastics, enabling their reprocessability. A series of new bio-based polyamide-polyamine vitrimers are synthesized starting from tris(2-aminoethyl) amine and epoxidized methyl oleate, a material that can be easily prepared from renewable resources obtainable both from natural products and waste. The incorporation of free amine groups in the network enables the transamination exchange reaction with the crosslinking amide functions; this reaction, if appropriately catalyzed, donates a full re-processability to the material. Boric acid, which is known to be a green, cheap and non-toxic catalyst for transamidation reactions, is employed in this work. Once the optimal condition for the transamidation reaction is found, different catalyst loadings are tested and the obtained materials are subjected to thermal and mechanical characterization. The obtained materials possess good thermal stability up to 300 °C and a  $T_g$  value ranging between 7 and 21 °C depending on the  $B(OH)_3$  content. Furthermore, it is possible to observe how the introduction of boric acid in the materials reduces the  $E_a$  (inferred from stress-relaxation experiments) of the transamidation reaction from  $130 \pm 8$  KJ  $mol^{-1}$  to a mean value of  $63 \pm 4$  KJ  $mol^{-1}$ .

See more at <https://doi.org/10.1002/app.52408>

## 2) Reusable adhesives

Article

### Self-Healing and Reprocessable Oleic Acid-Based Elastomer with Dynamic S-S Bonds as Solvent-Free Reusable Adhesive on Copper Surface

Luca Pettazzoni <sup>1,\*</sup>, Francesca Leonelli <sup>1,\*</sup>, Andrea Giacomo Marrani <sup>1</sup>, Luisa Maria Migneco <sup>1</sup>, Fabrizio Vetica <sup>1</sup>, Lorenzo Celio <sup>1</sup>, Valerio Napoleone <sup>1</sup>, Sara Alfano <sup>1</sup>, Andrea Colecchia <sup>1</sup>, Francesco Amato <sup>1</sup>, Valerio Di Lisio <sup>2</sup> and Andrea Martinelli <sup>1,\*</sup>

<sup>1</sup> Department of Chemistry, Sapienza University of Rome, 00185 Rome, Italy

<sup>2</sup> Donostia International Physics Center, Paseo Manuel de Lardizabal, 4, 20018 San Sebastian, Spain

\* Correspondence: luca.pettazzoni@uniroma1.it (L.P.); francesca.leonelli@uniroma1.it (F.L.); andrea.martinelli@uniroma1.it (A.M.)

In the last decade, the application of dynamic covalent chemistry in the field of polymeric materials has become the subject of an increasing number of studies, gaining applicative relevance. This is due to the fact that polymers containing dynamic functions possess a structure that affords reprocessability, recyclability and peculiar self-healing properties inconceivable for “classic” polymer networks. Consequently, the synthesis of a dynamic covalent chemistry-based polymer and its chemical, thermal, and mechanical characterizations are reported in the present research. In particular, oleic acid has been used as a starting material to follow the founding principles of the circular economy system and, thanks to the aromatic disulfide component, which is the foundation of the material dynamic characteristics, the obtained polymer resulted as being reprocessable and self-healable. Moreover, the polymer can strongly interact with copper surfaces through the formation of stable Cu-S bonds. Then, the application of the polymer as a solvent-free reusable adhesive for copper was investigated by lap joint shear tests and comparisons with the properties of an analogous material, devoid of the disulfide bonds, were conducted.

See more at <https://doi.org/10.3390/polym14224919>

## APPENDIX 2- Activities report

### 1. List of publications

- *Chlorine-free Extractions of Mixed-Culture Polyhydroxyalkanoates Produced from Fermented Sewage Sludge at Pilot Scale*

Salvatori, G.; Alfano, S.; Martinelli, A.; Gottardo, M.; Villano, M.; Ferreira, B.S.; Valentino, F.; Lorini, L.

Industrial and Engineering Chemistry Research, 2023.

<https://doi.org/10.1021/acs.iecr.3c02684>

- *Rapid Estimation of Poly(3-hydroxybutyrate-co-3-hydroxyvalerate) Composition by ATR-FTIR.*

Alfano, S.; Pagnanelli, F.; Martinelli, A.

Polymers, 2023, 15, 4127

<https://doi.org/10.3390/polym15204127>

- *Surface modification of polyesters films with polyfunctional amines: effect on bacterial biofilm formation*

Mallamaci G., Brugnoli B., Mariano A., d'Abusco A. S., Piozzi A., Di Lisio V., Sturabotti E., Alfano S., Francolini I.,

Surfaces and Interfaces 2023;39, 102924

<https://doi.org/10.1016/j.surfin.2023.102924>

- *Self-Healing and Reprocessable Oleic Acid-Based Elastomer with Dynamic S-S Bonds as Solvent-Free Reusable Adhesive on Copper Surface*

Pettazzoni, L.; Leonelli, F.; Marrani, A.G.; Migneco, L.M.; Vetica, F.; Celio, L.; Napoleone, V.; Alfano, S.; Colecchia, A.; Amato, F.; et al.

Polymers 2022; 14, 4919

<https://doi.org/10.3390/polym14224919>

- *Exploitation of wasted bread as substrate for polyhydroxyalkanoates production through the use of *Haloferax mediterranei* and seawater.*

Montemurro M, Salvatori G, Alfano S, Martinelli A, Verni M, Pontonio E, Villano M and Rizzello CG

Front. Microbiol. 2022;13, 1000962

<https://doi.org/10.3389/fmicb.2022.1000962>

- *Salute e sicurezza nelle biotecnologie agro-industriali: il Progetto europeo Res Urbis*

Pietrangeli B., Lauri R., Davolos D., Incocciati E., Lorin L., Villano M., Martinelli A., Palocci C., Petrangeli Papini M., Amanat N., Chronopoulou L., Alfano S., Valentino F., Pavan P., Moretto G., Bolzonella D., Rossetti S., Crognale S., Carfagnini A., Majone M.

Collana Ricerche INAIL 2022

ISBN 978-88-7484-753-2

<https://www.inail.it/cs/internet/comunicazione/pubblicazioni/catalogo-generale/pubblicazioni-salute-sicurezza-biot-indu-progetto-re-urbis.html>

- *Sewage sludge as renewable carbon source for polyhydroxyalkanoates production: from upstream to the final product*

Lorini L, Munarin G, Salvatori G, Alfano S, Pavan P, Majone M, Valentino F.

Journal of Cleaner Production. 2022; 354, 131728

<https://doi.org/10.1016/j.jclepro.2022.131728>

- *Transamidation based vitrimers from renewable sources*

L. Pettazzoni, F. Leonelli, A. Martinelli, L. M. Migneco, S. Alfano, D. Di Luca, L. Celio, V. Di Lisio.

J. Appl. Polym. Sci. 2022;25, 139

<https://doi.org/10.1002/app.52408>

- *A Polyhydroxybutyrate (PHB)-Biochar Reactor for the Adsorption and Biodegradation of Trichloroethylene: Design and Startup Phase*

Rossi, M.M.; Alfano, S.; Amanat, N.; Andreini, F.; Lorini, L.; Martinelli, A.; Petrangeli Papini, M.

Bioengineering 2022 ;9, 192

<https://doi.org/10.3390/bioengineering9050192>

- *Ethyl Esters as Green Solvents for the Extraction of Intracellular Polyhydroxyalkanoates Produced by Mixed Microbial Culture*

Alfano S, Lorini L, Majone M, Sciubba F, Valentino F, Martinelli A.

Polymers. 2021; 16, 2789

<https://doi.org/10.3390/polym13162789>

## 2. Conferences

- 4<sup>th</sup> Autumn Meeting for Young Chemists in Biomedical Sciences (AMYC BIOMED) 2023

"Sustainable Polyhydroxyalkanoates aminolysis by using Choline-Taurinate ionic liquid for nanoparticles preparation" *Poster*

Sara Alfano, Gianluca Forcina, Lorenzo Ceparano, Andrea Martinelli

16/10/2023 – 18/10/2023 – Firenze (FI), Italy

- MACROGIOVANI 2023

"Sustainable chemical modification of poly-hydroxyalkanoates (PHAs)" *Oral presentation*

Sara Alfano, Gianluca Forcina, Lorenzo Ceparano, Andrea Martinelli

21/06/2023 – 23/06/2023 – Catania (CT), Italy

- 38th Polymer Processing Society Conference (PPS)

"Tuned processability and mechanical properties of PHBV copolymers by using Boron Nitride (BN) and medium-chain-length-PHA (mcl-PHA) as additives" *Oral presentation.*

Sara Alfano, Estelle Doineau, Coline Perdrier, Andrea Martinelli, H el ene Angellier-Coussy

22/05/2023 – 26/05/2023 – St. Gallen, Switzerland



- 11th EPF Summer School 2023 on Polymers and Ionic Liquids  
 "Sustainable Polyhydroxyalkanoates aminolysis by using Choline-Taurinate ionic liquid for nanoparticles preparation" *Poster*  
 Sara Alfano, Gianluca Forcina, Lorenzo Ceparano, Andrea Martinelli  
 02/05/2023 – 05/05/2023 – Bertinoro (FC), Italy
  
- Bio-based polymers at the forefront of innovation in materials science  
 "Characterization of P(3HB- co-3HV) with different 3HV content: effect on properties, processability and miscibility with mcl-PHA" *Oral presentation*  
 Sara Alfano, Gaia Salvatori, Angela Marchetti, Estelle Doineau, Marianna Villano, H el ene Angellier-Coussy, Andrea Martinelli  
 12/04/2023 – 14/04/2023 – Bertinoro (FC), Italy
  
- Symposium for YouNg Chemist: Innovation and Sustainability (SYNC22)  
 "Characterization of MMC- produced PHAs with tailored chemical composition" *Oral presentation*  
 Sara Alfano, Gaia Salvatori, Angela Marchetti, Marianna Villano, Andrea Martinelli  
 20/06/2022 – 23/06/2022 – Rome, Italy
  
- XXIV Convegno Associazione Italiana Macromolecole (AIM)  
 "Influence of monomeric composition on properties of MMC-produced polyhydroxyalkanoates" *Oral presentation*  
 Sara Alfano, Angela Marchetti, Andrea Martinelli, Gaia Salvatori, Marianna Villano  
 04/09/2022 – 07/09/2022 – Trento, Italy
  
- 7th Mixed Microbial Culture PHA, properties and applications Workshop

"Thermal and morphological characterization of P(3HB-co-3HV) with high 3HV content" *Oral presentation*

Sara Alfano, Sara Paravisi, Gaia Salvatori, Marianna Villano, Andrea Martinelli

21/09/2021 – 22/09/2021 – Valencia, Spain

- 10th EPF Summer School 2021 on Polymers and Circular Economy  
"Extraction and characterization of poly-hydroxyalkanoates from mixed microbial cultures (MMC)" *Poster*

Sara Alfano, Laura Lorini, Andrea Martinelli, Francesco Valentino

Online event

### 3. Attended courses

- Applied Chemometric with MATLAB elements (6 CFU) Prof. Federico Marini
- Small Angle X-Ray Scattering, basics and applications (6 CFU) Dr Alessandra del Giudice
- Preparing artwork for scientific papers, getting started in scientific illustration (1 CFU) Dr. Giorgio Giardina e Prof. Stefano Gianni
- Master PhD Lessons (prof. Sylvain Marques Institut de Chimie Radicalaire, Université Aix-Marseille) 01-05/04/2022
  - o 01-05/04/2022 Solvent effects: Nitroxides/alkoxyamines as school cases
  - o 01-05/04/2022 How to use philosophical concepts in applied chemistry
- Scanning Probe Microscopy (3 CFU) Prof. Daniele Passeri
- Chemistry Ethics Prof. Luigi Campanella
- Natural organic substances and substances of food and pharmaceutical interest (1 CFU) Dr Marco Franceschin
- EsSENce Cost Action 3<sup>rd</sup> Training school -Smart sensing applications (Empa, Switzerland) Online

#### 4. Attended seminars

- 20/12/2020:
  - CRISPR/Cas9 What it is, where it comes from, how it works (prof. Giovanna Serino)
  - From municipal organic waste to biodegradable bioplastics: H2020 RES URBIS Project (prof. Mauro Majone)
  - Magic and Reality in Colloidal Systems (prof. Camillo La Mesa)
  - A Symphony of Data: Looking at Chemistry with Multivariate Eyes (prof. Federico Marini)
  - Chirality: A Journey Through the Looking Glass, From Molecules to Galaxies (prof. Donato Monti)
  
- 17/06/2021: Indices of the contribution of tobacco smoke to environmental particulate matter based on the molecular fingerprint of alkanes (Angelo Cecinato, University of Rome La Sapienza)
  
- 15/09/2021: Nuclear magnetic resonance spectroscopy-based metabolomics: a new frontier for the identification of predictive biomarkers of occupational exposure to risk factors (Ottavia Giampaoli, University of Rome La Sapienza)
  
- 19/07/2021: Encapsulation of bioactive compounds and other polymeric applications via emerging technologies (Cristina Prieto PhD, Spanish Council for Scientific Research)
  
- 21/10/2021 Bioremediation of sites contaminated with chlorinated solvents through the use of bioelectrochemical systems (Edoardo dell'Armi, University of Rome La Sapienza)
  
- 18/11/2021 Microfluidic Synthesis of Lipid Nanoparticles for In Vitro Transfer of

Plasmid DNA (Erica Quagliarini, University of Rome La Sapienza)

- 02/12/2021 Chitosan Modifications: Strategies and Applications (Ilaria Silvestro University of Rome La Sapienza)
  
- 20/12/2021:
  - o When Nature Inspires Science: Breaking Molecules Beyond the Looking Glass – (Dr. Fabrizio Vetica)
  - o The magic of catalysis – (Dr. Ida Pettiti)
  - o Omics Sciences: From the Dawn of Civilization to New Horizons for Nutrition and Health – (Prof. Anna Laura Capriotti)
  - o Energy from the sun: how could a chemist exploit this resource? – (Prof. Danilo Dini)
  - o The treatment and recycling of technological waste- (Prof. Francesca Pagnanelli)
  
- 27/01/2022 Functionalization of the CH bond using iron-based catalysts (Federico Fratello, University of Rome La Sapienza)
  
- 28/01/2022 Electrochemical Energy Storage and Conversion Devices: Materials and Scenarios of the Future. (Dr. Maria Assunta Navarra, University of Rome La Sapienza)
  
- 11/02/2022 Oxidation of C-H bonds by HAT processes: modification of selectivity (Marika Di Berto Mancini, Sapienza University of Rome)
  
- Workshop 03-04/03/2022: *Integrated Structural Biology Approach for Membrane Protein Research* (Membrane protein workshop)
  
- 17/03/2022 Photocyclization of 2-(hydroxyamino)-aldehydes through the Norrish-Yang reaction (Antonio di Sabato, University of Rome la Sapienza)

- 05/04/2022 Persistent radical effect: from polymer applications to potential new drugs (Prof. Sylvain Marques, Institut de Chimie Radicalaire, Université Aix-Marseille)
- 07/04/2022 Synthesis of Covalent Adaptable Networks from renewable sources (Luca Pettazzoni, University of Rome La Sapienza)
- 19/07/2022 Microbial Electrochemical Technologies: from bioremediation to microbial electrosynthesis (Dr Sebastà Pluig Laboratory of Chemical and Environmental Engineering (LEQUIA), University of Girona (UdG))
- 07/03/2023 Anionic block polymers as next generation of broad spectrum, self-sterilizing antimicrobial surfaces (Prof. Richard J. Spontak, University of North Carolina State University)
- 28/03/2023 Optical Activity at Varying Length Scales: From Molecular Chirality to Nanoscale Chirality (Dr Jatish Kumar, Indian Institute of Science Education & Research (IISER) Tirupati, India)
- 26/04/2023 Nanocoatings, degradable metals and 3D triple cell culture in bioreactors from collagen gel scaffolds for the innovation in reparative and regenerative medicine (Prof. Diego Mantovani, Laval University Canada)
- 30/05/2023 Greening-up polymers production: from Bio-Renewable building blocks to sustainable solvents (Dr. Vincenzo Taresco, University of Nottingham)
- 13/06/2023 Development, design and delivery of macromolecular medicines (Dr. Pratik Gurnani, University College London UK)

- 16/06/2023 Universal polymer crosslinkers: synthesis, structure-function relationships and application in material science (Prof. Jeremy Wulff, University of Victoria, Canada)
- 20/09/2023 Bio-instructive polymers for medical applications (Prof. Derek Irvine, University of Nottingham)
- 20/09/2023 Transforming fibronectin structures with customized 3D molecular architectures for advanced polymeric surfactants (Dr Valentina Cuzzucoli Crucitti, University of Nottingham)

## **5. Tutoring**

Graduate teaching assistant “General and Inorganic Chemistry” (Aerospace Engineering)  
Sapienza University of Rome (IT), 03/2023-07/2023

# ACKNOWLEDGEMENTS

At the end of this journey, it is necessary to make some thanks.

I thank my family for giving me the chance to continue pursuing my dream. I likewise thank my lifelong friends Giusy, Serena, Ludovica and Federica for their understanding and support.

A big thank you to all the people who made this path special and exciting, despite the ups and downs. First, thanks to my supervisor prof. Andrea Martinelli. It was a pleasure to be one of your students, master intern and finally PhD student. I will always carry with me your precious teachings.

Thanks to all the members of my research group Laboratorio Materiali Polimerici (LAMP): Benedetta Brugnoli, Clarissa Ciarlantini, Lorenzo Augusto Rocchi, David Albano, Elisabetta Lacolla, Riccardo Sergi, Valerio di Lisio, Elisa Sturabotti and professors Antonella Piozzi and Iolanda Francolini. Thanks for all the funny and crazy moments we lived together. I wish all the best to each of you.

A huge thank the members of the research group of Chemical Processes and Plants, professors Mauro Majone, Marianna Villano, Dr. Laura Lorini, Dr. Ing. Angela Marchetti and Gaia Salvatori for valuable discussions and help about the PHAs production.

A special mention to prof. H el ene Angellier-Coussy and her research group in Montpellier to hosting me for six months during my second year of PhD and to Jennifer and Valeria.

I would like to also thank Dr. Francesco Valentino, Dr Marco Gottardo for the economic analysis on PHAs extractions and prof. Francesca Pagnanelli and for the data analysis illustrated in chapter 4. Then thanks to prof. Francesca Leonelli and her research group (SYNERGY Lab) for involving me in biobased thermosets projects.

Last but not least, I cannot conclude without a big acknowledgment to my "little" helpers Sara Paravisi, Gianluca Forcina and Lorenzo Ceparano. Guiding you toward your master's degree was one of the most challenging, funny and precious experience of my young career.

# REFERENCES

- [1] R. Geyer, J.R. Jambeck, K.L. Law, Production, use, and fate of all plastics ever made, 2017. <https://www.science.org>.
- [2] J. Zheng, S. Suh, Strategies to reduce the global carbon footprint of plastics, *Nat Clim Chang*. 9 (2019) 374–378. <https://doi.org/10.1038/s41558-019-0459-z>.
- [3] L. Cabernard, S. Pfister, C. Oberschelp, S. Hellweg, Growing environmental footprint of plastics driven by coal combustion, *Nat Sustain*. 5 (2021) 139–148. <https://doi.org/10.1038/s41893-021-00807-2>.
- [4] W.W.Y. Lau, Y. Shiran, R.M. Bailey, E. Cook, M.R. Stuchtey, J. Koskella, C.A. Velis, L. Godfrey, J. Boucher, M.B. Murphy, R.C. Thompson, E. Jankowska, A. Castillo Castillo, T.D. Pilditch, B. Dixon, L. Koerselman, E. Kosior, E. Favoino, J. Gutberlet, S. Baulch, M.E. Atreya, D. Fischer, K.K. He, M.M. Petit, U.R. Sumaila, E. Neil, M. V. Bernhofen, K. Lawrence, J.E. Palardy, Evaluating scenarios toward zero plastic pollution, *Science* (1979). 369 (2020) 1455–1461. <https://doi.org/10.1126/science.aba9475>.
- [5] Day Robert H., Shaw David G., Ignell Steven E., Quantitative distribution and characteristics of neustonic plastic in the North Pacific Ocean, 1988.
- [6] S. Allen, D. Allen, V.R. Phoenix, G. Le Roux, P. Durántez Jiménez, A. Simonneau, S. Binet, D. Galop, Atmospheric transport and deposition of microplastics in a remote mountain catchment, *Nat Geosci*. 12 (2019) 339–344. <https://doi.org/10.1038/s41561-019-0335-5>.
- [7] M. Bergmann, S. Mützel, S. Primpke, M.B. Tekman, J. Trachsel, G. Gerdtts, White and wonderful? Microplastics prevail in snow from the Alps to the Arctic, *Sci Adv*. 5 (2019). <https://doi.org/10.1126/sciadv.aax1157>.



- [8] X. Zhao, Y. Zhou, C. Liang, J. Song, S. Yu, G. Liao, P. Zou, K.H.D. Tang, C. Wu, Airborne microplastics: Occurrence, sources, fate, risks and mitigation, *Science of The Total Environment*. 858 (2023) 159943.  
<https://doi.org/10.1016/j.scitotenv.2022.159943>.
- [9] Effects of pH and Temperature on the Leaching of Di(2-Ethylhexyl) Phthalate and Di-n-butyl Phthalate from Microplastics in Simulated Marine Environment, *Biointerface Res Appl Chem*. 13 (2022) 269. <https://doi.org/10.33263/BRIAC133.269>.
- [10] K. Molina-Besch, F. Wikström, H. Williams, The environmental impact of packaging in food supply chains – does life cycle assessment of food provide the full picture?, *Int J Life Cycle Assess*. 24 (2019) 37–50. <https://doi.org/10.1007/s11367-018-1500-6>.
- [11] P. Villarrubia-Gómez, S.E. Cornell, J. Fabres, Marine plastic pollution as a planetary boundary threat – The drifting piece in the sustainability puzzle, *Mar Policy*. 96 (2018) 213–220. <https://doi.org/10.1016/j.marpol.2017.11.035>.
- [12] E. Kosior, J. Mitchell, Current industry position on plastic production and recycling, in: *Plastic Waste and Recycling*, Elsevier, 2020: pp. 133–162.  
<https://doi.org/10.1016/B978-0-12-817880-5.00006-2>.
- [13] N. Ferronato, V. Torretta, Waste Mismanagement in Developing Countries: A Review of Global Issues, *Int J Environ Res Public Health*. 16 (2019) 1060.  
<https://doi.org/10.3390/ijerph16061060>.
- [14] United Nations, Transforming our world : The 2030 Agenda for Sustainable Development, in: *Division for Sustainable Development Goals*, New York, 2015.
- [15] V. Siracusa, I. Blanco, Bio-Polyethylene (Bio-PE), Bio-Polypropylene (Bio-PP) and Bio-Poly(ethylene terephthalate) (Bio-PET): Recent Developments in Bio-Based Polymers Analogous to Petroleum-Derived Ones for Packaging and Engineering Applications, *Polymers (Basel)*. 12 (2020) 1641.  
<https://doi.org/10.3390/polym12081641>.

- [16] C.M. Mendieta, M.E. Vallejos, F.E. Felissia, G. Chinga-Carrasco, M.C. Area, Review: Bio-polyethylene from Wood Wastes, *J Polym Environ.* 28 (2020) 1–16.  
<https://doi.org/10.1007/s10924-019-01582-0>.
- [17] B. Kamm, M. Kamm, *Biorefinery-Systems*, n.d.
- [18] S.Y. Lee, Bacterial polyhydroxyalkanoates, *Biotechnol Bioeng.* 49 (1996) 1–14.  
[https://doi.org/10.1002/\(SICI\)1097-0290\(19960105\)49:1<1::AID-BIT1>3.3.CO;2-1](https://doi.org/10.1002/(SICI)1097-0290(19960105)49:1<1::AID-BIT1>3.3.CO;2-1).
- [19] D. Jendrossek, R. Handrick, Microbial Degradation of Polyhydroxyalkanoates, *Annu Rev Microbiol.* 56 (2002) 403–432.  
<https://doi.org/10.1146/annurev.micro.56.012302.160838>.
- [20] B.H.A. Rehm, Bacterial polymers: biosynthesis, modifications and applications, *Nat Rev Microbiol.* 8 (2010) 578–592. <https://doi.org/10.1038/nrmicro2354>.
- [21] S.Y. Ong, J.Y. Chee, K. Sudesh, Degradation of Polyhydroxyalkanoate (PHA): a Review, *Journal of Siberian Federal University. Biology.* 10 (2017) 21–225.  
<https://doi.org/10.17516/1997-1389-0024>.
- [22] M. Zinn, B. Witholt, T. Egli, Occurrence, synthesis and medical application of bacterial polyhydroxyalkanoate, *Adv Drug Deliv Rev.* 53 (2001) 5–21.  
[https://doi.org/10.1016/S0169-409X\(01\)00218-6](https://doi.org/10.1016/S0169-409X(01)00218-6).
- [23] Y. Wang, J. Yin, G.-Q. Chen, Polyhydroxyalkanoates, challenges and opportunities, *Curr Opin Biotechnol.* 30 (2014) 59–65. <https://doi.org/10.1016/j.copbio.2014.06.001>.
- [24] R.A.J. Verlinden, D.J. Hill, M.A. Kenward, C.D. Williams, I. Radecka, Bacterial synthesis of biodegradable polyhydroxyalkanoates, *J Appl Microbiol.* 102 (2007) 1437–1449. <https://doi.org/10.1111/j.1365-2672.2007.03335.x>.
- [25] M. Zinn, R. Hany, Tailored Material Properties of Polyhydroxyalkanoates through Biosynthesis and Chemical Modification, *Adv Eng Mater.* 7 (2005) 408–411.  
<https://doi.org/10.1002/adem.200500053>.

- [26] R.A.J. Verlinden, D.J. Hill, M.A. Kenward, C.D. Williams, I. Radecka, Bacterial synthesis of biodegradable polyhydroxyalkanoates, *J Appl Microbiol.* 102 (2007) 1437–1449. <https://doi.org/10.1111/j.1365-2672.2007.03335.x>.
- [27] C. Dartiailh, W. Blunt, P.K. Sharma, S. Liu, N. Cicek, D.B. Levin, The Thermal and Mechanical Properties of Medium Chain-Length Polyhydroxyalkanoates Produced by *Pseudomonas putida* LS46 on Various Substrates, *Front Bioeng Biotechnol.* 8 (2021). <https://doi.org/10.3389/fbioe.2020.617489>.
- [28] L.L. Madison, G.W. Huisman, Metabolic Engineering of Poly(3-Hydroxyalkanoates): From DNA to Plastic, *Microbiology and Molecular Biology Reviews.* 63 (1999) 21–53. <https://doi.org/10.1128/MMBR.63.1.21-53.1999>.
- [29] A.J. Anderson, G.W. Haywood, E.A. Dawes, Biosynthesis and composition of bacterial poly(hydroxyalkanoates), *Int J Biol Macromol.* 12 (1990) 102–105. [https://doi.org/10.1016/0141-8130\(90\)90060-N](https://doi.org/10.1016/0141-8130(90)90060-N).
- [30] B. Kessler, B. Witholt, Synthesis, recovery and possible application of medium-chain-length polyhydroxyalkanoates: A short overview, *Macromol Symp.* 130 (1998) 245–260. <https://doi.org/10.1002/masy.19981300122>.
- [31] A. Steinbüchel, T. Lütke-Eversloh, Metabolic engineering and pathway construction for biotechnological production of relevant polyhydroxyalkanoates in microorganisms, *Biochem Eng J.* 16 (2003) 81–96. [https://doi.org/10.1016/S1369-703X\(03\)00036-6](https://doi.org/10.1016/S1369-703X(03)00036-6).
- [32] Guo-Qiang Chen, *Plastics Completely Synthesized by Bacteria: Polyhydroxyalkanoates*, in: Chen G. (Ed.), *Microbiology Monographs*, Springer-Verlag, Berlin, 2010: pp. 17–37.
- [33] O.P. Peoples, A.J. Sinskey, Poly- $\beta$ -hydroxybutyrate biosynthesis in *Alcaligenes eutrophus* H16, *Journal of Biological Chemistry.* 264 (1989) 15293–15297. [https://doi.org/10.1016/S0021-9258\(19\)84824-X](https://doi.org/10.1016/S0021-9258(19)84824-X).

- [34] B.H.A. Rehm, A. Steinbüchel, Biochemical and genetic analysis of PHA synthases and other proteins required for PHA synthesis, *Int J Biol Macromol.* 25 (1999) 3–19. [https://doi.org/10.1016/S0141-8130\(99\)00010-0](https://doi.org/10.1016/S0141-8130(99)00010-0).
- [35] K. Grage, A.C. Jahns, N. Parlane, R. Palanisamy, I.A. Rasiah, J.A. Atwood, B.H.A. Rehm, Bacterial Polyhydroxyalkanoate Granules: Biogenesis, Structure, and Potential Use as Nano-/Micro-Beads in Biotechnological and Biomedical Applications, *Biomacromolecules.* 10 (2009) 660–669. <https://doi.org/10.1021/bm801394s>.
- [36] M. Reis, M. Albuquerque, M. Villano, M. Majone, Mixed Culture Processes for Polyhydroxyalkanoate Production from Agro-Industrial Surplus/Wastes as Feedstocks, in: *Comprehensive Biotechnology*, Elsevier, 2011: pp. 669–683. <https://doi.org/10.1016/B978-0-08-088504-9.00464-5>.
- [37] B. Laycock, P. Halley, S. Pratt, A. Werker, P. Lant, The chemomechanical properties of microbial polyhydroxyalkanoates, *Prog Polym Sci.* 38 (2013) 536–583. <https://doi.org/10.1016/j.progpolymsci.2012.06.003>.
- [38] F. Valentino, A.A. Brusca, M. Beccari, A. Nuzzo, G. Zancaroli, M. Majone, Start up of biological sequencing batch reactor (SBR) and short-term biomass acclimation for polyhydroxyalkanoates production, *Journal of Chemical Technology & Biotechnology.* 88 (2013) 261–270. <https://doi.org/10.1002/jctb.3824>.
- [39] J.M.L. Dias, P.C. Lemos, L.S. Serafim, C. Oliveira, M. Eiroa, M.G.E. Albuquerque, A.M. Ramos, R. Oliveira, M.A.M. Reis, Recent Advances in Polyhydroxyalkanoate Production by Mixed Aerobic Cultures: From the Substrate to the Final Product, *Macromol Biosci.* 6 (2006) 885–906. <https://doi.org/10.1002/mabi.200600112>.
- [40] B. S. Kim, Production of Poly(3-Hydroxybutyrate) from Inexpensive Substrates, *Enzyme and Microbial Technology.* 27 (2000) 774–777.

- [41] H. Salehizadeh, M.C.M. Van Loosdrecht, Production of polyhydroxyalkanoates by mixed culture: recent trends and biotechnological importance, *Biotechnol Adv.* 22 (2004) 261–279. <https://doi.org/10.1016/j.biotechadv.2003.09.003>.
- [42] Y. Echegoyen, M.J. Fabra, J.L. Castro-Mayorga, A. Cherpinski, J.M. Lagaron, High throughput electro-hydrodynamic processing in food encapsulation and food packaging applications: Viewpoint, *Trends Food Sci Technol.* 60 (2017) 71–79. <https://doi.org/10.1016/j.tifs.2016.10.019>.
- [43] L.S. Serafim, P.C. Lemos, M.G.E. Albuquerque, M.A.M. Reis, Strategies for PHA production by mixed cultures and renewable waste materials, *Appl Microbiol Biotechnol.* 81 (2008) 615–628. <https://doi.org/10.1007/s00253-008-1757-y>.
- [44] J. Nikodinovic-Runic, M. Guzik, S.T. Kenny, R. Babu, A. Werker, K.E. O Connor, Carbon-Rich Wastes as Feedstocks for Biodegradable Polymer (Polyhydroxyalkanoate) Production Using Bacteria, in: 2013: pp. 139–200. <https://doi.org/10.1016/B978-0-12-407673-0.00004-7>.
- [45] D. Dionisi, M. Majone, V. Papa, M. Beccari, Biodegradable polymers from organic acids by using activated sludge enriched by aerobic periodic feeding, *Biotechnol Bioeng.* 85 (2004) 569–579. <https://doi.org/10.1002/bit.10910>.
- [46] M. Beccari, M. Majone, P. Massanisso, R. Ramadori, A bulking sludge with high storage response selected under intermittent feeding, *Water Res.* 32 (1998) 3403–3413. [https://doi.org/10.1016/S0043-1354\(98\)00100-6](https://doi.org/10.1016/S0043-1354(98)00100-6).
- [47] S. Bengtsson, A.R. Pisco, M.A.M. Reis, P.C. Lemos, Production of polyhydroxyalkanoates from fermented sugar cane molasses by a mixed culture enriched in glycogen accumulating organisms, *J Biotechnol.* 145 (2010) 253–263. <https://doi.org/10.1016/j.jbiotec.2009.11.016>.
- [48] S. Bengtsson, A. Werker, M. Christensson, T. Welander, Production of polyhydroxyalkanoates by activated sludge treating a paper mill wastewater, *Bioresour Technol.* 99 (2008) 509–516. <https://doi.org/10.1016/j.biortech.2007.01.020>.

- [49] M.G.E. Albuquerque, C.A.V. Torres, M.A.M. Reis, Polyhydroxyalkanoate (PHA) production by a mixed microbial culture using sugar molasses: Effect of the influent substrate concentration on culture selection, *Water Res.* 44 (2010) 3419–3433. <https://doi.org/10.1016/j.watres.2010.03.021>.
- [50] S. Campanari, F.A. e Silva, L. Bertin, M. Villano, M. Majone, Effect of the organic loading rate on the production of polyhydroxyalkanoates in a multi-stage process aimed at the valorization of olive oil mill wastewater, *Int J Biol Macromol.* 71 (2014) 34–41. <https://doi.org/10.1016/j.ijbiomac.2014.06.006>.
- [51] D. Dionisi, M. Beccari, S. Di Gregorio, M. Majone, M.P. Papini, G. Vallini, Storage of biodegradable polymers by an enriched microbial community in a sequencing batch reactor operated at high organic load rate, *Journal of Chemical Technology & Biotechnology.* 80 (2005) 1306–1318. <https://doi.org/10.1002/jctb.1331>.
- [52] M. Koller, I. Gasser, F. Schmid, G. Berg, Linking ecology with economy: Insights into polyhydroxyalkanoate-producing microorganisms, *Eng Life Sci.* 11 (2011) 222–237. <https://doi.org/10.1002/elsc.201000190>.
- [53] R. Kleerebezem, M.C. van Loosdrecht, Mixed culture biotechnology for bioenergy production, *Curr Opin Biotechnol.* 18 (2007) 207–212. <https://doi.org/10.1016/j.copbio.2007.05.001>.
- [54] F. Valentino, F. Morgan-Sagastume, S. Campanari, M. Villano, A. Werker, M. Majone, Carbon recovery from wastewater through bioconversion into biodegradable polymers, *N Biotechnol.* 37 (2017) 9–23. <https://doi.org/10.1016/j.nbt.2016.05.007>.
- [55] H. Bouallagui, Y. Touhami, R. Ben Cheikh, M. Hamdi, Bioreactor performance in anaerobic digestion of fruit and vegetable wastes, *Process Biochemistry.* 40 (2005) 989–995. <https://doi.org/10.1016/j.procbio.2004.03.007>.
- [56] F. Morgan-Sagastume, A. Karlsson, P. Johansson, S. Pratt, N. Boon, P. Lant, A. Werker, Production of polyhydroxyalkanoates in open, mixed cultures from a waste

- sludge stream containing high levels of soluble organics, nitrogen and phosphorus, *Water Res.* 44 (2010) 5196–5211. <https://doi.org/10.1016/j.watres.2010.06.043>.
- [57] M.A.M. Reis, L.S. Serafim, P.C. Lemos, A.M. Ramos, F.R. Aguiar, M.C.M. Van Loosdrecht, Production of polyhydroxyalkanoates by mixed microbial cultures, *Bioprocess Biosyst Eng.* 25 (2003) 377–385. <https://doi.org/10.1007/s00449-003-0322-4>.
- [58] H. Salehizadeh, M.C.M. Van Loosdrecht, Production of polyhydroxyalkanoates by mixed culture: recent trends and biotechnological importance, *Biotechnol Adv.* 22 (2004) 261–279. <https://doi.org/10.1016/j.biotechadv.2003.09.003>.
- [59] S. Philip, T. Keshavarz, I. Roy, Polyhydroxyalkanoates: Biodegradable polymers with a range of applications, *Journal of Chemical Technology and Biotechnology.* 82 (2007) 233–247. <https://doi.org/10.1002/jctb.1667>.
- [60] D. Shum-Tim, U. Stock, J. Hrkach, T. Shinoka, J. Lien, M.A. Moses, A. Stamp, G. Taylor, A.M. Moran, W. Landis, R. Langer, J.P. Vacanti, J.E. Mayer, Tissue engineering of autologous aorta using a new biodegradable polymer, *Ann Thorac Surg.* 68 (1999) 2298–2304. [https://doi.org/10.1016/S0003-4975\(99\)01055-3](https://doi.org/10.1016/S0003-4975(99)01055-3).
- [61] E. Romero-Castelán, A.I. Rodríguez-Hernández, N. Chavarría-Hernández, M.A. López-Ortega, M. del R. López-Cuellar, Natural antimicrobial systems protected by complex polyhydroxyalkanoate matrices for food biopackaging applications — A review, *Int J Biol Macromol.* 233 (2023). <https://doi.org/10.1016/j.ijbiomac.2023.123418>.
- [62] J.L. Castro-Mayorga, M.J. Fabra, L. Cabedo, J.M. Lagaron, On the use of the electrospinning coating technique to produce antimicrobial polyhydroxyalkanoate materials containing in situ-stabilized silver nanoparticles, *Nanomaterials.* 7 (2017). <https://doi.org/10.3390/nano7010004>.
- [63] P.A. Holmes, Applications of PHB - a microbially produced biodegradable thermoplastic, *Physics in Technology.* 16 (1985) 32–36. <https://doi.org/10.1088/0305-4624/16/1/305>.

- [64] V.C. Kalia, S.K.S. Patel, J.-K. Lee, Exploiting Polyhydroxyalkanoates for Biomedical Applications, *Polymers* (Basel). 15 (2023) 1937.  
<https://doi.org/10.3390/polym15081937>.
- [65] D.A. Gregory, C.S. Taylor, A.T.R. Fricker, E. Asare, S.S.V. Tetali, J.W. Haycock, I. Roy, Polyhydroxyalkanoates and their advances for biomedical applications, *Trends Mol Med*. 28 (2022) 331–342. <https://doi.org/10.1016/J.MOLMED.2022.01.007>.
- [66] A.I. Rodríguez-Cendal, I. Gómez-Seoane, F.J. de Toro-Santos, I.M. Fuentes-Boquete, J. Señarís-Rodríguez, S.M. Díaz-Prado, Biomedical Applications of the Biopolymer Poly(3-hydroxybutyrate-co-3-hydroxyvalerate) (PHBV): Drug Encapsulation and Scaffold Fabrication, *Int J Mol Sci*. 24 (2023) 11674.  
<https://doi.org/10.3390/ijms241411674>.
- [67] G. Pagliano, P. Galletti, C. Samorì, A. Zaghini, C. Torri, Recovery of Polyhydroxyalkanoates From Single and Mixed Microbial Cultures: A Review, *Front Bioeng Biotechnol*. 9 (2021). <https://doi.org/10.3389/fbioe.2021.624021>.
- [68] G. Mannina, D. Presti, G. Montiel-Jarillo, M.E. Suárez-Ojeda, Bioplastic recovery from wastewater: A new protocol for polyhydroxyalkanoates (PHA) extraction from mixed microbial cultures, *Bioresour Technol*. 282 (2019) 361–369.  
<https://doi.org/10.1016/J.BIORTECH.2019.03.037>.
- [69] J. Choi, S.Y. Lee, MINI-REVIEW Factors affecting the economics of polyhydroxyalkanoate production by bacterial fermentation, n.d.
- [70] C. Pérez-Rivero, J.P. López-Gómez, I. Roy, A sustainable approach for the downstream processing of bacterial polyhydroxyalkanoates: State-of-the-art and latest developments, *Biochem Eng J*. 150 (2019) 107283.  
<https://doi.org/10.1016/J.BEJ.2019.107283>.
- [71] N. Jacquél, C.W. Lo, Y.H. Wei, H.S. Wu, S.S. Wang, Isolation and purification of bacterial poly(3-hydroxyalkanoates), *Biochem Eng J*. 39 (2008) 15–27.  
<https://doi.org/10.1016/J.BEJ.2007.11.029>.



- [72] S. Dubey, P. Bharmoria, P. Singh Gehlot, V. Agrawal, A. Kumar, S. Mishra, 1-Ethyl-3-methylimidazolium Diethylphosphate Based Extraction of Bioplastic “Polyhydroxyalkanoates” from Bacteria: Green and Sustainable Approach, *ACS Sustainable Chemistry & Engineering*. 6 (2017) 766–773. <https://doi.org/10.1021/acssuschemeng.7b03096>.
- [73] D.L. Kurdikar, F.E. Strauser, A.J. Solodar, M.D. Paster, High Temperature PHA Extraction Using PHA-Poor Solvents, 1998.
- [74] D.L. Kurdikar, F.E. Strauser, A.J. Solodar, M.D. Paster, J. Asrar, Methods of PHA Extraction and Recovery Using Non-Halogenated Solvents, 1998.
- [75] G. Jiang, B. Johnston, D. Townrow, I. Radecka, M. Koller, P. Chaber, G. Adamus, M. Kowalczyk, Biomass Extraction Using Non-Chlorinated Solvents for Biocompatibility Improvement of Polyhydroxyalkanoates, *Polymers (Basel)*. 10 (2018) 731. <https://doi.org/10.3390/polym10070731>.
- [76] N. Yabueng, S.C. Napathorn, Toward non-toxic and simple recovery process of poly(3-hydroxybutyrate) using the green solvent 1,3-dioxolane, *Process Biochemistry*. 69 (2018) 197–207. <https://doi.org/10.1016/J.PROCBIO.2018.02.025>.
- [77] A. Rosengart, M.T. Cesário, M.C.M.D. de Almeida, R.S. Raposo, A. Espert, E.D. de Apodaca, M.M.R. da Fonseca, Efficient P(3HB) extraction from *Burkholderia sacchari* cells using non-chlorinated solvents, *Biochem Eng J*. 103 (2015) 39–46. <https://doi.org/10.1016/J.BEJ.2015.06.013>.
- [78] S.L. Riedel, C.J. Brigham, C.F. Budde, J. Bader, C. Rha, U. Stahl, A.J. Sinskey, ARTICLE Recovery of Poly(3-Hydroxybutyrate-co-3-Hydroxyhexanoate) From *Ralstonia eutropha* Cultures With Non-Halogenated Solvents, *Biotechnol. Bioeng*. 110 (2013) 461–470. <https://doi.org/10.1002/bit.24713/abstract>.
- [79] C. Samorì, M. Basaglia, S. Casella, L. Favaro, P. Galletti, L. Giorgini, D. Marchi, L. Mazzocchetti, C. Torri, E. Tagliavini, Dimethyl carbonate and switchable anionic surfactants: Two effective tools for the extraction of polyhydroxyalkanoates from

microbial biomass, *Green Chemistry*. 17 (2015) 1047–1056.

<https://doi.org/10.1039/c4gc01821d>.

- [80] B. Mongili, A. Abdel Azim, S. Fraterrigo Garofalo, E. Batuecas, A. Re, S. Bocchini, D. Fino, Novel insights in dimethyl carbonate-based extraction of polyhydroxybutyrate (PHB), *Biotechnol Biofuels*. 14 (2021). <https://doi.org/10.1186/s13068-020-01849-y>.
- [81] G.A. de Souza Reis, M.H.A. Michels, G.L. Fajardo, I. Lamot, J.H. de Best, Optimization of Green Extraction and Purification of PHA Produced by Mixed Microbial Cultures from Sludge, *Water (Basel)*. 12 (2020) 1185. <https://doi.org/10.3390/w12041185>.
- [82] M.L. Fiorese, F. Freitas, J. Pais, A.M. Ramos, G.M.F. De Aragão, M.A.M. Reis, Recovery of polyhydroxybutyrate (PHB) from *Cupriavidus necator* biomass by solvent extraction with 1,2-propylene carbonate, *Eng Life Sci*. 9 (2009) 454–461. <https://doi.org/10.1002/elsc.200900034>.
- [83] C.M. Chan, P. Johansson, P. Magnusson, L.J. Vandi, M. Arcos-Hernandez, P. Halley, B. Laycock, S. Pratt, A. Werker, Mixed culture polyhydroxyalkanoate-rich biomass assessment and quality control using thermogravimetric measurement methods, *Polym Degrad Stab*. 144 (2017) 110–120. <https://doi.org/10.1016/J.POLYMDEGRADSTAB.2017.07.029>.
- [84] M. Koller, R. Bona, E. Chiellini, G. Braunegg, Extraction of short-chain-length poly-[(R)-hydroxyalkanoates] (scl-PHA) by the “anti-solvent” acetone under elevated temperature and pressure, *Biotechnol Lett*. 35 (2013) 1023–1028. <https://doi.org/10.1007/s10529-013-1185-7>.
- [85] T. Yılmaz Nayır, S. Konuk, S. Kara, Extraction of polyhydroxyalkanoate from activated sludge using supercritical carbon dioxide process and biopolymer characterization, *J Biotechnol*. 364 (2023) 50–57. <https://doi.org/10.1016/j.jbiotec.2023.01.011>.

- [86] H.K.S. Souza, M. Matos, M.A.M. Reis, J.A. Covas, L. Hilliou, Can Biomass Mastication Assist the Downstreaming of Polyhydroxyalkanoates Produced from Mixed Microbial Cultures?, *Molecules*. 28 (2023).  
<https://doi.org/10.3390/molecules28020767>.
- [87] S. Mondal, U.T. Syed, C. Gil, L. Hilliou, A.F. Duque, M.A.M. Reis, C. Brazinha, A novel sustainable PHA downstream method, *Green Chemistry*. 25 (2023) 1137–1149.  
<https://doi.org/10.1039/D2GC04261D>.
- [88] Y. Zou, M. Yang, Q. Tao, K. Zhu, X. Liu, C. Wan, M.K. Harder, Q. Yan, B. Liang, I. Ntaikou, G. Antonopoulou, G. Lyberatos, Y. Zhang, Recovery of polyhydroxyalkanoates (PHAs) polymers from a mixed microbial culture through combined ultrasonic disruption and alkaline digestion, *J Environ Manage*. 326 (2023) 116786. <https://doi.org/10.1016/j.jenvman.2022.116786>.
- [89] D. Kobayashi, K. Fujita, N. Nakamura, H. Ohno, A simple recovery process for biodegradable plastics accumulated in cyanobacteria treated with ionic liquids, *Appl Microbiol Biotechnol*. 99 (2015) 1647–1653. <https://doi.org/10.1007/s00253-014-6234-1>.
- [90] S. Dubey, P. Bharmoria, P. Singh Gehlot, V. Agrawal, A. Kumar, S. Mishra, 1-Ethyl-3-methylimidazolium Diethylphosphate Based Extraction of Bioplastic “Polyhydroxyalkanoates” from Bacteria: Green and Sustainable Approach, *ACS Sustainable Chemistry & Engineering*. 6 (2017) 766–773.  
<https://doi.org/10.1021/acssuschemeng.7b03096>.
- [91] V. Kachrimanidou, N. Kopsahelis, A. Vlysidis, S. Papanikolaou, I.K. Kookos, B. Monje Martínez, M.C. Escrig Rondán, A.A. Koutinas, Downstream separation of poly(hydroxyalkanoates) using crude enzyme consortia produced via solid state fermentation integrated in a biorefinery concept, *Food and Bioproducts Processing*. 100 (2016) 323–334. <https://doi.org/10.1016/J.FBP.2016.08.002>.
- [92] M. Saavedra del Oso, M. Mauricio-Iglesias, A. Hospido, Evaluation and optimization of the environmental performance of PHA downstream processing,

Chemical Engineering Journal. 412 (2021) 127687.

<https://doi.org/10.1016/j.cej.2020.127687>.

- [93] L. De Donno Novelli, S. Moreno Sayavedra, E.R. Rene, Polyhydroxyalkanoate (PHA) production via resource recovery from industrial waste streams: A review of techniques and perspectives, *Bioresour Technol.* 331 (2021) 124985. <https://doi.org/10.1016/j.biortech.2021.124985>.
- [94] C. Fernández-Dacosta, J.A. Posada, R. Kleerebezem, M.C. Cuellar, A. Ramirez, Microbial community-based polyhydroxyalkanoates (PHAs) production from wastewater: Techno-economic analysis and ex-ante environmental assessment, *Bioresour Technol.* (2015). <https://doi.org/10.1016/j.biortech.2015.03.025>.
- [95] L. Lorini, G. Salvatori, L.N. Tayou, F. Valentino, M. Villano, Innovative Strategy for Polyhydroxyalkanoates Recovery from Mixed Microbial Cultures: Effects of Aqueous Phase and Solvent Extraction on Polymer Properties, *Chem Eng Trans.* 92 (2022) 529–534. <https://doi.org/10.3303/CET2292089>.
- [96] B. Xiong, Q. Fang, T. Wei, Z. Wang, R. Shen, M. Cheng, W. Zhou, Chemical digestion method to promote activated sludge cell wall breaking and optimize the polyhydroxyalkanoate (PHA) extraction process, *Int J Biol Macromol.* 240 (2023) 124369. <https://doi.org/10.1016/j.ijbiomac.2023.124369>.
- [97] G. Montiel-Jarillo, D.A. Morales-Urrea, E.M. Contreras, A. López-Córdoba, E.Y. Gómez-Pachón, J. Carrera, M.E. Suárez-Ojeda, Improvement of the Polyhydroxyalkanoates Recovery from Mixed Microbial Cultures Using Sodium Hypochlorite Pre-Treatment Coupled with Solvent Extraction, *Polymers (Basel)*. 14 (2022) 1–17. <https://doi.org/10.3390/polym14193938>.
- [98] M. Saavedra del Oso, M. Mauricio-Iglesias, A. Hospido, Evaluation and optimization of the environmental performance of PHA downstream processing, *Chemical Engineering Journal.* 412 (2021) 127687. <https://doi.org/10.1016/J.CEJ.2020.127687>.

- [99] L. di Bitonto, S. Menegatti, C. Pastore, Process intensification for the production of the ethyl esters of volatile fatty acids using aluminium chloride hexahydrate as a catalyst, *J Clean Prod.* 239 (2019) 118122.  
<https://doi.org/10.1016/J.JCLEPRO.2019.118122>.
- [100] G. Moretto, I. Russo, D. Bolzonella, P. Pavan, M. Majone, F. Valentino, An urban biorefinery for food waste and biological sludge conversion into polyhydroxyalkanoates and biogas, *Water Res.* 170 (2020) 115371.  
<https://doi.org/10.1016/J.WATRES.2019.115371>.
- [101] D. Prat, A. Wells, J. Hayler, H. Sneddon, C.R. McElroy, S. Abou-Shehada, P.J. Dunn, CHEM21 selection guide of classical- and less classical-solvents, *Green Chemistry.* 18 (2015) 288–296. <https://doi.org/10.1039/c5gc01008j>.
- [102] D. Prat, J. Hayler, A. Wells, A survey of solvent selection guides, *Green Chemistry.* 16 (2014) 4546–4551. <https://doi.org/10.1039/c4gc01149j>.
- [103] F. Valentino, G. Moretto, L. Lorini, D. Bolzonella, P. Pavan, M. Majone, Pilot-Scale Polyhydroxyalkanoate Production from Combined Treatment of Organic Fraction of Municipal Solid Waste and Sewage Sludge, *Industrial & Engineering Chemistry Research.* 58 (2019) 12149–12158. <https://doi.org/10.1021/acs.iecr.9b01831>.
- [104] G. Braunegg, B. Sonnleimer, R.M. Lafferty, A Rapid Gas Chromatographic Method for the Determination of Poly- $\gamma$ -hydroxybutyric Acid in Microbial Biomass, 1978.
- [105] R.H. Marchessault, K. Okamura, C.J. Su, Physical Properties of Poly (3-Hydroxy Butyrate). II. Conformational Aspects in Solution., *Macromolecules.* 3 (1970) 735–740.
- [106] S. Hu, A.G. McDonald, E.R. Coats, Characterization of polyhydroxybutyrate biosynthesized from crude glycerol waste using mixed microbial consortia, *J Appl Polym Sci.* 129 (2013) 1314–1321. <https://doi.org/10.1002/app.38820>.
- [107] L. Lorini, A. Martinelli, G. Capuani, N. Frison, M. Reis, B. Sommer Ferreira, M. Villano, M. Majone, F. Valentino, Characterization of Polyhydroxyalkanoates

Produced at Pilot Scale From Different Organic Wastes, *Front Bioeng Biotechnol.* 9 (2021). <https://doi.org/10.3389/fbioe.2021.628719>.

- [108] F.D. Kopinke, M. Remmler, K. Mackenzie, Thermal decomposition of biodegradable polyesters—I: Poly( $\beta$ -hydroxybutyric acid), *Polym Degrad Stab.* 52 (1996) 25–38. [https://doi.org/10.1016/0141-3910\(95\)00221-9](https://doi.org/10.1016/0141-3910(95)00221-9).
- [109] H. Xiang, X. Wen, X. Miu, Y. Li, Z. Zhou, M. Zhu, Thermal depolymerization mechanisms of poly(3-hydroxybutyrate-co-3-hydroxyvalerate), *Progress in Natural Science: Materials International.* 26 (2016) 58–64. <https://doi.org/10.1016/J.PNSC.2016.01.007>.
- [110] C. Samorì, F. Abbondanzi, P. Galletti, L. Giorgini, L. Mazzocchetti, C. Torri, E. Tagliavini, Extraction of polyhydroxyalkanoates from mixed microbial cultures: Impact on polymer quality and recovery, *Bioresour Technol.* 189 (2015) 195–202. <https://doi.org/10.1016/J.BIORTECH.2015.03.062>.
- [111] M. Terada, R.H. Marchessault, Determination of solubility parameters for poly(3-hydroxyalkanoates), *Int J Biol Macromol.* 25 (1999) 207–215. [https://doi.org/10.1016/S0141-8130\(99\)00036-7](https://doi.org/10.1016/S0141-8130(99)00036-7).
- [112] G.Q. Chen, G. Zhang, S.J. Park, S.Y. Lee, Industrial scale production of poly(3-hydroxybutyrate-co-3-hydroxyhexanoate), *Appl Microbiol Biotechnol.* 57 (2001) 50–55. <https://doi.org/10.1007/s002530100755>.
- [113] T. Manangan, S. Shawaphun, Quantitative extraction and determination of polyhydroxyalkanoate accumulated in *Alcaligenes latus* dry cells, *ScienceAsia.* 36 (2010) 199–203. <https://doi.org/10.2306/scienceasia1513-1874.2010.36.199>.
- [114] A. Aramvash, N. Gholami-Banadkuki, F. Moazzeni-Zavareh, S. Hajizadeh-Turchi, An environmentally friendly and efficient method for extraction of PHB biopolymer with non-halogenated solvents, *J Microbiol Biotechnol.* 25 (2015) 1936–1943. <https://doi.org/10.4014/jmb.1505.05053>.

- [115] G. Gahlawat, S. Kumar Soni, Study on sustainable recovery and extraction of Polyhydroxyalkanoates (PHAs) produced by *Cupriavidus necator* using waste glycerol for medical applications, *Chem Biochem Eng Q.* 33 (2019) 99–110. <https://doi.org/10.15255/CABEQ.2018.1471>.
- [116] A.G. Werker, P.S.T. Johansson, O.G. Magnusson, *Process for the Extraction of Polyhydroxyalkanoates from Biomass*, 2014.
- [117] L. Devdatt, D.L. Kurdikar, F.E. Strauser, A.J. Solodar, M.D. Paster, *High Temperature PHA Extraction Using PHA-Poor Solvents.* , 2000.
- [118] N. Grassie, E.J. Murray, P.A. Holmes, *The Thermal Degradation of Poly(-D)-/~-Hydroxybutyric Acid): Part 1 Identification and Quantitative Analysis of Products*, 1984.
- [119] G.Y. and R.H.M. Sophie Nguyen, *Thermal degradation of Poly(3-hydroxyalkanoates):Preparation of well-defined Oligomers*, *Biomacromolecules.* (2002) 219–224.
- [120] L. Lorini, G. Munarin, G. Salvatori, S. Alfano, P. Pavan, M. Majone, F. Valentino, *Sewage sludge as carbon source for polyhydroxyalkanoates: a holistic approach at pilot scale level*, *J Clean Prod.* 354 (2022) 131728. <https://doi.org/10.1016/j.jclepro.2022.131728>.
- [121] G. Moretto, L. Lorini, P. Pavan, S. Crognale, B. Tonanzi, S. Rossetti, M. Majone, F. Valentino, *Biopolymers from urban organic waste: Influence of the solid retention time to cycle length ratio in the enrichment of a Mixed Microbial Culture (MMC)*, *ACS Sustain Chem Eng.* 8 (2020). <https://doi.org/10.1021/acssuschemeng.0c04980>.
- [122] L. Lorini, A. Martinelli, G. Capuani, N. Frison, M. Reis, B. Sommer Ferreira, M. Villano, M. Majone, F. Valentino, *Characterization of Polyhydroxyalkanoates Produced at Pilot Scale From Different Organic Wastes*, *Front Bioeng Biotechnol.* 9 (2021) 1–13. <https://doi.org/10.3389/fbioe.2021.628719>.

- [123] S. Alfano, L. Lorini, M. Majone, F. Sciubba, F. Valentino, A. Martinelli, Ethylic esters as green solvents for the extraction of intracellular polyhydroxyalkanoates produced by mixed microbial culture, *Polymers (Basel)*. 13 (2021).  
<https://doi.org/10.3390/polym13162789>.
- [124] L. Lorini, A. Martinelli, P. Pavan, M. Majone, F. Valentino, Downstream processing and characterization of polyhydroxyalkanoates (PHAs) produced by mixed microbial culture (MMC) and organic urban waste as substrate, *Biomass Convers Biorefin.* 11 (2021) 693–703. <https://doi.org/10.1007/s13399-020-00788-w>.
- [125] A.M. Rodrigues, R.G.F. Dias, M. Dionísio, C. Sevrin, C. Grandfils, M.A.M. Reis, N.D. Lourenço, Polyhydroxyalkanoates from a Mixed Microbial Culture: Extraction Optimization and Polymer Characterization, *Polymers (Basel)*. 14 (2022) 2115.
- [126] G. Mannina, D. Presti, G. Montiel-Jarillo, M.E. Suárez-Ojeda, Bioplastic recovery from wastewater: A new protocol for polyhydroxyalkanoates (PHA) extraction from mixed microbial cultures, *Bioresour Technol.* 282 (2019) 361–369.  
<https://doi.org/10.1016/j.biortech.2019.03.037>.
- [127] M. Villano, F. Valentino, A. Barbetta, L. Martino, M. Scandola, M. Majone, Polyhydroxyalkanoates production with mixed microbial cultures: From culture selection to polymer recovery in a high-rate continuous process, *N Biotechnol.* 31 (2014) 289–296. <https://doi.org/10.1016/j.nbt.2013.08.001>.
- [128] N. Jacquél, C.W. Lo, Y.H. Wei, H.S. Wu, S.S. Wang, Isolation and purification of bacterial poly(3-hydroxyalkanoates), *Biochem Eng J.* 39 (2008) 15–27.  
<https://doi.org/10.1016/j.bej.2007.11.029>.
- [129] S.K. Hahn, Y.K. Chang, B. Engineering, A THERMOGRAVIMETRIC FOR POLY ( 3-HYDROXYBUTYRATE ) ANALYSIS, 9 (1995) 873–878.
- [130] M.A.M. Reis, M. Albuquerque, M. Villano, M. Majone, Mixed Culture Processes for Polyhydroxyalkanoate Production from Agro-Industrial Surplus/Wastes as



Feedstocks, *Comprehensive Biotechnology*. (2011) 669–683.

<https://doi.org/10.1016/B978-0-08-088504-9.00464-5>.

- [131] M. Majone, L. Chronopoulou, L. Lorini, A. Martinelli, C. Palocci, S. Rossetti, F. Valentino, M. Villano, PHA copolymers from microbial mixed cultures: Synthesis, extraction and related properties, in: *Current Advances in Biopolymer Processing and Characterization*, Nova Science Publishers, Inc., 2017: pp. 223–276.
- [132] L. Lorini, G. Munarin, G. Salvatori, S. Alfano, P. Pavan, M. Majone, F. Valentino, Sewage sludge as carbon source for polyhydroxyalkanoates: a holistic approach at pilot scale level, *J Clean Prod.* 354 (2022).  
<https://doi.org/10.1016/j.jclepro.2022.131728>.
- [133] A.P. Khedulkar, B. Pandit, V.D. Dang, R. an Doong, Agricultural waste to real worth biochar as a sustainable material for supercapacitor, *Science of The Total Environment.* 869 (2023) 161441. <https://doi.org/10.1016/J.SCITOTENV.2023.161441>.
- [134] P. Ghosh, R.A. Afre, T. Soga, T. Jimbo, A simple method of producing single-walled carbon nanotubes from a natural precursor: Eucalyptus oil, *Mater Lett.* 61 (2007) 3768–3770. <https://doi.org/10.1016/J.MATLET.2006.12.030>.
- [135] M.M. Rossi, S. Alfano, N. Amanat, F. Andreini, L. Lorini, A. Martinelli, M.P. Papini, A Polyhydroxybutyrate (PHB)-Biochar Reactor for the Adsorption and Biodegradation of Trichloroethylene: Design and Startup Phase, *Bioengineering.* 9 (2022). <https://doi.org/10.3390/bioengineering9050192>.
- [136] J. Shi, R. Zhang, X. Liu, Y. Zhang, Y. Du, H. Dong, Y. Ma, X. Li, P.C.K. Cheung, F. Chen, Advances in multifunctional biomass-derived nanocomposite films for active and sustainable food packaging, *Carbohydr Polym.* 301 (2023) 120323.  
<https://doi.org/10.1016/J.CARBPOL.2022.120323>.
- [137] B.D. Mattos, B.L. Tardy, W.L.E. Magalhães, O.J. Rojas, Controlled release for crop and wood protection: Recent progress toward sustainable and safe nanostructured

biocidal systems, *Journal of Controlled Release*. 262 (2017) 139–150.

<https://doi.org/10.1016/J.JCONREL.2017.07.025>.

- [138] I.J. Hall Barrientos, E. Paladino, P. Szabó, S. Brozio, P.J. Hall, C.I. Oseghale, M.K. Passarelli, S.J. Moug, R.A. Black, C.G. Wilson, R. Zelkó, D.A. Lamprou, Electrospun collagen-based nanofibres: A sustainable material for improved antibiotic utilisation in tissue engineering applications, *Int J Pharm*. 531 (2017) 67–79.  
<https://doi.org/10.1016/J.IJPHARM.2017.08.071>.
- [139] C.T.J.I.C.-M. and I.R. L. R. Lizarraga-Valderrama, *Tissue Engineering: Polyhydroxyalkanoate-Based Materials and Composites*, in: *Encyclopedia of Polymer Applications*, CRC Press Taylor & Francis Group, 2018.  
<https://doi.org/10.1201/9781351019422-140000458>.
- [140] P. Basnett, K.Y. Ching, M. Stolz, J.C. Knowles, A.R. Boccaccini, C. Smith, I.C. Locke, T. Keshavarz, I. Roy, Novel Poly(3-hydroxyoctanoate)/Poly(3-hydroxybutyrate) blends for medical applications, *React Funct Polym*. 73 (2013) 1340–1348.  
<https://doi.org/10.1016/J.REACTFUNCTPOLYM.2013.03.019>.
- [141] C. Del Gaudio, L. Fioravanzo, M. Folin, F. Marchi, E. Ercolani, A. Bianco, Electrospun tubular scaffolds: On the effectiveness of blending poly( $\epsilon$ -caprolactone) with poly(3-hydroxybutyrate-co-3-hydroxyvalerate), *J Biomed Mater Res B Appl Biomater*. 100 B (2012) 1883–1898. <https://doi.org/10.1002/jbm.b.32756>.
- [142] A. V. Bagdadi, M. Safari, P. Dubey, P. Basnett, P. Sofokleous, E. Humphrey, I. Locke, M. Edirisinghe, C. Terracciano, A.R. Boccaccini, J.C. Knowles, S.E. Harding, I. Roy, Poly(3-hydroxyoctanoate), a promising new material for cardiac tissue engineering, *J Tissue Eng Regen Med*. 12 (2018) e495–e512. <https://doi.org/10.1002/term.2318>.
- [143] S. Vigneswari, V. Murugaiyah, G. Kaur, H.P.S. Abdul Khalil, A.A. Amirul, Simultaneous dual syringe electrospinning system using benign solvent to fabricate nanofibrous P(3HB-co-4HB)/collagen peptides construct as potential leave-on

wound dressing, *Materials Science and Engineering: C*. 66 (2016) 147–155.  
<https://doi.org/10.1016/J.MSEC.2016.03.102>.

- [144] C. Del Gaudio, L. Fioravanzo, M. Folin, F. Marchi, E. Ercolani, A. Bianco, Electrospun tubular scaffolds: On the effectiveness of blending poly( $\epsilon$ -caprolactone) with poly(3-hydroxybutyrate-co-3-hydroxyvalerate), *J Biomed Mater Res B Appl Biomater*. 100 B (2012) 1883–1898. <https://doi.org/10.1002/jbm.b.32756>.
- [145] E. Marcello, M. Maqbool, R. Nigmatullin, M. Cresswell, P.R. Jackson, P. Basnett, J.C. Knowles, A.R. Boccaccini, I. Roy, Antibacterial Composite Materials Based on the Combination of Polyhydroxyalkanoates With Selenium and Strontium Co-substituted Hydroxyapatite for Bone Regeneration, *Front Bioeng Biotechnol*. 9 (2021). <https://doi.org/10.3389/fbioe.2021.647007>.
- [146] J. Lim, M. You, J. Li, Z. Li, Emerging bone tissue engineering via Polyhydroxyalkanoate (PHA)-based scaffolds, *Materials Science and Engineering C*. 79 (2017) 917–929. <https://doi.org/10.1016/j.msec.2017.05.132>.
- [147] E. Chiellini, C. Errico, C. Bartoli, F. Chiellini, Poly(hydroxyalkanoates)-based polymeric nanoparticles for drug delivery, *J Biomed Biotechnol*. 2009 (2009). <https://doi.org/10.1155/2009/571702>.
- [148] T.R.J. Heathman, W.R. Webb, J. Han, Z. Dan, G.Q. Chen, N.R. Forsyth, A.J. El Haj, Z.R. Zhang, X. Sun, Controlled production of poly (3-hydroxybutyrate-co-3-hydroxyhexanoate) (PHBHHx) nanoparticles for targeted and sustained drug delivery, *J Pharm Sci*. 103 (2014) 2498–2508. <https://doi.org/10.1002/jps.24035>.
- [149] Y.C. Xiong, Y.C. Yao, X.Y. Zhan, G.Q. Chen, Application of polyhydroxyalkanoates nanoparticles as intracellular sustained drug-release vectors, *J Biomater Sci Polym Ed*. 21 (2010) 127–140. <https://doi.org/10.1163/156856209X410283>.
- [150] T.G. Vladkova, Surface engineered polymeric biomaterials with improved biocontact properties, *Int J Polym Sci*. 2010 (2010). <https://doi.org/10.1155/2010/296094>.

- [151] P. Kingshott, G. Andersson, S.L. McArthur, H.J. Griesser, Surface modification and chemical surface analysis of biomaterials, *Curr Opin Chem Biol.* 15 (2011) 667–676. <https://doi.org/10.1016/j.cbpa.2011.07.012>.
- [152] H. T. Phan, A. J. Haes, What Does Nanoparticle Stability Mean?, *The Journal of Physical Chemistry C.* 123 (2019) 16495–16507. <https://doi.org/10.1021/acs.jpcc.9b00913>.
- [153] D.A. Donkor, X.S. Tang, Tube length and cell type-dependent cellular responses to ultra-short single-walled carbon nanotube, *Biomaterials.* 35 (2014) 3121–3131. <https://doi.org/10.1016/J.BIOMATERIALS.2013.12.075>.
- [154] J. Choi, Q. Zhang, V. Reipa, N.S. Wang, M.E. Stratmeyer, V.M. Hitchins, P.L. Goering, Comparison of cytotoxic and inflammatory responses of photoluminescent silicon nanoparticles with silicon micron-sized particles in RAW 264.7 macrophages, *Journal of Applied Toxicology.* 29 (2009) 52–60. <https://doi.org/10.1002/jat.1382>.
- [155] H. Cortés, H. Hernández-Parra, S.A. Bernal-Chávez, M.L. Del Prado-Audelo, I.H. Caballero-Florán, F. V. Borbolla-Jiménez, M. González-Torres, J.J. Magaña, G. Leyva-Gómez, Non-ionic surfactants for stabilization of polymeric nanoparticles for biomedical uses, *Materials.* 14 (2021). <https://doi.org/10.3390/ma14123197>.
- [156] S.D. Tröster, U. Müller, J. Kreuter, Modification of the body distribution of poly(methyl methacrylate) nanoparticles in rats by coating with surfactants, *Int J Pharm.* 61 (1990) 85–100. [https://doi.org/10.1016/0378-5173\(90\)90047-8](https://doi.org/10.1016/0378-5173(90)90047-8).
- [157] J. Kreuter, V.E. Petrov, D.A. Kharkevich, R.N. Alyautdin, Influence of the type of surfactant on the analgesic effects induced by the peptide dalargin after its delivery across the blood–brain barrier using surfactant-coated nanoparticles, *Journal of Controlled Release.* 49 (1997) 81–87. [https://doi.org/10.1016/S0168-3659\(97\)00061-8](https://doi.org/10.1016/S0168-3659(97)00061-8).
- [158] B. Wilson, Y. Lavanya, S.R.B. Priyadarshini, M. Ramasamy, J.L. Jenita, Albumin nanoparticles for the delivery of gabapentin: Preparation, characterization and

pharmacodynamic studies, *Int J Pharm.* 473 (2014) 73–79.

<https://doi.org/10.1016/J.IJPHARM.2014.05.056>.

- [159] W.C. Hueper, Carcinogenic Studies on Water-Soluble and Insoluble Macromolecules., *Arch. Pathol.* . 67 (1959).
- [160] S.O. Badmus, H.K. Amusa, T.A. Oyehan, T.A. Saleh, Environmental risks and toxicity of surfactants: overview of analysis, assessment, and remediation techniques, (n.d.). <https://doi.org/10.1007/s11356-021-16483-w/Published>.
- [161] S. Rebello, A.K. Asok, S. Mundayoor, M.S. Jisha, Surfactants: Toxicity, remediation and green surfactants, *Environ Chem Lett.* 12 (2014) 275–287.  
<https://doi.org/10.1007/s10311-014-0466-2>.
- [162] P. Charoensit, W. Pompimon, N. Khorana, S. Sungthongjeen, Effect of amide linkage of PEG-lipid conjugates on the stability and cytotoxic activity of goniodiol loaded in PEGylated liposomes, *J Drug Deliv Sci Technol.* 50 (2019) 1–8.  
<https://doi.org/10.1016/J.JDDST.2019.01.004>.
- [163] F. D. Souza, B. S. Souza, D. W. Tondo, E. C. Leopoldino, H. D. Fiedler, F. Nome, Imidazolium-Based Zwitterionic Surfactants: Characterization of Normal and Reverse Micelles and Stabilization of Nanoparticles, *Langmuir.* 31 (2015) 3587–3595.  
<https://doi.org/10.1021/la504802k>.
- [164] W. Smulek, N. Burlaga, M. Hricovíni, A. Medved'ová, E. Kaczorek, Z. Hricovíniová, Evaluation of surface active and antimicrobial properties of alkyl D-lyxosides and alkyl L-rhamnosides as green surfactants, *Chemosphere.* 271 (2021) 129818.  
<https://doi.org/10.1016/J.CHEMOSPHERE.2021.129818>.
- [165] M. Sanjivkumar, M. Deivakumari, G. Immanuel, Investigation on spectral and biomedical characterization of rhamnolipid from a marine associated bacterium *Pseudomonas aeruginosa* (DKB1), *Arch Microbiol.* 203 (2021) 2297–2314.  
<https://doi.org/10.1007/s00203-021-02220-x>.

- [166] A. Carrio, G. Schwach, J. Coudane, M. Vert, Preparation and degradation of surfactant-free PLGA microspheres, 1995.
- [167] A. Martinelli, A. Bakry, L. D'Ilario, I. Francolini, A. Piozzi, V. Taresco, Release behavior and antibiofilm activity of usnic acid-loaded carboxylated poly(l-lactide) microparticles, *European Journal of Pharmaceutics and Biopharmaceutics*. 88 (2014) 415–423. <https://doi.org/10.1016/J.EJPB.2014.06.002>.
- [168] Y. Bu, J. Ma, J. Bei, S. Wang, Surface Modification of Aliphatic Polyester to Enhance Biocompatibility, *Front Bioeng Biotechnol*. 7 (2019). <https://doi.org/10.3389/fbioe.2019.00098>.
- [169] L. Lao, H. Tan, Y. Wang, C. Gao, Chitosan modified poly(l-lactide) microspheres as cell microcarriers for cartilage tissue engineering, *Colloids Surf B Biointerfaces*. 66 (2008) 218–225. <https://doi.org/10.1016/J.COLSURFB.2008.06.014>.
- [170] T. I. Croll, A. J. O'Connor, G. W. Stevens, J. J. Cooper-White, Controllable Surface Modification of Poly(lactic-co-glycolic acid) (PLGA) by Hydrolysis or Aminolysis I: Physical, Chemical, and Theoretical Aspects, *Biomacromolecules*. 5 (2004) 463–473. <https://doi.org/10.1021/bm0343040>.
- [171] J.M. Goddard, J.H. Hotchkiss, Polymer surface modification for the attachment of bioactive compounds, *Prog Polym Sci*. 32 (2007) 698–725. <https://doi.org/10.1016/J.PROGPOLYMSCI.2007.04.002>.
- [172] U. Hersel, C. Dahmen, H. Kessler, RGD modified polymers: biomaterials for stimulated cell adhesion and beyond, *Biomaterials*. 24 (2003) 4385–4415. [https://doi.org/10.1016/S0142-9612\(03\)00343-0](https://doi.org/10.1016/S0142-9612(03)00343-0).
- [173] Y.-P. Jiao, F.-Z. Cui, Surface modification of polyester biomaterials for tissue engineering, *Biomedical Materials*. 2 (2007) R24–R37. <https://doi.org/10.1088/1748-6041/2/4/R02>.
- [174] R. A. Bakare, C. Bhan, D. Raghavan, Synthesis and Characterization of Collagen Grafted Poly(hydroxybutyrate–valerate) (PHBV) Scaffold for Loading of Bovine

Serum Albumin Capped Silver (Ag/BSA) Nanoparticles in the Potential Use of Tissue Engineering Application, *Biomacromolecules*. 15 (2013) 423–435.  
<https://doi.org/10.1021/bm401686v>.

- [175] C. Zhijiang, H. Chengwei, Y. Guang, Poly(3-hydroxybutyrate-co-4-hydroxybutyrate)/bacterial cellulose composite porous scaffold: Preparation, characterization and biocompatibility evaluation, *Carbohydr Polym*. 87 (2012) 1073–1080. <https://doi.org/10.1016/J.CARBPOL.2011.08.037>.
- [176] L.Y. Wang, Y.J. Wang, D.R. Cao, Surface modification of poly(3-hydroxybutyrate-co-3-hydroxyvalerate) membrane by combining surface aminolysis treatment with collagen immobilization, *Journal of Macromolecular Science, Part A: Pure and Applied Chemistry*. 46 (2009) 765–773. <https://doi.org/10.1080/10601320903004517>.
- [177] G. Mallamaci, B. Brugnoli, A. Mariano, A.S. d’Abusco, A. Piozzi, V. Di Lisio, E. Sturabotti, S. Alfano, I. Francolini, Surface modification of polyester films with polyfunctional amines: Effect on bacterial biofilm formation, *Surfaces and Interfaces*. 39 (2023). <https://doi.org/10.1016/j.surfin.2023.102924>.
- [178] L. Pellegrino, R. Cocchiola, I. Francolini, M. Lopreiato, A. Piozzi, R. Zanoni, A. Scotto d’Abusco, A. Martinelli, Taurine grafting and collagen adsorption on PLLA films improve human primary chondrocyte adhesion and growth, *Colloids Surf B Biointerfaces*. 158 (2017) 643–649. <https://doi.org/10.1016/J.COLSURFB.2017.07.047>.
- [179] A.C. De Felice, V. Di Lisio, I. Francolini, A. Mariano, A. Piozzi, A. Scotto d’Abusco, E. Sturabotti, A. Martinelli, One-Pot Preparation of Hydrophilic Polylactide Porous Scaffolds by Using Safe Solvent and Choline Taurinate Ionic Liquid, *Pharmaceutics*. 14 (2022) 158. <https://doi.org/10.3390/pharmaceutics14010158>.
- [180] Y. Zhu, Z. Mao, C. Gao, Aminolysis-based surface modification of polyesters for biomedical applications, *RSC Adv*. 3 (2013) 2509–2519.  
<https://doi.org/10.1039/c2ra22358a>.

- [181] M. Cocchietto, N. Skert, P. Nimis, G. Sava, A review on usnic acid, an interesting natural compound, *Naturwissenschaften*. 89 (2002) 137–146.  
<https://doi.org/10.1007/s00114-002-0305-3>.
- [182] S. Sato, D. Gondo, T. Wada, S. Kanehashi, K. Nagai, Effects of various liquid organic solvents on solvent-induced crystallization of amorphous poly(lactic acid) film, *J Appl Polym Sci*. 129 (2013) 1607–1617. <https://doi.org/10.1002/app.38833>.
- [183] J. Gao, L. Duan, G. Yang, Q. Zhang, M. Yang, Q. Fu, Manipulating poly(lactic acid) surface morphology by solvent-induced crystallization, *Appl Surf Sci*. 261 (2012) 528–535. <https://doi.org/10.1016/j.apsusc.2012.08.050>.
- [184] A.K. Kulshreshtha, A.H. Khan, G.L. Madan, X-ray diffraction study of solvent-induced crystallization in polyester filaments, *Polymer (Guildf)*. 19 (1978) 819–823.  
[https://doi.org/10.1016/0032-3861\(78\)90011-3](https://doi.org/10.1016/0032-3861(78)90011-3).
- [185] B. Salgaonkar, J. Bragança, Utilization of Sugarcane Bagasse by Halogeometricum borinquense Strain E3 for Biosynthesis of Poly(3-hydroxybutyrate-co-3-hydroxyvalerate), *Bioengineering*. 4 (2017) 50.  
<https://doi.org/10.3390/bioengineering4020050>.
- [186] T. I. Croll, A. J. O'Connor, G. W. Stevens, J. J. Cooper-White, Controllable Surface Modification of Poly(lactic-co-glycolic acid) (PLGA) by Hydrolysis or Aminolysis I: Physical, Chemical, and Theoretical Aspects, *Biomacromolecules*. 5 (2004) 463–473. <https://doi.org/10.1021/bm0343040>.
- [187] Y. Zhu, C. Gao, X. Liu, J. Shen, Surface Modification of Polycaprolactone Membrane via Aminolysis and Biomacromolecule Immobilization for Promoting Cytocompatibility of Human Endothelial Cells, *Biomacromolecules*. 3 (2002) 1312–1319. <https://doi.org/10.1021/bm020074y>.
- [188] Z. Yang, M. Zhengwei, S. Huayu, G. Changyou, In-depth study on aminolysis of poly( $\epsilon$ -caprolactone): Back to the fundamentals, *Sci China Chem*. 55 (2012) 2419–2427. <https://doi.org/10.1007/s11426-012-4540-y>.



- [189] A.N. Kuskov, P.P. Kulikov, A. V. Goryachaya, M.N. Tzatzarakis, A.M. Tsatsakis, K. Velonia, M.I. Shtilman, Self-assembled amphiphilic poly- *N* -vinylpyrrolidone nanoparticles as carriers for hydrophobic drugs: Stability aspects, *J Appl Polym Sci.* 135 (2018). <https://doi.org/10.1002/app.45637>.
- [190] P.L. Jacob, L.A. Ruiz Cantu, A.K. Pearce, Y. He, J.C. Lentz, J.C. Moore, F. Machado, G. Rivers, E. Apebende, M.R. Fernandez, I. Francolini, R. Wildman, S.M. Howdle, V. Taresco, Poly (glycerol adipate) (PGA) backbone modifications with a library of functional diols: Chemical and physical effects, *Polymer (Guildf).* 228 (2021) 123912. <https://doi.org/10.1016/j.polymer.2021.123912>.
- [191] M. Sanna, G. Sicilia, A. Alazzo, N. Singh, F. Musumeci, S. Schenone, K.A. Spriggs, J.C. Burley, M.C. Garnett, V. Taresco, C. Alexander, Water Solubility Enhancement of Pyrazolo[3,4- *d* ]pyrimidine Derivatives via Miniaturized Polymer–Drug Microarrays, *ACS Med Chem Lett.* 9 (2018) 193–197. <https://doi.org/10.1021/acsmchemlett.7b00456>.
- [192] D. Garcia-Garcia, L. Quiles-Carrillo, R. Balart, S. Torres-Giner, M.P. Arrieta, Innovative solutions and challenges to increase the use of Poly(3-hydroxybutyrate) in food packaging and disposables, *Eur Polym J.* 178 (2022) 111505. <https://doi.org/10.1016/J.EURPOLYMJ.2022.111505>.
- [193] D.Z. Bucci, L.B.B. Tavares, I. Sell, Biodegradation and physical evaluation of PHB packaging, *Polym Test.* 26 (2007) 908–915. <https://doi.org/10.1016/J.POLYMERTESTING.2007.06.013>.
- [194] J.K. Hobbs, P.J. Barham, The fracture of poly(hydroxybutyrate) Part III Fracture morphology in thin films and bulk systems, n.d.
- [195] W. v. Srubar, Z.C. Wright, A. Tsui, A.T. Michel, S.L. Billington, C.W. Frank, Characterizing the effects of ambient aging on the mechanical and physical properties of two commercially available bacterial thermoplastics, in: *Polym Degrad Stab*, 2012: pp. 1922–1929. <https://doi.org/10.1016/j.polymdegradstab.2012.04.011>.

- [196] Y. Wang, S. Yamada, N. Asakawa, T. Yamane, N. Yoshie, Y. Inoue, Comonomer Compositional Distribution and Thermal and Morphological Characteristics of Bacterial Poly(3-hydroxybutyrate-co-3-hydroxyvalerate)s with High 3-Hydroxyvalerate Content, *Biomacromolecules*. 2 (2001) 1315–1323. <https://doi.org/10.1021/bm010128o>.
- [197] H.M. Ye, J. Xu, B.H. Guo, T. Iwata, Left- or right-handed lamellar twists in poly[(R)-3-hydroxyvalerate] banded spherulite: dependence on growth axis, *Macromolecules*. 42 (2009) 694–701. <https://doi.org/10.1021/ma801653p>.
- [198] B. Melendez-Rodriguez, M.A.M. Reis, M. Carvalheira, C. Sammon, L. Cabedo, S. Torres-Giner, J.M. Lagaron, Development and Characterization of Electrospun Biopapers of Poly(3-hydroxybutyrate- co-3-hydroxyvalerate) Derived from Cheese Whey with Varying 3-Hydroxyvalerate Contents, *Biomacromolecules*. 22 (2021) 2935–2953. <https://doi.org/10.1021/acs.biomac.1c00353>.
- [199] M. Abbasi, D. Pokhrel, E.R. Coats, N.M. Guho, A.G. McDonald, Effect of 3-Hydroxyvalerate Content on Thermal, Mechanical, and Rheological Properties of Poly(3-hydroxybutyrate-co-3-hydroxyvalerate) Biopolymers Produced from Fermented Dairy Manure, *Polymers (Basel)*. 14 (2022) 4140. <https://doi.org/10.3390/polym14194140>.
- [200] J. Mai, C.J. Garvey, C.M. Chan, S. Pratt, B. Laycock, Synthesis and characterisation of poly(3-hydroxybutyrate-co-3-hydroxyvalerate) (PHBV) multi-block copolymers comprising blocks of differing 3-hydroxyvalerate contents, *Chemical Engineering Journal*. (2023) 146175. <https://doi.org/10.1016/J.CEJ.2023.146175>.
- [201] W. Ma, J. Wang, Y. Li, L. Yin, X. Wang, Poly(3-hydroxybutyrate-co-3-hydroxyvalerate) co-produced with l-isoleucine in *Corynebacterium glutamicum* WM001, *Microb Cell Fact*. 17 (2018) 93. <https://doi.org/10.1186/s12934-018-0942-7>.
- [202] I.S. Aldor, S.-W. Kim, K.L.J. Prather, J.D. Keasling, Metabolic Engineering of a Novel Propionate-Independent Pathway for the Production of Poly(3-Hydroxybutyrate- co

- 3-Hydroxyvalerate) in Recombinant *Salmonella enterica* Serovar Typhimurium, *Appl Environ Microbiol.* 68 (2002) 3848–3854. <https://doi.org/10.1128/AEM.68.8.3848-3854.2002>.
- [203] I. Aldor, J.D. Keasling, Metabolic engineering of poly(3-hydroxybutyrate-co-3-hydroxyvalerate) composition in recombinant *Salmonella enterica* serovar typhimurium, *Biotechnol Bioeng.* 76 (2001) 108–114. <https://doi.org/10.1002/bit.1150>.
- [204] A. Ferre-Guell, J. Winterburn, Biosynthesis and Characterization of Polyhydroxyalkanoates with Controlled Composition and Microstructure, *Biomacromolecules.* 19 (2018) 996–1005. <https://doi.org/10.1021/acs.biomac.7b01788>.
- [205] B. Laycock, M. V. Arcos-Hernandez, A. Langford, S. Pratt, A. Werker, P.J. Halley, P.A. Lant, Crystallisation and fractionation of selected polyhydroxyalkanoates produced from mixed cultures, *N Biotechnol.* 31 (2014) 345–356. <https://doi.org/10.1016/j.nbt.2013.05.005>.
- [206] M. V. Arcos-Hernández, B. Laycock, B.C. Donose, S. Pratt, P. Halley, S. Al-Luaibi, A. Werker, P.A. Lant, Physicochemical and mechanical properties of mixed culture polyhydroxyalkanoate (PHBV), *Eur Polym J.* 49 (2013) 904–913. <https://doi.org/10.1016/j.eurpolymj.2012.10.025>.
- [207] A. Langford, C.M. Chan, S. Pratt, C.J. Garvey, B. Laycock, The morphology of crystallisation of PHBV/PHBV copolymer blends, *Eur Polym J.* 112 (2019) 104–119. <https://doi.org/10.1016/j.eurpolymj.2018.12.022>.
- [208] E. DOINEAU, C. PERDRIER, F. ALLAYAUD, E. BLANCHET, L. PREZIOSI-BELLOU, E. GROUSSEAU, N. GONTARD, H. ANGELLIER-COUSSY, Designing Poly(3-Hydroxybutyrate-co-3-Hydroxyvalerate) P(3HB-co-3HV) films with tailored mechanical properties, *Mater Today Commun.* (2023) 106848. <https://doi.org/10.1016/J.MTCOMM.2023.106848>.
- [209] W. Kai, Y. He, Y. Inoue, Fast crystallization of poly(3-hydroxybutyrate) and poly(3-hydroxybutyrate-co-3-hydroxy-valerate) with talc and boron nitride as nucleating

agents, *Polymer International Polym Int.* 54 (2005) 780–789.

<https://doi.org/10.1002/pi.1758>.

- [210] Y. Miao, C. Fang, D. Shi, Y. Li, Z. Wang, Coupling effects of boron nitride and heat treatment on crystallization, mechanical properties of poly (3-hydroxybutyrate-co-3-hydroxyvalerate) (PHBV), *Polymer (Guildf)*. 252 (2022).  
<https://doi.org/10.1016/j.polymer.2022.124967>.
- [211] L.N. Carli, J.S. Crespo, R.S. Mauler, PHBV nanocomposites based on organomodified montmorillonite and halloysite: The effect of clay type on the morphology and thermal and mechanical properties, *Compos Part A Appl Sci Manuf.* 42 (2011) 1601–1608. <https://doi.org/10.1016/J.COMPOSITESA.2011.07.007>.
- [212] I.T. Seoane, E. Fortunati, D. Puglia, V.P. Cyras, L.B. Manfredi, Development and characterization of bionanocomposites based on poly(3-hydroxybutyrate) and cellulose nanocrystals for packaging applications, *Polym Int.* 65 (2016) 1046–1053.  
<https://doi.org/10.1002/pi.5150>.
- [213] T.-M. Don, C.-Y. Chung, S.-M. Lai, H.-J. Chiu, Preparation and properties of blends from poly(3-hydroxybutyrate) with poly(vinyl acetate)-modified starch, *Polym Eng Sci.* 50 (2010) 709–718. <https://doi.org/10.1002/pen.21575>.
- [214] S.J. Modi, K. Cornish, K. Koelling, Y. Vodovotz, Fabrication and improved performance of poly(3-hydroxybutyrate-co-3-hydroxyvalerate) for packaging by addition of high molecular weight natural rubber, *J Appl Polym Sci.* 133 (2016).  
<https://doi.org/10.1002/app.43937>.
- [215] X. Zhao, V. Venoor, K. Koelling, K. Cornish, Y. Vodovotz, Bio-based blends from poly(3-hydroxybutyrate- co -3-hydroxyvalerate) and natural rubber for packaging applications, *J Appl Polym Sci.* 136 (2019). <https://doi.org/10.1002/app.47334>.
- [216] C.S. Ha, W.J. Cho, Miscibility, properties, and biodegradability of microbial polyester containing blends, *Prog Polym Sci.* 27 (2002) 759–809.  
[https://doi.org/10.1016/S0079-6700\(01\)00050-8](https://doi.org/10.1016/S0079-6700(01)00050-8).

- [217] L. Yu, K. Dean, L. Li, Polymer blends and composites from renewable resources, *Prog Polym Sci.* 31 (2006) 576–602.  
<https://doi.org/10.1016/j.progpolymsci.2006.03.002>.
- [218] P. Feijoo, K. Samaniego-Aguilar, E. Sánchez-Safont, S. Torres-Giner, J.M. Lagaron, J. Gamez-Perez, L. Cabedo, Development and Characterization of Fully Renewable and Biodegradable Polyhydroxyalkanoate Blends with Improved Thermoformability, *Polymers (Basel)*. 14 (2022) 2527.  
<https://doi.org/10.3390/polym14132527>.
- [219] S.M. Martelli, J. Sabirova, F.M. Fakhoury, A. Dyzma, B. de Meyer, W. Soetaert, Obtention and characterization of poly(3-hydroxybutyric acid-co-hydroxyvaleric acid)/mcl-PHA based blends, *LWT*. 47 (2012) 386–392.  
<https://doi.org/10.1016/j.lwt.2012.01.036>.
- [220] L. Zhang, C. Xiong, X. Deng, Miscibility, crystallization and morphology of poly(P-hydroxybutyrate)/ poly(d,l-lactide) blends, 1996.
- [221] R.K. Sadi, R.S. Kurusu, G.J.M. Fachine, N.R. Demarquette, Compatibilization of polypropylene/poly(3-hydroxybutyrate) blends, *J Appl Polym Sci.* 123 (2012) 3511–3519. <https://doi.org/10.1002/app.34853>.
- [222] M. Przybysz, M. Marć, M. Klein, M.R. Saeb, K. Formela, Structural, mechanical and thermal behavior assessments of PCL/PHB blends reactively compatibilized with organic peroxides, *Polym Test*. 67 (2018) 513–521.  
<https://doi.org/10.1016/J.POLYMERTESTING.2018.03.014>.
- [223] C. Perdrier, E. Doineau, L. Leroyer, M. Subileau, H. Angellier-Coussy, L. Preziosi-Belloy, E. Grousseau, Impact of overflow vs. limitation of propionic acid on poly(3-hydroxybutyrate-co-3-hydroxyvalerate) biosynthesis, *Process Biochemistry*. (2023).  
<https://doi.org/10.1016/J.PROCBIO.2023.02.006>.
- [224] J. Bossu, N. Le Moigne, P. Dieudonné-George, L. Dumazert, V. Guillard, H. Angellier-Coussy, Impact of the processing temperature on the crystallization

behavior and mechanical properties of poly[R-3-hydroxybutyrate-co-(R-3-hydroxyvalerate)], *Polymer (Guildf)*. 229 (2021).  
<https://doi.org/10.1016/j.polymer.2021.123987>.

- [225] H. Mitomo, P.J. Barham, A. Keller, *Crystallization and Morphology of Poly(p-hydroxybutyrate) and Its Copolymer*, 1987.
- [226] K.S. Anderson, M.A. Hillmyer, Melt preparation and nucleation efficiency of polylactide stereocomplex crystallites, *Polymer (Guildf)*. 47 (2006) 2030–2035.  
<https://doi.org/10.1016/J.POLYMER.2006.01.062>.
- [227] P. Song, Z. Wei, J. Liang, G. Chen, W. Zhang, Crystallization behavior and nucleation analysis of poly( $\epsilon$ -lactic acid) with a multiamide nucleating agent, *Polym Eng Sci*. 52 (2012) 1058–1068. <https://doi.org/10.1002/pen.22172>.
- [228] W.J. Liu, H.L. Yang, Z. Wang, L.S. Dong, J.J. Liu, Effect of nucleating agents on the crystallization of poly(3-hydroxybutyrate-co-3-hydroxyvalerate), *J Appl Polym Sci*. 86 (2002) 2145–2152. <https://doi.org/10.1002/app.11023>.
- [229] G.X. Chen, G.J. Hao, T.Y. Guo, M.D. Song, B.H. Zhang, Structure and mechanical properties of poly(3-hydroxybutyrate-co-3-hydroxyvalerate) (PHBV)/clay nanocomposites, n.d.
- [230] M.J. Meziani, W.-L. Song, P. Wang, F. Lu, Z. Hou, A. Nderson, H. Aimaiti, Y.-P. Sun, *Boron Nitride Nanomaterials for Thermal Management Applications*, n.d.  
[www.chemphyschem.org](http://www.chemphyschem.org).
- [231] Q. Weng, X. Wang, X. Wang, Y. Bando, D. Golberg, Functionalized hexagonal boron nitride nanomaterials: emerging properties and applications, *Chem. Soc. Rev.* 45 (2016) 3989. <https://doi.org/10.1039/c5cs00869g>.
- [232] J. Yu, X. Huang, C. Wu, X. Wu, G. Wang, P. Jiang, Interfacial modification of boron nitride nanoplatelets for epoxy composites with improved thermal properties, *Polymer (Guildf)*. 53 (2012) 471–480. <https://doi.org/10.1016/J.POLYMER.2011.12.040>.

- [233] M.L. Focarete, G. Ceccorulli, M. Scandola, M. Kowalczyk, Further evidence of crystallinity-induced biodegradation of synthetic atactic poly(3-hydroxybutyrate) by PHB-depolymerase A from *Pseudomonas lemoignei*. Blends of atactic poly(3-hydroxybutyrate) with crystalline polyesters, *Macromolecules*. 31 (1998) 8485–8492. <https://doi.org/10.1021/ma981115e>.
- [234] M.J. Jenkins, Y. Cao, L. Howell, G.A. Leeke, Miscibility in blends of poly(3-hydroxybutyrate-co-3-hydroxyvalerate) and poly( $\epsilon$ -caprolactone) induced by melt blending in the presence of supercritical CO<sub>2</sub>, *Polymer (Guildf)*. 48 (2007) 6304–6310. <https://doi.org/10.1016/j.polymer.2007.08.033>.
- [235] X. Wang, Z. Chen, X. Chen, J. Pan, K. Xu, Miscibility, crystallization kinetics, and mechanical properties of poly(3-hydroxybutyrate-co-3-hydroxyvalerate)(PHBV)/poly(3-hydroxybutyrate-co-4-hydroxybutyrate)(P3/4HB) blends, *J Appl Polym Sci*. 117 (2010) 838–848. <https://doi.org/10.1002/app.31215>.
- [236] B. Dodson, I.C. Mcneill, *Degradation of Polymer Mixtures. VI. Blends of Poly(vinyl Chloride) with Polystyrene*, 1976.
- [237] O. Miguel, J.J. Iruin, Water transport properties in poly(3-hydroxybutyrate) and poly(3-hydroxybutyrate-co-3-hydroxyvalerate) biopolymers, *J Appl Polym Sci*. 73 (1999) 455–468. [https://doi.org/10.1002/\(SICI\)1097-4628\(19990725\)73:4<455::AID-APP1>3.0.CO;2-Y](https://doi.org/10.1002/(SICI)1097-4628(19990725)73:4<455::AID-APP1>3.0.CO;2-Y).
- [238] A. Oehmen, B. Keller-Lehmann, R.J. Zeng, Z. Yuan, J. Keller, Optimisation of poly- $\beta$ -hydroxyalkanoate analysis using gas chromatography for enhanced biological phosphorus removal systems, *J Chromatogr A*. 1070 (2005) 131–136. <https://doi.org/10.1016/J.CHROMA.2005.02.020>.
- [239] S. Bloembergen, D.A. Holden, G.K. Hamer, T.L. Bluhm, R.H. Marchessault, Studies of composition and crystallinity of bacterial poly( $\beta$ -hydroxybutyrate-co- $\beta$ -hydroxyvalerate), *Macromolecules*. 19 (1986) 2865–2871. <https://doi.org/10.1021/ma00165a034>.

- [240] M. Kansiz, A. Domínguez-Vidal, D. McNaughton, B. Lendl, Fourier-transform infrared (FTIR) spectroscopy for monitoring and determining the degree of crystallisation of polyhydroxyalkanoates (PHAs), *Anal Bioanal Chem.* 388 (2007) 1207–1213. <https://doi.org/10.1007/s00216-007-1337-5>.
- [241] J. Xu, B.H. Guo, R. Yang, Q. Wu, G.Q. Chen, Z.M. Zhang, In situ FTIR study on melting and crystallization of polyhydroxyalkanoates, *Polymer (Guildf)*. 43 (2002) 6893–6899. [https://doi.org/10.1016/S0032-3861\(02\)00615-8](https://doi.org/10.1016/S0032-3861(02)00615-8).
- [242] J. Zhang, H. Sato, I. Noda, Y. Ozaki, Conformation Rearrangement and Molecular Dynamics of Poly(3-hydroxybutyrate) during the Melt-Crystallization Process Investigated by Infrared and Two-Dimensional Infrared Correlation Spectroscopy, *Macromolecules*. 38 (2005) 4274–4281. <https://doi.org/10.1021/ma0501343>.
- [243] V. Jost, M. Schwarz, H.-C. Langowski, Investigation of the 3-hydroxyvalerate content and degree of crystallinity of P3HB-co-3HV cast films using Raman spectroscopy, *Polymer (Guildf)*. 133 (2017) 160–170. <https://doi.org/10.1016/j.polymer.2017.11.026>.
- [244] L. Lorini, A. Martinelli, P. Pavan, M. Majone, F. Valentino, Downstream processing and characterization of polyhydroxyalkanoates (PHAs) produced by mixed microbial culture (MMC) and organic urban waste as substrate, *Biomass Convers Biorefin.* 11 (2021) 693–703. <https://doi.org/10.1007/s13399-020-00788-w>.
- [245] Montgomery Douglas C., *Design and Analysis of Experiments*, 8th ed., Wiley, 2012.
- [246] Klaus Danzer, Lloyd A. Currie, *Guidelines for Calibration in Analytical Chemistry. Part I. Fundamentals and Single Component Calibration*, in: IUPAC Recommendations 1998, De Gruyter, 1998.
- [247] M. Scandola, G. Ceccorulli, M. Pizzoli, M. Gazzano, Study of the Crystal Phase and Crystallization Rate of Bacterial Poly(3-hydroxybutyrate-co-3-hydroxyvalerate), 1992. <https://pubs.acs.org/sharingguidelines>.
- [248] H. Sato, J. Dybal, R. Murakami, I. Noda, Y. Ozaki, Infrared and Raman spectroscopy and quantum chemistry calculation studies of C–H···O hydrogen bondings and



thermal behavior of biodegradable polyhydroxyalkanoate, *J Mol Struct.* 744–747 (2005) 35–46. <https://doi.org/10.1016/j.molstruc.2004.10.069>.

- [249] H. Sato, R. Murakami, J. Zhang, K. Mori, I. Takahashi, H. Terauchi, I. Noda, Y. Ozaki, Infrared Spectroscopy and X-Ray Diffraction Studies of C<sub>3</sub>H<sub>6</sub>O Hydrogen Bonding and Thermal Behavior of Biodegradable Poly(hydroxyalkanoate), *Macromol Symp.* 230 (2005) 158–166. <https://doi.org/10.1002/masy.200551155>.
- [250] Y. Kann, M. Shurgalin, R.K. Krishnaswamy, FTIR spectroscopy for analysis of crystallinity of poly(3-hydroxybutyrate-co-4-hydroxybutyrate) polymers and its utilization in evaluation of aging, orientation and composition, *Polym Test.* 40 (2014) 218–224. <https://doi.org/10.1016/j.polymertesting.2014.09.009>.
- [251] C.M.S. Izumi, M.L.A. Temperini, FT-Raman investigation of biodegradable polymers: Poly(3-hydroxybutyrate) and poly(3-hydroxybutyrate-co-3-hydroxyvalerate), *Vib Spectrosc.* 54 (2010) 127–132. <https://doi.org/10.1016/J.VIBSPEC.2010.07.011>.
- [252] S.N. Gorodzha, A.R. Muslimov, D.S. Syromotina, A.S. Timin, N.Y. Tcvetkov, K. V. Lepik, A. V. Petrova, M.A. Surmeneva, D.A. Gorin, G.B. Sukhorukov, R.A. Surmenev, A comparison study between electrospun polycaprolactone and piezoelectric poly(3-hydroxybutyrate-co-3-hydroxyvalerate) scaffolds for bone tissue engineering, *Colloids Surf B Biointerfaces.* 160 (2017) 48–59. <https://doi.org/10.1016/j.colsurfb.2017.09.004>.
- [253] T.G. Volova, N.O. Zhila, E.I. Shishatskaya, P. V. Mironov, A.D. Vasil'ev, A.G. Sukovatyi, A.J. Sinskey, The physicochemical properties of polyhydroxyalkanoates with different chemical structures, *Polymer Science Series A.* 55 (2013) 427–437. <https://doi.org/10.1134/S0965545X13070080>.
- [254] A. Narayanan, V.A. Sajeev Kumar, K.V. Ramana, Production and Characterization of Poly (3-Hydroxybutyrate-co-3-Hydroxyvalerate) from *Bacillus mycoides* DFC1

Using Rice Husk Hydrolyzate, Waste Biomass Valorization. 5 (2014) 109–118.  
<https://doi.org/10.1007/s12649-013-9213-3>.

- [255] A. Kovalcik, S. Obruca, M. Kalina, M. Machovsky, V. Enev, M. Jakesova, M. Sobkova, I. Marova, Enzymatic Hydrolysis of Poly(3-Hydroxybutyrate-co-3-Hydroxyvalerate) Scaffolds, *Materials*. 13 (2020) 2992.  
<https://doi.org/10.3390/ma13132992>.
- [256] Y. Marois, Z. Zhang, M. Vert, X. Deng, R. Lenz, R. Guidoin, Mechanism and rate of degradation of polyhydroxyoctanoate films in aqueous media: A long-term in vitro study, *J Biomed Mater Res*. 49 (2000) 216–224. [https://doi.org/10.1002/\(SICI\)1097-4636\(200002\)49:2<216::AID-JBM9>3.0.CO;2-X](https://doi.org/10.1002/(SICI)1097-4636(200002)49:2<216::AID-JBM9>3.0.CO;2-X).
- [257] M.A. Porras, M.A. Cubitto, M.A. Villar, A new way of quantifying the production of poly(hydroxyalkanoate)s using FTIR, *Journal of Chemical Technology & Biotechnology*. 91 (2016) 1240–1249. <https://doi.org/10.1002/jctb.4713>.
- [258] C. Koch, A.E. Posch, H.C. Goicoechea, C. Herwig, B. Lendl, Multi-analyte quantification in bioprocesses by Fourier-transform-infrared spectroscopy by partial least squares regression and multivariate curve resolution, *Anal Chim Acta*. 807 (2014) 103–110. <https://doi.org/10.1016/j.aca.2013.10.042>.



